THE CRYSTAL AND MOLECULAR STRUCTURE OF SOME TRANSITION METAL COMPLEXES DERIVED FROM (i) POLYPYRIDYL (ii) 1,4-DI(2'-PYRIDYL)AMINOPHTHALAZINE LIGANDS

WASANTHA A. WICKRAMASINGHE

A THESIS

IN

THE DEPARTMENT

OF

CHEMISTRY

PRESENTED IN PARTIAL FULFILMENT OF THE REQUIREMENTS

FOR THE DEGREE OF DOCTOR OF PHILOSOPHY AT

CONCORDIA UNIVERSITY

MONTREAL, QUEBEC, CANADA

FEBRUARY 1982

To My Parents

ABSTRACT

THE CRYSTAL AND MOLECULAR STRUCTURE OF SOME TRANSITION METAL COMPLEXES DERIVED FROM

(i) POLYPYRIDYL

(ii) 1,4-DI(2'-PYRIDYL)AMINOPHATHALAZINE

LIGANDS

Wasantha A. Wickramasinghe, Ph.D

Concordia University, 1982.

The thesis describes the crystal and molecular structure of five transition metal complexes as determined by X-ray diffraction techniques. The first three compounds are derived from polypyridyl ligands, and have photochemical importance. The last two compounds are bimetallic compounds derived from 1,4 di(2'-pyridyl)aminophthalazine, and have biological importance.

The structure of $[Ir(bpy)_2(bpy')]^{3+}$, which was believed to contain either a monodentate or a covalently hydrated bipyridyl ligand contains neither of these; instead all three bipyridine ligands are chelated to iridium(III) as in the case of a tris chelate, but one bipyridine ligand is ligated via the nitrogen of one ring and C(3) carbon of the other ring. The water of hydration is hydrogen-bonded to the uncoordinated nitrogen atom.

$[Cr(terpy)_2]^{3+}$ cation adopts a distorted meridional configuration

about chromium(III), with a mean Cr-N distance of 2.03(4) °A. There are 8 ClO_4 anions about the $[Cr(terpy)_2]^{3+}$ cation within 3.32 °A of a non-hydrogen atom. The water of hydration does not occupy a site in the intra-ligand pockets, but is hydrogen-bonded to a ClO_4 ion.

The structure of $[Cr(bpy)_2(H_2O)Cl]^{2+}$ cation consists of two N-chelated bipyridyl groups, and a Cl^- and a H_2O molecule attached in a cis manner. There are 6 perchlorate units about the cation within 3.3 °A of a non-hydrogen atom. The two waters of crystallization are hydrogen-bonded to bound water.

The last two compounds are binuclear complexes of Co(III) and Ni(II). The Co(III) dimer consist of approximately octahedrally arranged two Co(III) atoms linked by two symmetrically bridging OH^- groups and by the adjacent N atoms of a diazine ring of a phthalazine ligand. In addition each Co(III) atom is linked to another phthalazine group which acts in a bidentate fashion. The mean Co-N and Co-O distances are 1.92 and 1.91 °A respectively. The bonding in the Ni(II) dimer is virtually identical to that of the Co(III) complex, except the two nickel atoms are linked by a di-aquo bridge. The mean Ni-N and Ni-O distances are 2.07 and 2.15 °A respectively. In both complexes uncoordinated nitrogen atoms are hydrogen-bonded to the bridging oxygens.

CONTENTS

ACKNOWLEDGEMENT

I wish to acknowledge the debt I owe to my research director, Dr. P.H.Bird; his continued help and encouragement has been a great inspiration to me throughout the course of this work. Also I wish to express my sincere thanks to Dr. N.Serpone and Dr. L.D.Colebrook for their valuable advice, helpful discussions and continual encouragement.

I wish to acknowledge the generous help given by the technical staff of the Chemistry Department, especially by John Schultz.

Finally I wish to thank my family, to my parents, sisters and to my wife, Dilanthi, for their patience and understanding.

1.1 CRYSTALLOGRAPHY GENERAL - THEORY

This section of the thesis describes the theoretical aspects of X-ray crystallography. However, it does not serve as a complete text; for this, the reader is referred elsewhere, (see for eg. references 15,16,20,21).

1.1.1 The Unit Cell

Crystals are composed of groups of atoms, repeated at regular intervals in three-dimensions with the same molecular orientations. The fundamental unit which is repeated infinitely by translation in three-dimensions is known as the unit cell. The size and the shape of the unit cell is defined by the lengths a, b and c of the three independent non-coplanar edges and by the three angles α, β and γ between them (figure 1). There are 7 crystal systems, which can be expanded to 14 Bravais lattices. When combined with the 32 point groups, the 230 space groups are derived. All the known crystalline solids are confined to these 230 space groups [1-10].

1.1.2 Diffraction of x-rays

In as much as a crystal has a periodic structure, it could act as a three-dimensional diffraction grating for electromagnetic radiation of suitable wave-length. The

wave-lengths of X-rays are comparable to the interatomic distances of molecules, hence X-rays should show diffraction by crystals. This effect was discovered by Max von Laue in 1912 [11].

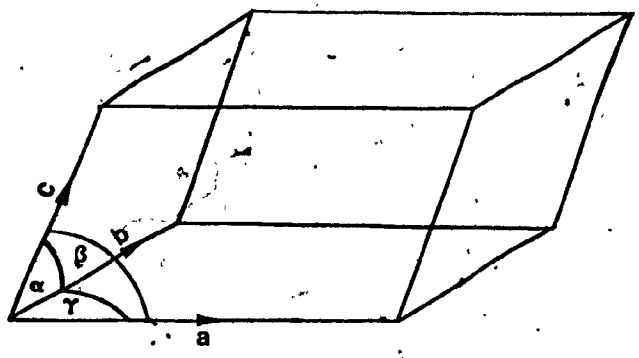

Figure 1.1

1.1.3 Bragg's Law

The geometric nature of a diffraction pattern is best explained by the Bragg's law [12-14].

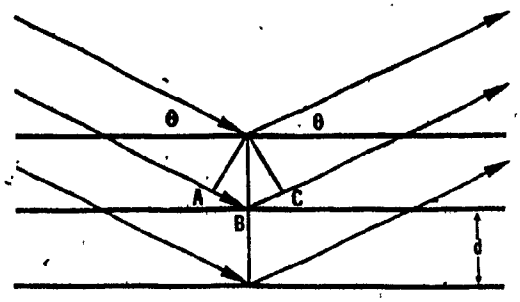

Figure 1.2

Because of the three-dimensional periodicity of a crystal structure it is possible to construct sets of many planes that are parallel with each other, equally spaced and containing identical atomic arrangements. If an incident X-ray beam makes an angle θ with such a set of planes, the reflected beam also makes an angle θ with the planes. Reflections from successive planes will interfere with each other. There will be constructive interference only when the difference in path length between rays from successive planes is equal to a whole number of wave-lengths. In figure 1.2 the ray striking the second plane travels a distance AB+BC farther than the ray striking the first plane. These two rays will be in phase only if,

$$AB + BC = n\lambda$$

where n is an integer.

Since $AB = BC = d \sin \theta$,

$$2d \sin \theta = n\lambda \qquad (1.1)$$

This is the well known Bragg's law.

1.1.4 The Scattering of X-rays by Atoms [15-17]

The geometric nature of the scattered radiation depends

upon the dimensions of the crystal lattice, but the intensities of the different diffracted beams depend only on the nature and arrangement of the atoms within the unit cell.

The electrons of the individual atoms within a unit cell are responsible for the scattering of X-rays. In order to evaluate the combined scattering from the atoms in the unit cell, it is necessary to consider the amplitudes of the waves scattered by the atoms; ie. the atomic scattering factors. The atomic scattering factor depends upon the nature of the atom, the direction of scattering, the wavelength of the X-rays used, and on the amplitude of the thermal vibrations of the atom. The atomic scattering factor can be taken as a measure of the efficiency with which an atom scatters X-radiation with respect to a single electron. The general form of the variation of f_j with $\sin \theta/\lambda$ is shown in figure 1.3.

The curve shown in figure 1.3, fits very well to the analytical expression given by the equation 1.2. The values of a_i, b_i, and C have been calculated by Cromer and Waber [18], among others, for most of the elements in the periodic table.

$$f_{(\sin \theta/\lambda)} = \sum_{i=1}^{4} a_i \exp[-b_i(\sin \theta/\lambda)^2] + c \qquad (1.2)$$

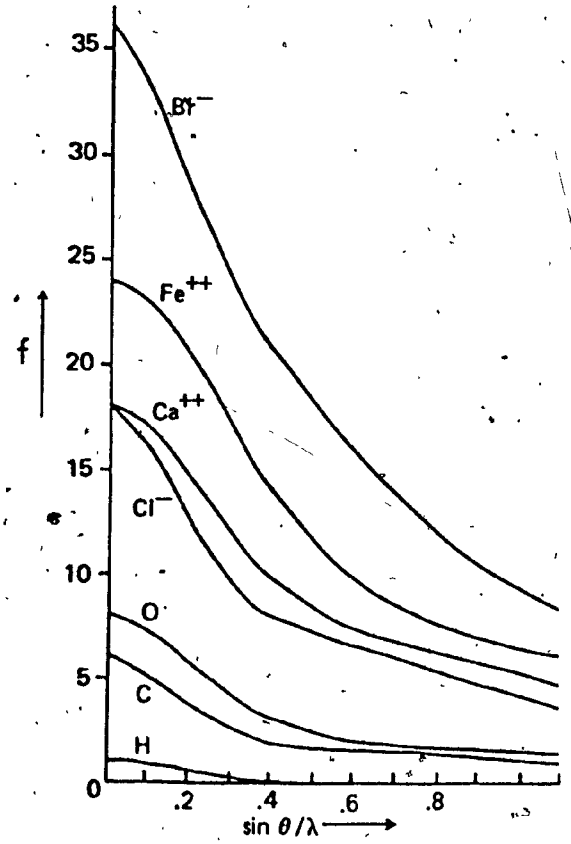

Figure 1.3

The amplitude of scattering from an atom is affected by the thermal motion of the atom. If each atom in a structure vibrates in an isotropic manner, then temperature factor correction for the j^{th} atom can be expressed as,

$$T_{j,\theta} = \exp[-B_j(\sin^2 \theta/\lambda^2)] \qquad (1.3)$$

$$B_j = 8\pi^2 U_j^2 \qquad (1.4)$$

where U_j is the mean square amplitude vibration of the atom from its equilibrium position in a direction normal to the reflecting plane. This is a function of temperature.

The temperature corrected scattering factor could be expressed as,

$$g_j = f_{j,\theta} \cdot T_{j,\theta} \qquad (1.5)$$

If the atoms of a structure have preferred vibrations in certain directions, a more accurate description of the thermal motion of an atom may be needed. The usual correction, which describes an ellipsoid of root mean square displacements, can be expressed as,

$$T_{j,\theta} = \exp[-2\pi^2(U_{11}h^2a^{*2}+U_{22}k^2b^{*2}+U_{33}l^2c^{*2}+2U_{12}hka^*b^* + 2U_{13}hla^*c^*+2U_{23}klb^*c^*)] \qquad (1.6)$$

where a^*, b^* and c^* are reciprocal lattice constants and U_{jk}'s are anisotropic thermal parameters.

So far, the scattering factors for elements have been considered real, but if the absorption edge of an element is close to the incident X-ray wave length, then the scattering process shows an unusual behaviour. This is caused by an anomalous phase-shift of the scattered wave. This effect is known as anomalous dispersion, and is usually significant only for those elements of the scattering material having an atomic number close to that of the target material of the X-ray tube. When an anomalous scatterer is

present the scattering factor takes the form given by equation 1.7.

$$f_A = f + \Delta f' + i\,\Delta f'' \qquad (1.7)$$

The values of $\Delta f'$ and $\Delta f''$ have been tabulated in the International Tables for X-ray Crystallography [19]. When an anomalous scatterer is present Friedel's law no longer holds (see section 1.1.6).

1.1.5 The Structure Factor [20]

The structure factor F(hkl) of a particular reflection expresses the combined scattering of all atoms in the unit cell compared to that of a single electron. For N atoms present in the unit cell, the structure factor for a reflection hkl, can be written as,

$$F(hkl) = \sum_{j=1}^{N} g_j \exp(2\Pi i \alpha_j) \qquad (1.8)$$

where $\alpha_j = (hx_j + ky_j + lz_j)$ and (x_j, y_j, z_j) are the fractional coordinates of the j^{th} atom.

Being a complex quantity, the structure factor could be broken down to its real and imaginary parts as,

$$F(hkl) = A(hkl) + i\,B(hkl) \qquad (1.9)$$

where

$$A(hkl) = \sum_{j=1}^{N} g_j \cos 2\pi(hx_j+ky_j+lz_j) \qquad (1.10)$$

$$B(hkl) = \sum_{j=1}^{N} g_j \sin 2\pi(hx_j+ky_j+lz_j) \qquad (1.11)$$

The amplitude of the structure factor F(hkl) is given by $|F(hkl)|$ and could be expressed as,

$$|F(hkl)| = \sqrt{\{A^2(hkl) + B^2(hkl)\}} \qquad (1.12)$$

Further, the structure factor can also be written as,

$$F(hkl) = |F(hkl)| \exp(i\phi) \qquad (1.13)$$

where $\tan \phi = B/A$, and ϕ is known as the phase angle.

1.1.6 Intensity-Structure Factor Relationship [21]

The most important quantity that is measured in an X-ray diffraction experiment is the relative intensity of a reflection hkl. The observed intensity, $I_o(hkl)$ of a reflection hkl is related to the observed structure factor modulus by,

$$I_o(hkl) \propto |F_o(hkl)|^2 \qquad (1.14)$$

or

$$I_o(hkl) = K^2 c(hkl) |F_o(hkl)|^2 \qquad (1.15)$$

The factor K is a scale factor associated with $|F_o(hkl)|$. C(hkl) combines several geometric and physical factors which depend upon both hkl and the actual experimental conditions, especially Lorentz, polarization and absorption corrections. These will be discussed in the sections 1.1.8 and 1.1.9.

Equation 1.15 forms the basis of X-ray structure analysis. The experimentally measured intensities, $I_o(hkl)$s are related to the structure through the structure factor modulus $|F_o(hkl)|$.

The structure factor given in (1.9) can be represented in an Argand diagram as shown in figure 1.4. It can be shown that for reflections hkl and its centrosymmetrically related partner $\bar{h}\bar{k}\bar{l}$,

$$|F(hkl)| = |F(\bar{h}\bar{k}\bar{l})|$$

which means

$$I_o(hkl) = I_o(\bar{h}\bar{k}\bar{l})$$

This is Friedel's law. The recorded diffraction pattern will appear centrosymmetric even though the structure itself may not possess a centre of symmetry. Deviations from Friedel's law occur when an anomalous scatterer is present in the structure.

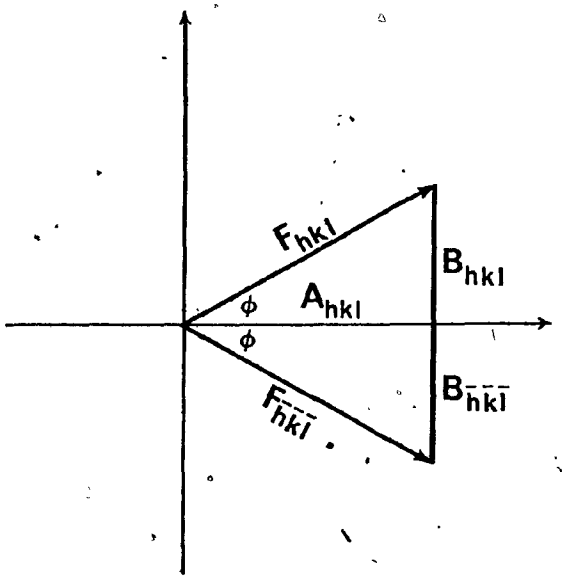

Figure 1.4

1.1.7 Absolute Scale Factor and Overall Thermal Parameter

In any structure analysis, it is necessary to calculate structure factors for a trial structure for comparison with the experimental data. To do this successfully, an overall temperature factor for the atomic scattering factors, and a scale factor for F_o are necessary. These can be derived approximately by Wilson's method [22]. For a unit cell containing a random distribution of N identical atoms, the local average value of $|F(hkl)|^2$ is given by,

$$\overline{\left|F(hkl)\right|^2} \simeq \sum g_j^2(hkl) \qquad (1.16)$$

This approximation holds satisfactorily only if the $\left|F(hkl)\right|$ are averaged over small ranges of $(\sin\theta)/\lambda$.

If an overall isotropic temperature factor B for all atoms and a scale factor K for the experimental $\left|F_o(hkl)\right|$ are assumed, then:

$$K^2\overline{\left|F_o(hkl)\right|^2} = \exp[-2B(\sin^2\theta_r)/\lambda^2]\sum f_{j,\theta_r}^2 \qquad (1.17)$$

where θ_r is a representative value of θ for each range of $(\sin\theta)/\lambda$. Rearranging and taking logarithms,

$$\ln q_r = 2 \ln K + 2B(\sin^2\theta_r)/\lambda^2 \qquad (1.18)$$

where q_r is given by

$$q_r = \left(\sum f_{j,\theta_r}^2\right) \Big/ \overline{\left|F_o(hkl)\right|^2_{\theta_r}} \qquad (1.19)$$

If $\ln q_r$ is plotted against $(\sin^2\theta)/\lambda^2$, and the best straight line is drawn, the slope is equal to 2B and the intercept is equal to 2 ln K.

1.1.8 Lorentz and Polarization Correction [23-24]

This correction, usually abreviated as the Lp-correction, consists of the Lorentz correction L and a polarization correction p. The partial polarization of the unpolarized primary beam, which occurs in the diffraction process is taken account of by p, which depends only on the diffraction angle 2θ, and can be expressed analytically as:

$$p = \frac{1 + \cos^2 2\theta}{2} \qquad (1.20)$$

If a crystal monochromator is used to monochromatize the X-ray beam further polarization occurs at this crystal and p becomes more complicated and can be expressed as,

$$p = \frac{(\cos^2 2\theta_m + \cos^2 2\theta_s)}{(\cos^2 2\theta_m + 1)} \qquad (1.21)$$

where $2\theta_m$ and $2\theta_s$ are the diffraction angles at the monochromator and the sample crystal, respectively.

The Lorentz factor, L, arises because the time required for a reciprocal lattice point to pass through the sphere of reflection is not constant; it is different for different 2θ values. For the 2θ or ω scanning techniques, this can be expressed as,

$$L = \frac{1}{\sin 2\theta} \qquad (1.22)$$

The combined Lorentz-polarization correction Lp is thus expressed as,

$$Lp = \frac{(\cos^2 2\theta_m + \cos^2 2\theta_s)}{\sin 2\theta_s(\cos^2 2\theta_m + 1)} \qquad (1.23)$$

1.1.9 Absorption Correction [15]

X-rays are attenuated when passing through matter. If an X-ray beam of primary intensity I_o passes a sample of homogeneous material of thickness dx, the loss dI at the element dx is proportional to I_o and dx,

$$dI = -\mu I_o dx \qquad (1.24)$$

By integration,

$$I = I_o \exp(-\mu x) \qquad (1.25)$$

where μ is the linear absorption coefficient of the material. Absorption is an additive atomic property of matter, which is nearly independent of the physical or chemical state of the constituent atoms under consideration. Mass absorption coefficient μ_m is defined as $\mu_m = \frac{\mu}{\rho}$ where ρ = density of the material.

The linear absorption coefficient, μ, for a crystal can be calculated from the expression given by the equation 1.26.

$$\mu = \rho \sum x_i \left(\frac{\mu}{\rho}\right)_i \qquad (1.26)$$

where x_i is the weight fraction of the element i. The mass absorption coefficient, $\left(\frac{\mu}{\rho}\right)_i$, for all the elements for different X-ray wave lengths are tabulated in the International Tables for X-ray Crystallography [19].

Several methods for the application of absorption corrections are available [25]. They are all based on the calculation of path lengths through the crystal, which vary from reflection to reflection. Precise measurement of crystal dimensions under a microscope is necessary for making a successful absorption correction.

1.1.10 Electron Density [26-29]

It was mentioned earlier that the electrons in a crystal are responsible for the scattering of X-rays. The structure factor can also be written in terms of electron density. This is given by,

$$F(hkl) = \int_0^a \int_0^b \int_0^c \rho(xyz) \exp[2\pi i(hx + ky + lz_j)]dxdydz \qquad (1.27)$$

In as much as the electron density $\rho(xyz)$ is a function with periodicity of the lattice, it can be written as a Fourier series,

$$\rho(xyz) = \frac{1}{V_c} \sum_{hkl} F(hkl) \exp[-2\pi i(hx+ky+lz)] \qquad (1.28)$$

Here V_c is the unit cell volume.

Since

$$F(hkl) = \left|F(hkl)\right| \exp[-2\pi i(hx_j+ky_j+lz_j)] \qquad (1.29)$$

$\rho(xyz)$ could be written as

$$\rho(xyz) = \frac{1}{V_c} \sum_{hkl} \left|F(hkl)\right| \exp(i\phi_{hkl}) \exp[-2\pi i(hx+ky+lz)] \qquad (1.30)$$

or

$$\rho(xyz) = \frac{1}{V_c} \sum_{hkl} \left|F(hkl)\right| \cos[2\pi(hx+ky+lz) - \phi(hkl)] \qquad (1.31)$$

Since $\left|F(hkl)\right|$ can be obtained from intensity data, if $\phi(hkl)$ is known, the electron density at any point could be calculated according to equation 1.30.

1.1.11 The Phase Problem

The determination of a crystal structure cannot proceed directly from the observed intensity data. The structure analysis is hampered fundamentally by the inability to determine, by an X-ray diffraction experiment, the complete vectorial structure factor. The structure factor modulus $|F(hkl)|$ can be obtained from the intensity data, but the corresponding phase angle $\phi(hkl)$ is not directly measurable. To determine the structure completely, it is necessary to determine both the amplitude and the phase angle. The method of obtaining the phase angle is the central problem in X-ray structure analysis. There are two basic ways to overcome this problem,

by (i) the heavy atom method, and by

(ii) "direct" methods.

These will be discussed in the sections 1.1.12 and 1.1.13.

1.1.12 The Heavy Atom Method

The heavy atom method or the Patterson method was first introduced by A.L.Patterson in 1935 [30-31]. A Fourier series, analogous to equation 1.28, in which the coefficients F(hkl) are replaced by $|F(hkl)|^2$ can be written as,

$$P(UVW) = \frac{1}{V_c} \sum_{hkl} |F(hkl)|^2 \exp[-2\pi i(hU+kV+lW)] \quad (1.32)$$

or

$$P(UVW) = \frac{1}{V_c} \sum_{hkl} |F(hkl)|^2 \cos 2\pi(hU+kV+lW) \quad (1.35)$$

The above summation is directly derivable from the primary experimental quantities, that is, the angular positions and intensities of the diffracted beam. The Patterson function P(UVW) at each point UVW of a three-dimensional grid of the size and shape of the unit cell can be evaluated.

The Patterson function P(UVW) will be non zero at the point UVW only when there exists points xyz such that $\rho(xyz)$ and $\rho(x+U, y+V, z+W)$ are both non zero. The Patterson function will reach maximum values at points UVW which correspond to the coordinates of vectors between pairs of atoms. The Patterson function gives a map of the vectors between the atoms. If a unit cell contains N atoms, there will be N^2 interatomic vectors. Out of this, N vectors lie in the origin, so there will be $N^2 - N$ peaks other than the origin peak.

The relative intensity of a Patterson peak resulting from the vectors between two atoms of atomic number Z_1 and Z_2 is $Z_1 Z_2 / \sum Z_i$. This means that, if there is a heavy atom present in the structure then the intensity of this peak will be significantly larger than the other peaks (except

for the origin peak). The location of this atom in the unit cell can be determined.

1.1.13 The Direct Methods of Phase Determination [32-35]

The principles of direct methods are based on the fact that the experimentally obtained $|F(hkl)|$ already contain information about the phases of the structure factors. This was first pointed out by Harker and Kasper in 1948 [36]. The technique involved is to determine a set of phases by probabilistic calculations.

1.1.14 E-Values

The initial stage is to convert $|F(hkl)|$ to the corresponding normalized structure factor $|E(hkl)|$ according to

$$|E(hkl)|^2 = \frac{K^2 |F_o(hkl)|^2}{\epsilon \sum_{j=1}^{N} g_j^2} \qquad (1.33)$$

where K is the scale factor, g(j) is the temperature corrected scattering factor of the j^{th} atom.

ϵ is an integer which depends upon the crystal system and the reflection parity group.

1.1.15 Σ_2-relationships

If three reflections $\vec{h}_1$, $\vec{h}_2$ and $\vec{h}_3$ satisfy the equation $\vec{h}_1 + \vec{h}_2 + \vec{h}_3 = 0$, then these reflections are said to be related by a Σ_2 -relation. These Σ_2-relations play an important role in direct methods. Once E values are calculated, the next step is to find as many Σ_2-relationships as possible.

1.1.16 Origin Definition

Applications of direct methods requires a set of reflections with known phases. A set of up to three known phases can be obtained by the definition of the origin. The origin of a unit cell is chosen to be in a special position relative to the symmetry elements. In the case of a centrosymmetric cell, the origin must always coincide with the inversion centre. In every centric unit cell inversion centres are present in eight possible positions, (0 0 0), (1/2 0 0), (0 1/2 0), (0 0 1/2), (1/2 1/2 0), (1/2 0 1/2), (0 1/2 1/2) and (1/2 1/2 1/2). These eight centres of symmetry are not identical. For origin definition purposes, the reflections are categorized in to eight parity groups, eee oee, eoe, eeo, ooe, oeo, eoo and ooo where o = odd and e = even. A set of up to three reflections are chosen so that no reflection or combination of two or three reflections add to give an eee combination. Arbitary phases

are assigned to these reflections.

1.1.17 Convergence Mapping

The aim of convergence mapping is to determine the 'best' reflections for origin and enantiomorph definition. Such a starting set could be found by using the probabilistic quantities defined by Karle and Karle [37]. A quantity α_h is defined as,

$$\alpha_h^2 = \left[\sum K_{hh'} \cos(\phi_{h'}+\phi_{h-h'})\right]^2 + \left[\sum K_{hh'} \sin(\phi_h+\phi_{h-h'})\right]^2 \quad (1.34)$$

where

$$K_{hh'} = \frac{2\sigma_3}{\sigma_2^{2/3}} \left| E_h . E_{h'} . E_{h-h'} \right| \quad (1.36)$$

and $\sigma_k = \sum_{j=1}^{N} n_j^k$ and $n_j = \frac{f_j}{\sum_{j=1}^{N} f_j}$.

The quantity K_{hh} is a measure of the reliability with which the phase ϕ_h may be determined using the tangent formula [38-39]; see section 1.1.18.

In the absence of any phase information as in the case of the beginning of the structure determination, a quantity

α_E, the expectation value of α_h is defined as [40],

$$\alpha_E^2 = \sum K_{hh'}^2 + 2\sum\sum K_{hh'} K_{hh''} \left[\frac{I_1(K_{hh'})\ I_1(K_{hh''})}{I_0(K_{hh'})\ I_0(K_{hh''})} \right] \quad (1.37)$$

where I_0 and I_1 are modified Bessel functions of the zero and first orders respectively. For computational purposes the following polynomial in the range $0 < K < 6$ can be used.

$$I_1(K)/I_0(K) \simeq 0.5658K - 0.1304K^2 + 0.0106K^3 \quad (1.38)$$

The value α_E for all the reflections with greater than E_{min} is estimated. The reflection with smallest α_E is eliminated from the data set, along with all the phase relationships in which this reflection is involved. The process is repeated, the worst reflection being eliminated at each stage, the remaining group of reflections are linked together with much better phase relationships. As each reflection is eliminated, those remaining are examined to ensure they contain all the necessory reflections for origin definition. If the reflection just eliminated is the last of a certain parity group which is necessary for origin fixing, then this reflection is reinserted and becomes one of the origin fixing reflections. All the reflections necessary for the origin definition are selected at the end

of convergence.

1.1.18 Sign Determination Formulae

The sign s(hkl) of a reflection hkl is $F(hkl)/|F(hkl)|$. For a centrosymmetric space group, s(hkl) could takeup only two possible values, +1 or -1.

For sufficiently large E(hkl) values, which are related by Σ_2-relationship,

$$s(h) = s(h').s(h-h') \tag{1.39}$$

if $-h=h_1$, $h'=h_2$ and $h-h'=h_3$ then

$$s(h_1) = s(h_2).s(h_3) \tag{1.40}$$

The probability, P, that equation 1.40 holds can be expressed as [41-42]

$$P = \frac{1}{2} + \frac{1}{2}\tanh\left[\frac{\sigma_3}{\sigma_2^{3/2}}\left|E(h_1)E(h_2)E(h_3)\right|\right] \tag{1.41}$$

For a structure containing N atoms of equal type the equation 1.41 will reduce to

$$P = \frac{1}{2} + \frac{1}{2}\tanh\left[\frac{1}{\sqrt{N}}\left|E(h_1)E(h_2)E(h_3)\right|\right] \tag{1.42}$$

If the unknown reflection is involved in more than one Σ_2-relation, then,

$$s(h) = \sum s(h').s(h-h') \qquad (1.43)$$

is a better approximation than equation 1.39. The probability P that equation 1.43 holds is given by,

$$P = \frac{1}{2} + \frac{1}{2}\tanh\left[\frac{\sigma_3}{\sigma_2^{3/2}}\left|E(h)\right|\sum E(h')E(h-h')\right] \qquad (1.44)$$

Equation 1.43 is a special case of the Sayre's [35] equation applicable to centrosymmetric crystal classes.

$$E(h) = T\sum E(h').E(h-h') \qquad (1.45)$$

The tangent formula derived by Karle and Hauptman in 1956 [39] is applicable to acentric crystal classes as well. A weighted tangent formula proposed by Germain, Main and Woolfson in 1971 [43] can be written as

$$\tan\phi_h \approx \frac{\sum_{h'} w_{h'} w_{h-h'} \left|E_{h'} E_{h-h'}\right| \sin(\phi_{h'} + \phi_{h-h'})}{\sum_{h'} w_{h'} w_{h-h'} \left|E_{h'} E_{h-h'}\right| \cos(\phi_{h'} + \phi_{h-h'})} = \frac{T_h}{B_h} \qquad (1.46)$$

where w_h is the weight associated with the phase angle ϕ_h. Each weight is computed from,

$$w_h = \tanh\left(\tfrac{1}{2}\alpha_h\right) . \qquad (1.47)$$

$$\alpha_h = |E_h|\sqrt{(T_h^2 + B_h^2)} \qquad (1.48)$$

The process of phase determination by application of equations 1.43 or 1.46 are in principle the same. Σ_2-relations have to be found and if the phases of two reflections are known, this relation can be used as input to equations 1.43 or 1.46 to determine the third.

1.1.19 The Refinement of Structure [21,44]

The positional parameters found for the atoms are used to create a model of the contents of the unit cell. The accuracy of this model can be determined by calculating structure factors $F_c(hkl)$ based on this model and comparing them to those observed $F_o(hkl)$. A quantitative measure of the agreement between $F_o(hkl)$ and $F_c(hkl)$ is given by the discrepancy index, R:

$$R = \left[\frac{\sum || F_o |_{hkl} - | F_c |_{hkl}|}{\sum | F_o |_{hkl}}\right] \qquad (1.49)$$

where the summation is over all the reflections.

Initially only few atomic positions are known. For example if the structure contains a heavy atom, position of this might be the only known position in the unit cell. An extremly valuable approach to find the other constituent atoms in the unit cell lies in the Δ F or difference Fourier synthesis. This can be expressed as,

$$\Delta\rho(xyz) = \frac{1}{V_c}\sum\left(|F_o| - |F_c|\right)\exp(i\phi_c) \exp[-2\pi i(hx + ky + lz)] \qquad (1.50)$$

where ϕ_c is the calculated phase angle based on the few known atomic positions of the unit cell. Missing atoms, which are not included in the above summation will appear as peaks in a three-dimensional map drawn at different points, xyz. Once a new atom has been found, the position of its maximum density can be picked off either by inspection or by a more accurate curve fitting method.

The positional and thermal parameters obtained by difference Fourier or Fourier techniques have to be refined in order to get a better set of values. This can be done by the method of least-squares.

The function minimized in the least-squares refinement is represented in equation 1.51.

$$D = \sum w_{hkl}\left(|F_o| - |k F_c|\right)^2 \qquad (1.51)$$

where k is the scale factor and w_{hkl} is defined as,

$$w_{hkl} = \frac{1}{\sigma^2} \tag{1.52}$$

The derivative of the above expression (equation 1.51) with respect to each parameter is set to zero, equation 1.53. The normal equations are expanded by a Taylor series and all but the linear terms are neglected.

$$\sum w_{hkl}\left(|F_o| - |kF_c(p_1, p_2, \ldots p_n)|\right)\frac{\partial |kF_c(p_1 \ldots p_n)|}{\partial p_j} = 0 \tag{1.53}$$

$$\begin{pmatrix} a_{11} & a_{12} & \ldots\ldots a_{1n} \\ a_{21} & a_{22} & \ldots\ldots a_{2n} \\ \vdots & & \\ a_{n1} & a_{n2} & \ldots\ldots a_{nn} \end{pmatrix} \begin{pmatrix} x_1 \\ x_2 \\ \vdots \\ x_n \end{pmatrix} = \begin{pmatrix} v_1 \\ v_2 \\ \vdots \\ v_n \end{pmatrix} \tag{1.54}$$

where

$$a_{ij} = \sum w_r \frac{\partial |F_c|_{hkl}}{\partial p_i} \cdot \frac{\partial |F_c|_{hkl}}{\partial p_j} \tag{1.55}$$

$$x_j = \Delta p_j \tag{1.56}$$

$$V_i = \sum w_r(\Delta F_{hkl}) \frac{\partial |F_c|_{hkl}}{\partial P_i} \qquad (1.57)$$

The set of normal equations given in equation 1.53 can be written in a more compact form as,

$$Ax = V$$

If the normal equations given above have a solution, then, an inverse matrix, A^{-1}, exists such that,

$$A^{-1}A = E$$

where E is the unit matrix. Then,

$$A^{-1}Ax = A^{-1}V$$

$$x = A^{-1}V \qquad (1.58)$$

The x's are the shifts in the refined parameters which are added to the p_is to obtain new parameters.

The estimated standard deviation of parameter p_i, σ_{p_i}, was computed according to the equation 1.59.

$$\sigma_{p_i} = \sqrt{b_{ii}\left(\sum w_{hkl}\Delta F_{hkl}^2\right) \Big/ (m-n)} \qquad (1.59)$$

where b_{ii} is the i^{th} diagonal element of the inverse

matrix A^{-1}, w(hkl) is the weight of the reflection hkl and $\Delta F(hkl)$ is given by the equation 1.60,

$$\Delta F_{hkl} = \left(|F_o|_{hkl} - |F_c|_{hkl} \right) \qquad (1.60)$$

and m is the number of observations (reflections greater than 3σ usually) and n is the number of parameters.

A least-squares refinement involves an extensive calculation. For this, a large computer storage facility and a fair amount of computer time is necessary. To cut down the computer time and memory requirements, some approximations may have to be made.

In the matrix given in equation 1.54, the diagonal elements a_{ii}'s are always sums of squares, whereas the off diagonal elements are sums of products which may be either positive or negative. It is reasonable to assume that the off diagonal elements are smaller than the diagonal elements. If the off-diagonal elements are neglected, only the diagonal elements are needed to be calculated. Such an approximation is known as diagonal-least-squares approximation. But, if the parameters are correlated in some way, the contributing terms will not cancel out in a random fashion. The elements could have a large negative or positive value. An alternative method to the diagonal-least-squares approximation is the block-diagonal

least-squares approximation. A block-diagonal matrix is shown in figure 1.5. Non-zero elements are divided in to blocks along the principal diagonal. Each atom is described by a single block. The blocks shown in figure 1.5 are 4 X 4, three positional parameters and one thermal parameter. In the case of anisotropic refinement, each atom occupies a 9 X 9 block. All the other elements of the matrix are neglected.

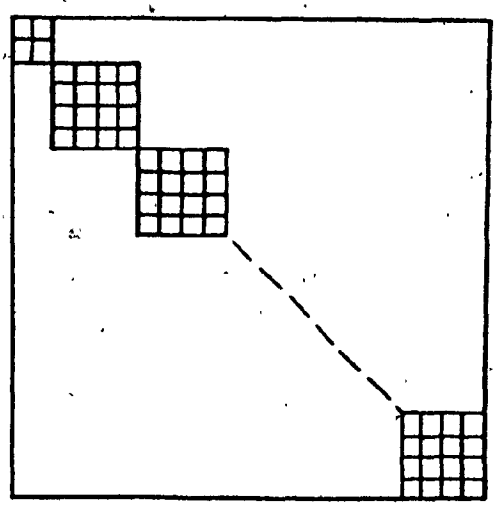

Figure 1.5

1.2 EXPERIMENTAL-GENERAL CRYSTALLOGRAPHY

1.2.1 Crystal Mounting

A suitable crystal was chosen under a low powered microscope. This was affixed to a borosilicate glass fibre using fast drying epoxy glue. The fibre was then fixed to a flexible copper wire attached to a brass pin. This was then mounted on a goniometer head, figure 1.6.

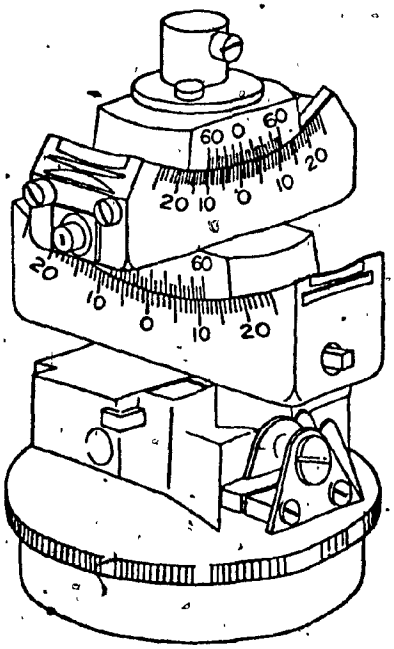

Figure 1.6

1.2.2 Weissenberg and Rotation Photography [45-47]

The goniometer was set on the Weissenberg camera. Rotation photographs taken in two mutually perpendicular directions with 10° rotations were used to align the crystal.

The Weissenberg and rotation photographs were obtained on a Charles Supper Co. Weissenberg camera. Both the Weissenberg and the precession camera were operated using Zr filtered, molybdenum X-ray tube. The tube was powered by a Picker Nuclear model 809B X-ray generator. Kodak 'No Screen' film was used during the course of the photographic study.

Weissenberg photographs provide a distorted record of a reciprocal lattice plane. The camera has been designed so that 1 mm in 2θ direction on the film is equal to 2° in 2θ and 1 mm in sideways motion corresponds to a 2° rotation of ϕ. Figure 1.7 is a schematic representation of a Weissenberg camera.

1.2.3 Precession Photography [48]

Precession photographs provide a undistorted record of a reciprocal lattice plane.

In the precession camera, a crystal axis makes a constant angle with the X-ray beam. The crystal axis precesses so as to maintain this angle. During this process, various planes successively pass through reflecting position. A schematic representation of a precession camera is shown in figure 1.8.

1.2.4 Space Group Determination

By examining the symmetry information and systematic absences present in both Weissenberg and precession photographs, the possible space groups could be narrowed down to a few possibilities. In certain cases, such as space group $P2_1/c$ the systematic absences uniquely establish the space group.

1.2.5 Data Collection

This section of the thesis deals with the collection of relative intensity data.

Except in the case of $[Cr(terpy)_2](ClO_4)_3.H_2O$, the intensity measurements were made on a fully automated Picker Nuclear FACS-1, four circle diffractometer coupled to PDP-8A minicomputer. The data collection package DIFFRAC [49] supplied by the NRC of Canada was used. The data were collected using graphite monochromatized Mo K_α radiation. A

Picker-Nuclear constant potential diffraction generator, model 6238E, provided the power to the Philips Mo X-ray tube. The tube was operated at 40 kV and 30 mA. The take off angle was 3.0 degrees for the direct beam and this was monochromatized using the 002 face of a graphite monochromator "crystal".

The Mo K_α radiation was collimated by passing through a 1 mm diameter pinhole collimator directed at the sample. The intensity measurements were carried out using a scintillation counter. The scintillation counter was equipped with a 31/32" diameter 1/32" thick Tl activated NaI crystal with a 0.005" thick Be window, optically coupled to a XP-1010 Amperex photomultiplier tube. The detector was operated at about 1 kV, and a pulse height analyzer was set to receive 100% Mo K_α radiation.

Weissenberg angles were set on the goniometer head and it was mounted on the diffractometer. A strong reflection at a low 2θ angle was chosen from the zero level Weissenberg photograph. The 2θ angle of this reflection was set and ω, χ and ϕ circles were brought to zero. A ϕ scan was done manually until the chosen reflection was located.

Another reflection was located on the zero level by the same procedure and the angular values of these reflections were optimized by an alignment routine supplied with the

data collection package. These two reflections and the film measured approximate cell parameters were used to locate the third axis. Angular scans on each of the axes were done to ensure the proper orientation of the crystal. A third reflection was chosen and its angular values were optimized. The angular values of these three reflections were used to calculate an approximate orientation matrix.

About 15 reflections, widely separated in reciprocal space were chosen from zero and upper level Weissenberg and precession photographs. These and their Friedel equivalents were centered in the detector aperture. The slits in the receiving collimators were partly shut to ensure higher accuracy. The angular values thus obtained were used in a least-squares refinement to obtain an orientation matrix and final unit cell parameters with their estimated standard deviations. The orientation matrix was used in the subsequent data collection.

Several test scans were done with low and high angle reflections to establish a proper scan width. The values of minimum and maximum 2θ, scan rate and the time for back ground measurements were specified. Three standards were chosen and their intensities were measured. These standards were remeasured after every 50 reflections, to check the crystal and instrument stability.

Data were collected using θ-2θ scan technique with profile analysis mode [50]. Here, the reflection profile is accumulated at 0.01 degree intervals and the profile variations are minimized by 5-point smoothing. The reflection profile is examined to determine at what point the background is significantly flat. This point is taken to be the point at which the peak ends and the background begins. Backgrounds were measured at each end of the peak for 10% of the total scan time. Beyond 10^4 cps, pre calibrated attenuators made of Ni foil were automatically inserted. The data were recorded on a magnetic disk.

1.2.6 Data Reduction

Except in the case of $[Cr(terpy)_2](ClO_4)_3.H_2O$, all the computations were carried out on the PDP-8A minicomputer. Data reduction was accomplished using the NRC DATRD2 program [51]. The intensities were corrected for backgrounds according to the equation 1.61.

$$I = N - (B_l + B_h).\frac{t_s}{2t_b} \qquad (1.61)$$

where, N is the peak count in the scan time t_s, B_h and B_l are the background counts on eithe side of the peak, each measured for t_b seconds; t_b was usually taken as $t_s/10$. The standard deviation of a reflection was computed according to equation 1.62.

$$\sigma(I) = [N + (B_h + B_l)(t_s/t_b)^2 + (pN)^2] \qquad (1.62)$$

where p is an ignorance factor, usually given a value 0.01 or 0.02. A reflection was considered as unobserved if the intensity, I computed was less than zero or less than $3\sigma(I)$.

The intensities were corrected for Lorentz and polarization effects but not for absorption. An approximate scale factor and an overall thermal parameter was obtained by means of a Wilson plot [22].

1.2.7 Structure Solution

The structure solution was accomplished either by heavy atom method or by direct method. The Patterson synthesis was carried out using the NRC program FOURR [52] and MULTAN [53] was used in the case of direct methods. Scattering factors and the anomalous dispersion correction terms were taken from the International Tables for X-ray Crystallography, Vol.IV [54].

Observed and difference Fourier maps were calculated using the NRC program FOURR. Structure factor calculations and least-squares refinement were accomplished using the NRC program LSTSQ [55].

The goodness of fit is defined according to the equation 1.63. The unweighted and weighted descrepancy indices were computed using the equations 1.64 and 1.65 respectively.

$$GOF = \left[\sum w_{hkl} \Delta F^2_{hkl}\right] / (m-n) \qquad (1.63)$$

$$R = \frac{\sum \left| \left| F_o \right|_{hkl} - \left| F_c \right|_{hkl} \right|}{\sum \left| F_o \right|_{hkl}} \qquad (1.64)$$

$$R_w = \left[\frac{\sum w_{hkl} \left\{ \left| F_o \right|_{hkl} - \left| F_c \right|_{hkl} \right\}^2}{\sum w_{hkl} \left\{ \left| F_o \right|_{hkl} \right\}^2} \right]^{\frac{1}{2}} \qquad (1.65)$$

1.2.8 Interpretative Programs

The NRC package DISPOW [56] was used to compute the various interatomic distances and to calculate bond angles. The program first converts the positional parameters to orthogonal coordinates, and the bond lengths, and angles were computed using standard techniques. "Ortep" by Johnson [57] was used to prepare plots. This program was run on

Concordia University, Control Data Cyber 170 computer, interfaced with a HP 1000 minicomputer. Plots were made on a Complot X-Y plotter.

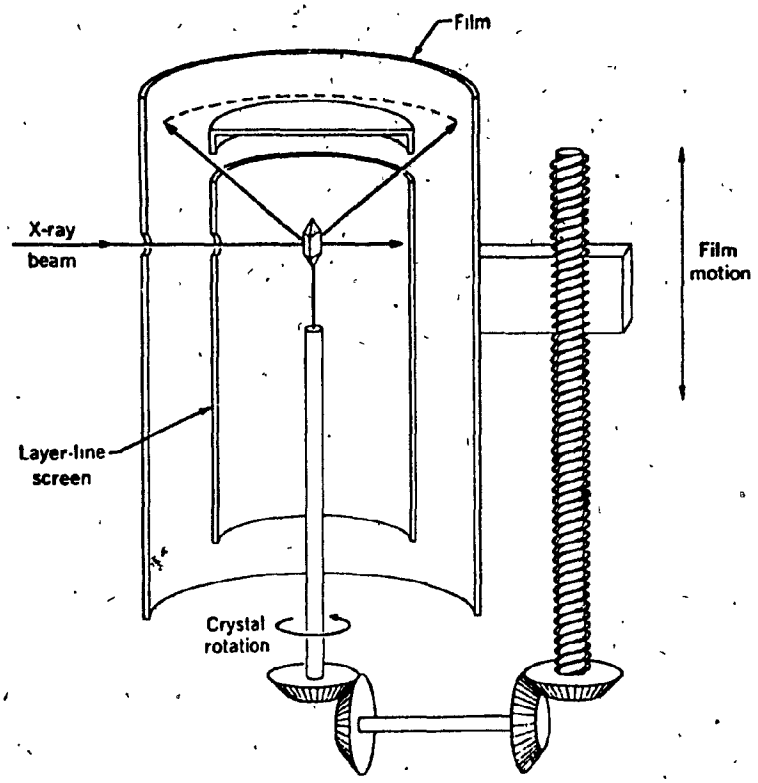

Figure 1.7. A schematic representation of a Weissenberg camera [27]

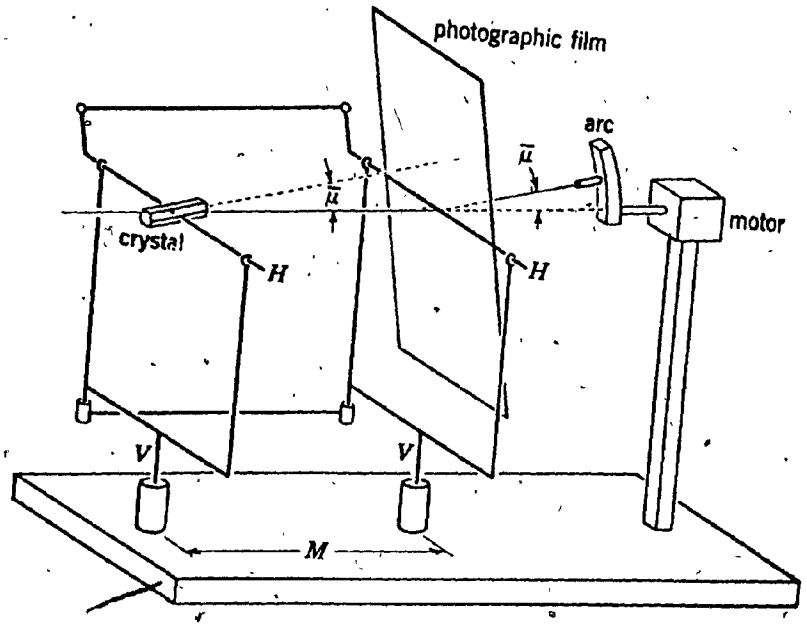

Figure 1.8. A schematic representation of a precession camera [15]

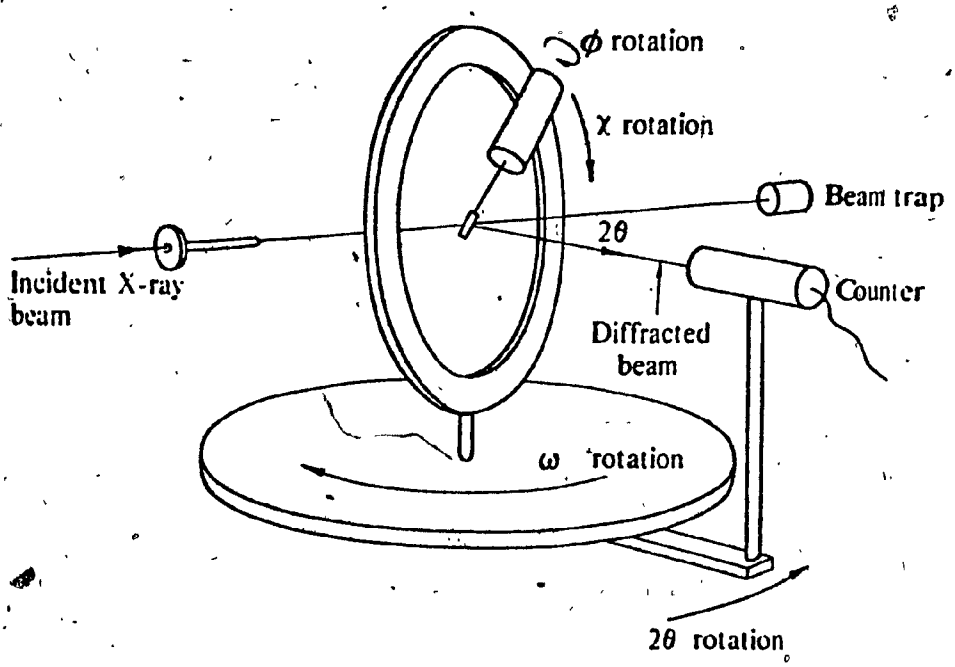

Figure 1.9. A schematic representation of a four-circle diffractometer [27]

2.1 INTRODUCTION-POLYPYRIDYL COMPLEXES

Complexes derived from 2,2'-bipyridine(I), 2,2',2''-terpyridine(II), 1,10-phenanthroline(III) and their substituted derivatives are known as polypyridyl complexes.

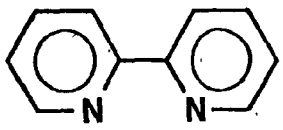

I

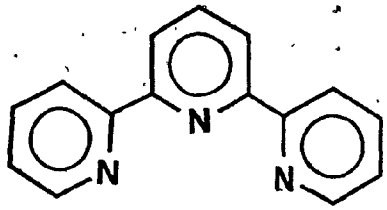

II

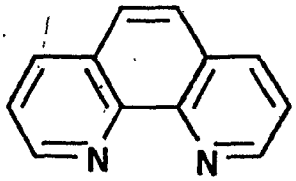

III

Polypyridyl complexes of Ru(II), Os(II), Ir(III) and Cr(III) have been extensively studied for their photochemical

behaviour [58-62].

The electronic excited states of molecules can be obtained by irradiating with visible or U.V radiation. Reactions of the molecules in their excited states are called photochemical reactions. One of the most important consequences of electronic excitation is that of increasing the electronic affinity, and decreasing the ionization potential of a molecule. This means that an electronically excited state is a better oxidant and a better reductant with respect to its ground state. If the lifetime of the excited state is sufficiently long, the excited molecule can engage in bimolecular electron and energy transfer reactions.

Recent investigations of the behaviour of the excited states of transition metal complexes have shown that they can engage in homogeneous electron and energy transfer in solution media [63-64], or heterogeneous electron transfer at semiconductor electrodes [61]. Such processes are viewed as having potential applicability in converting radiant energy to useful chemical or electrical energy.

Very often, to get a better understanding about the details of a reaction mechanism, it is necessary to know the exact molecular structure. Sometimes the structure itself can be a puzzle. If the compound under study can be

obtained as a crystalline solid, x-ray diffraction studies offer the best way of determining the molecular structure.

This section of the thesis describes the molecular structure of three polypyridyl complexes of Cr(III) and Ir(III), as determined by x-ray diffraction studies. They were

(1) $[Ir(bpy)_2(bpy')](ClO_4)_3.H_2O$

(2) $[Cr(terpy)_2](ClO_4)_3.H_2O$

(3) $[Cr(bpy)_2(H_2O)Cl](ClO_4)_2.2H_2O$

2.2 MOLECULAR STRUCTURE OF "$[Ir(bpy)_2(bpy')](ClO_4)_3 \cdot H_2O$"

2.2.1 Introduction

Tris bipyridyl complexes of d^6 transition metals, Fe(II), Ru(II), Os(II), Co(III) and Rh(III) have been known for some time, but the first successful isolation of a tris(bipyridine)Iridium(III) complex was reported only in 1974 by Flynn and Demas [65-66]. The tris(bipyridine) Iridium(III) ion had been previously reported to be the sole product of the reaction between $[IrCl_6]^{3-}$ and bypyridine [67]. The nature of this complex was later reexamined by DeSimone and Drago [68] and found to be cis-dichlorobis(bipyridine)Iridium(III). The carbon-13 NMR spectrum of the compound isolated by Flynn and Demas showed five well resolved peaks at -89.46, -83.77, -76.69, -63.34, and -60.05 ppm, relative to dioxane [66]. The five lines correspond to the five distinct carbon atoms of a D_3-symmetry tris complex. The proton NMR of the complex in DMSO-d_6 has two doublets, at 9.28 and 8.14, and two triplets, at 8.74 and 8.08 ppm, with respect to TMS. The spectrum strongly resembles the spectra of $[Os(bpy)_3]^{2+}$ and $[Fe(bpy)_3]^{2+}$ [68-69]. The emission spectra of the Ir(III) complex and $[Rh(bpy)_3]^{3+}$ [70] have virtually identical properties. Based on this spectroscopic evidence and elemental analysis, which has shown the Ir to bipyridine molar ratio to be 1:3, the complex has been identified as

$[Ir(bpy)_3]^{3+}$.

In 1977 Watts and co-workers [71] isolated another Iridium(III) compound with the molecular formula $[Ir(bpy)_2(bpy')H_2O]Cl_3$, which also contained three moles of bipyridine per mole of Iridium. Surprisingly, this compound has shown totally different spectroscopic and photophysical properties to a conventional tris chelated bipyridyl metal complex. The nature of this compound has been the subject of a controversy since then [71,72-74].

According to Watts and co-workers, the most likely alternatives to a tris complex are:

(1) a six coordinated Ir(III) bound to two chelating bipyridines, one monodentate bipyridine and water.

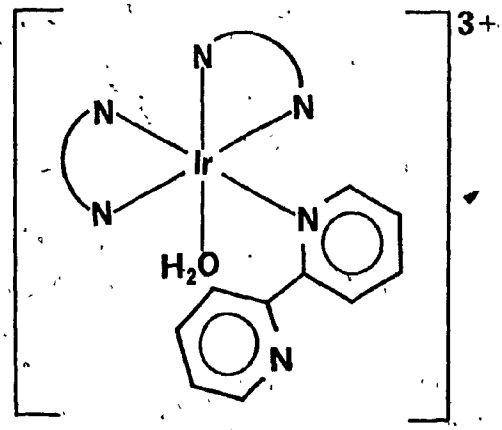

I

(2) a six coordinated Ir(III) bound to two bidentate bipyridines and one covalently hydrated bipyridine.

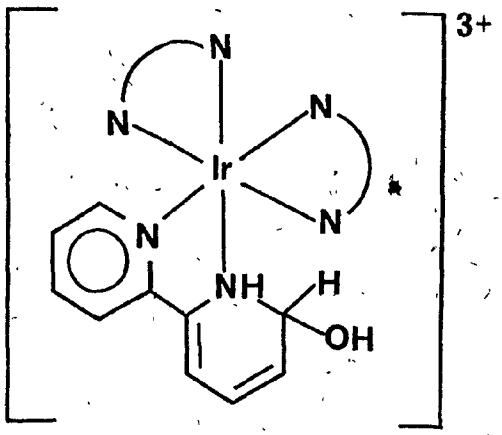

II

(3) a six coordinated Ir(III) bound to two bidentate bipyridines, one monodentate bipyridine and coordinated chloride,

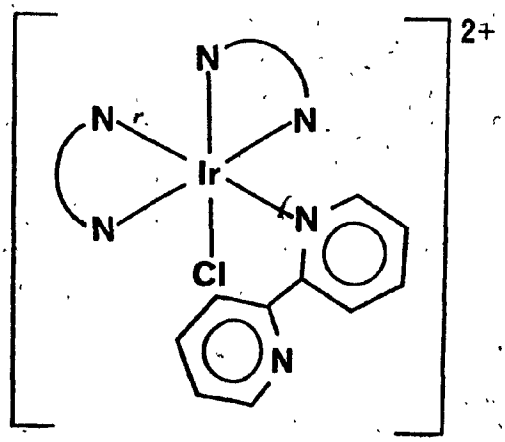

III

(4) a seven coordinated Ir(III) bound to three bidentate bipyridines and one water.

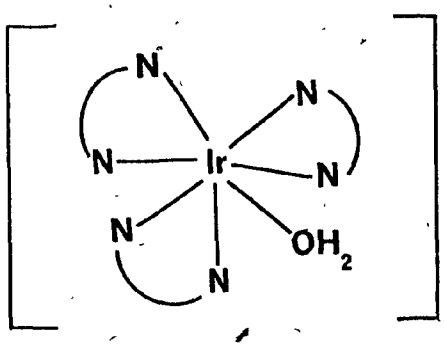

IV

A seven coordinated Ir(III) bound to three bidentate bipyridines and one chloride has been ruled out due to the absence of any acidic proton in the structure.

Ionic halide analysis have shown that non-ionic chlorides are not present in the structure, thus ruling out III.

The appearence of a N-H stretch in the infra-red spectrum at $\nu = 2650\ cm^{-1}$ of the acidic form of the complex is not consistent with all three bipyridines chelating to Ir(III). Hence the structure IV has been ruled out. This left the monodentate or covalently hydrated species as the possible candidates.

The ligands such as 1,2-diamino-ethane (V) form complexes in which they may behave either in a mono or bidentate fashion, but 2,2'-bipyridine always displays bidentate behaviour [75-77]. In reactions where dissociation of one or more bipyridines from a metal complex occur, the bipyridine ligand must be present as a unidentate ligand at least for a short period of time. A platinum complex of 1,10-phenanthroline, which is closely related to 2,2'-bipyridine, has been shown by X-ray structure analysis to contain a monodentate phenanthroline ligand [78]. However, such a complex is not known with bipyridine.

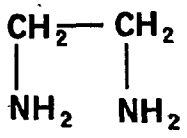

V

In a classical scheme proposed by Gillard [79] for the OH^- attack upon a tris(bipyridyl) complex, a covalently hydrated species has been considered as a common intermediate. This is given in the scheme 2.1.

It has been postulated that this covalently hydrated intermediate could undergo an intramolecular hydroxyl shift by protonation to give the conjugate acid. This is followed by an intra molecular shift of water from C(2) to metal or by deprotonation with hydroxide giving the conjugate base.

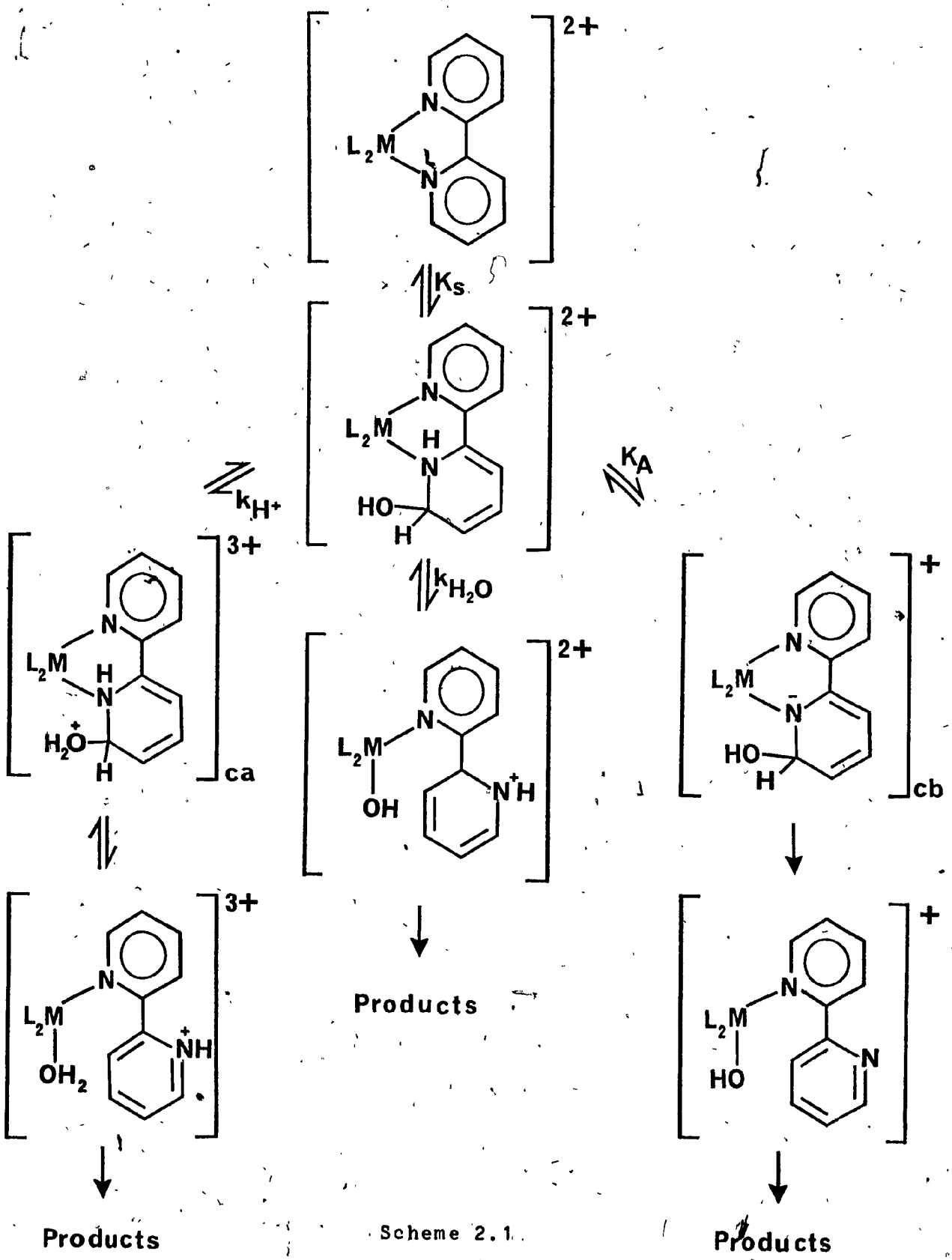

Scheme 2.1

The conjugate base then reacts by an intra molecular OH^- shift from C(2) to metal M.

Studying the dissociation of $[Fe(terpy)_2]^{3+}$ in aqueous sulphuric acid media, Gillard and co-workers observed that in the absence of water no dissociation occurs. They take this as evidence of covalent hydrate formation prior to the dissociation step [80]. In a recent communication [81] similar covalent hydrate formation has been proposed with $[Pt(py)_4Cl_2]^{2+}$ upon hydroxide attack.

Based on the above considerations, Watts and co-workers have chosen the species containing the monodentate bipyridyl ligand as the most probable structure (I). Their choice was reinforced on the basis of the observation that, when the complex is dissolved in aqueous acid and base different emission spectra are obtained, whereas when $[Ir(bpy)_3]^{3+}$ is dissolved in aqueous acid or base the same emission spectrum is observed. This latter spectrum is different to the former two. This compelled Watts and co-workers to believe that, in solution, there is no facile equilibrium between the tris complex and a covalently hydrated species.

The proton NMR spectrum of the title complex in DMSO-d_6 is reported in the literature [72]. This is considerably different from that of a conventional tris chelated metal complex of bipyridine possessing D_3-symmetry. It consists

of broad multiplets at 9.2, 8.4 and 7.8 ppm with respect to TMS. In addition, a doublet at 6.65 ppm and a doublet of doublets at 7.14 ppm have also been observed. The highest field signals observed for free bipyridine occur at 7.12 and 7.35 in CCl_4 and methanol respectively (for 5,5' H's).

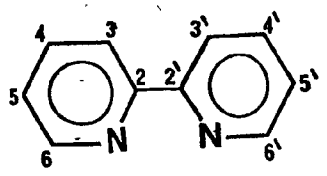

VI

The signal observed as a doublet at 6.65 ppm for the complex is at much higher field than for any other known bipyridyl complex of a metal ion, or that of free bipyridine. Gillard and co-workers [72] interpret this as evidence for the existence of a covalently hydrated species. They assign the 6.65 ppm doublet to the proton on the tetrahedral carbon of II. The appearance of the band at 2650 cm^{-1} in the infra-red spectrum of the complex has been taken as further evidence for the covalent hydrate formulation.

Interestingly, the PMR spectrum of the complex in DCl/D_2O differ greatly from that in DMSO-d_6 [73]. The high field multiplets are not present in acidified D_2O. As expected, the carbon-13 spectrum of the complex shows about 25 peaks in the range 120 - 160 ppm with respect to TMS [73,82]. Carbon-13 resonances for covalently hydrated

quinazolines and pteridines occur around 70 ppm down-field of TMS [83-84]. Since no resonance signals are visible in this region of the carbon-13 spectrum for an sp^3 carbon, Watts and co-workers reject the hypothesis of covalent hydrate formation. The solvent dependent nature of the PMR spectrum and the absence of any sp^3 hybridized carbon atom in the carbon-13 spectrum have been considered to be consistent with the presence of a monodentate bipyridyl fragment in the structure.

This controversial debate led to our solid state structure analysis by X-ray diffraction techniques [74].

2.2.2 Experimental

Preliminary Weissenberg and precession photographs indicated a primitive monoclinic crystal system with, on h0l, l odd absent, and on 0k0, k odd absent. These data uniquely established the space group as $P2_1/c$ (No. 14), with b as the unique axis. Accurate cell dimensions were obtained by centering 15 high angle reflections with $17 < 2\theta < 30$ (and their Friedel equivalents) in the detector aperture of the four-circle diffractometer.

A unique set of data were collected in the range $3.5 < 2\theta < 40.0$ for $\pm h, +k, +l$. The three standards monitored after every 50 reflections showed random variation not more than 2%. The scaled reflections were corrected for Lorentz and polarization effects. Of 3218 reflections collected, 2376 with $I > 3\sigma(I)$ were used in subsequent calculations.

The structure was solved by the heavy atom method and Fourier techniques. The Ir atom position was obtained by a three-dimensional sharpened Patterson map. The position thus obtained was refined by the full-matrix least-squares technique. Two cycles of refinement followed by a structure factor calculation reduced the R factor to 28%. A difference Fourier map phased using the Ir position revealed all the non-hydrogen atoms, except the oxygens of one of the perchlorate units. These oxygens were subsequently located

by another difference Fourier map, and found to be disordered, probably due to one or more different orientations. The resolution of this disorder was not possible. These oxygens have high thermal parameters when compared to others. The structure was refined by the block-diagonal least-squares technique with all the non hydrogen atoms refined anisotropically to a final R = 4.39% and R_w = 5.09%. A final difference Fourier map was featureless.

2.2.3 Results and Discussion

The structure of the Λ isomer is depicted in figure 2.1, and the molecular numbering scheme is given in figure 2.2. The unit cell constants are tabulated in table A.1. The structure contains neither a covalent hydrate nor a monodentate bipyridyl ligand. All three bipyridyl ligands are chelated to Ir(III) ion as in the case of $[Ir(bpy)_3]^{3+}$ ion, but as noted below one of the pyridyl rings is believed to be attached to Ir(III) through a carbon atom and not through a nitrogen atom. The Ir(III) is thus in a distorted octahedral arrangement bound to five nitrogens and a carbon atom.

The mean Ir-N distance is 2.05(3)°A [85], somewhat shorter than that reported for compounds containing N-coordinated pyridines where the average Ir-N bond distance is 2.16 °A [86-88].

Bipyridine, which has a more extended atomic frame work than pyridine, has a stronger π-acceptor character. Delocalization of electrons over this extended carbon frame work, tends to lower the energies of both π-HOMO and π-LUMO. The shorter Ir-N bond length in the present complex suggests that, there is considerable π-bonding between the delocalized π^* orbitals of the bipyridyl ligands and the t_{2g} orbital of the Ir(III) core [89-90].

Ir-C bond length of 2.007(10) °A is in good agreement with other known Ir(III)-C bond distances reported [91-95].

Intraligand bond angles of the complex vary from 78.2 to 80.8. These are comparable to those found in $[Ni(bpy)_3]^{2+}$ [96-97], $[Ru(bpy)_3]^{2+}$ [89] and $[Co(bpy)_3]^{2+}$ [98]. The important bond lengths and angles are tabulated in table 2.1.

The closest approach of the water oxygen to a bipyridyl non-hydrogen atom is 2.75 °A, about 1.4 °A longer than the expected C-O distance (C-O ≈ 1.4 °A) if a carbon atom is covalently hydrated. The water oxygen is also about 2.56 °A away from a ClO_4^- oxygen. These distances indicate that the water molecule is hydrogen-bonded not only to a perchlorate oxygen but also to a bipyridyl ring atom. The reported average hydrogen-bond distances [99] are, C-H····O 3.23 °A, N-H····O 2.93 °A and N····H-O 2.78 °A. The most likely candidate for this ring atom is a nitrogen atom, which helps identify the cyclometallated pyridyl ring. This type of cyclometallated ring is known to exist with Ir and other metals.

Nonayama [100] has reported the structure of a chloro-bridged dimer, depicted below, where M is Iridium. The ligand, Benzo(h)quinoline, is known to form such complexes with Pd(II), Pt(II), and Rh(III) [101-102]. Even

though cyclometallation is known with other ligands it has not been reported for polypyridyl ligands such as bipyridine, terpyridine and 1,10 phenanthrolines.

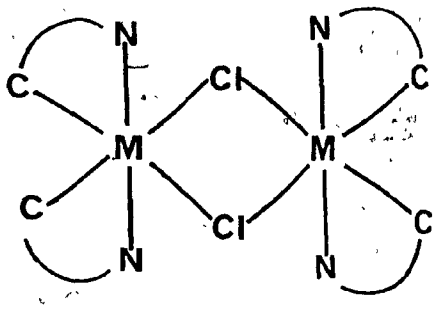

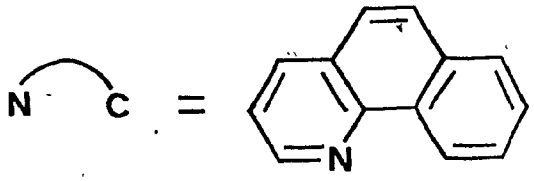

VII

The total structure contains one water molecule and three ClO_4 units per Ir. To balance the charge, since the cyclometallated bipyridyl residue carries a net negative charge, one proton should be present in the structure. The most likely place to find this is on uncoordinated N or on water as H_3O^+. Watts and co-workers in their original paper [72], report the absence of an acidic proton in the molecule. This and the observed N-H stretch in the infra-red spectrum at 2650 cm^{-1} of the acidic form of the structure suggests the most probable structure to be the one represented below (VIII).

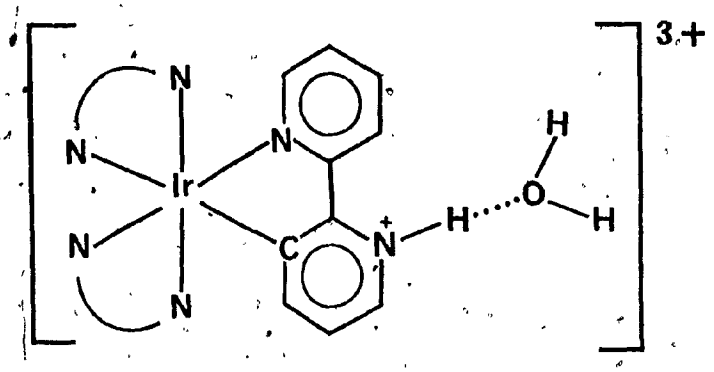

The x-ray crystallographic data do not easily distinguish between the carbon and nitrogen atoms because of the almost identical scattering power of these atomic types. However a slightly worse discrepancy index was obtained on interchanging the scattering factors for atoms C(3) and N(1). By applying Hamilton's significance test [103], the hypothesis that the conventional tris chelate being correct could be rejected at a significance level lower than 0.5%. The possibility of the presence of two non coordinated N atoms could be ruled out on the basis of the observation of a single pK_a value of 3.0 [104].

A stereoscopic view of the molecule with eight of its nearest neighbours is shown in figure 2.4. There are seven ClO_4 units about the $[Ir(bpy)_2(bpy')]^{3+}$ cation within 3.1-3.3 °A of a non hydrogen atom. Six of these ClO_4 ions have oxygens wedged into the intra-ligand pockets such that

in the solid state the cation and the anions form tight ion pairs [105].

The mean Cl-O distance is 1.37(6) °A and the mean O-Cl-O angle is 109(5) similar to those previously reported [105-108].

The individual pyridyl groups retain planarity, the equations of the least-squares planes calculated, and the deviation of the atoms from their respective planes are listed in table 2.2. Each pyridyl group is tilted with respect to the other bonded to it: the dihedral angles vary from 2.4 to 4.2.

A stereo packing diagram of the complex is shown in figure 2.5. It contains alternately arranged Δ and Λ isomers of the cation. The final atomic coordinates and the anisotropic thermal parameters are listed in table A.3.

Table 2.1

Bond Distances and Angles of $[Ir(bpy)_2(bpy')](ClO_4)_3 \cdot H_2O$, standard deviation is given in paranthesis.

Bond Distances in Angstroms.

Ir-C(3)	2.007(10)	C(12)-C(13)	1.363(25)
Ir-N(2)	2.058(11)	C(13)-C(14)	1.410(24)
Ir-N(3)	2.046(11)	C(14)-C(15)	1.378(19)
Ir-N(4)	2.084(10)	C(15)-C(16)	1.434(21)
Ir-N(5)	2.068(10)	N(4)-C(16)	1.396(17)
Ir-N(6)	2.010(10)	N(4)-C(20)	1.370(18)
C(3)-C(4)	1.397(18)	C(16)-C(17)	1.442(20)
C(3)-C(2)	1.355(18)	C(17)-C(18)	1.437(24)
C(4)-C(5)	1.414(21)	C(18)-C(19)	1.358(24)
C(5)-C(1)	1.396(24)	C(19)-C(20)	1.391(21)
C(1)-N(1)	1.434(21)	N(5)-C(21)	1.374(18)
N(1)-C(2)	1.396(19)	N(5)-C(25)	1.361(17)
C(2)-C(6)	1.463(19)	C(21)-C(22)	1.451(20)
N(2)-C(6)	1.370(18)	C(22)-C(23)	1.370(24)
N(2)-C(10)	1.398(17)	C(23)-C(24)	1.395(22)
C(6)-C(7)	1.345(18)	C(24)-C(25)	1.391(18)
C(7)-C(8)	1.324(23)	C(25)-C(26)	1.463(19)
C(8)-C(9)	1.437(26)	N(6)-C(26)	1.393(17)
C(9)-C(10)	1.441(20)	N(6)-C(30)	1.373(17)
N(3)-C(11)	1.357(18)	C(26)-C(27)	1.374(20)
N(3)-C(15)	1.366(18)	C(27)-C(28)	1.401(23)
C(11)-C(12)	1.397(22)	C(28)-C(29)	1.398(23)

C(29)-C(30)	1.426(21)	Cl(2)-O(7)	1.377(12)
Cl(1)-O(1)	1.266(18)	Cl(2)-O(8)	1.396(13)
Cl(1)-O(2)	1.322(19)	Cl(3)-O(9)	1.405(13)
Cl(1)-O(3)	1.290(19)	Cl(3)-O(10)	1.405(13)
Cl(1)-O(4)	1.287(20)	Cl(3)-O(11)	1.404(11)
Cl(2)-O(5)	1.418(11)	Cl(3)-O(12)	1.424(12)
Cl(2)-O(6)	1.435(13)		

Bond Angles in Degrees.

C(3)-Ir-N(2)	79.7(5)	Ir-N(2)-C10)	123(1)
C(3)-Ir-N(3)	96.8(4)	Ir-N(3)-C(11)	124.4(9)
C(3)-Ir-N(4)	176.0(4)	Ir-N(3)-C(15)	114.4(9)
C(3)-Ir-N(5)	96.6(4)	Ir-N(4)-C(16)	110.7(9)
C(3)-Ir-N(6)	87.3(4)	Ir-N(4)-C(20)	125.4(9)
N(2)-Ir-N(3)	88.6(4)	Ir-N(5)-C(21)	120.8(9)
N(2)-Ir-N(4)	97.1(4)	Ir-N(5)-C(25)	116.2(8)
N(2)-Ir-N(5)	174.5(4)	Ir-N(6)-C(26)	118.1(8)
N(2)-Ir-N(6)	97.6(4)	Ir-N(6)-C(30)	124.2(8)
N(3)-Ir-N(4)	80.8(4)	C(4)-C(3)-C(2)	118(1)
N(3)-Ir-N(5)	95.9(4)	C(3)-C(4)-C(5)	121(1)
N(3)-Ir-N(6)	173.2(4)	C(4)-C(5)-C(1)	121(1)
N(4)-Ir-N(5)	86.8(4)	C(5)-C(1)-N(1)	118(1)
N(4)-Ir-N(6)	95.4(4)	C(1)-N(1)-C(2)	118(1)
N(5)-Ir-N(6)	78.2(4)	N(1)-C(2)-C(3)	124(1)
Ir-C(3)-C(4)	125.8(9)	N(1)-C(2)-C(6)	120(1)
Ir-C(3)-C(2)	115.7(9)	N(1)-C(2)-C(6)	116(1)
Ir-N(2)-C(6)	115.1(9)		

C(2)-C(6)-C(7)	125(1)	C(22)-C(23)-C(24)	122(1)
C(2)-C(6)-N(2)	113(1)	C(23)-C(24)-C(25)	118(1)
N(2)-C(6)-C(7)	122(1)	N(5)-C(25)-C(24)	120(1)
C(6)-N(2)-C(10)	122(1)	N(5)-C(25)-C(26)	115(1)
C(6)-C(7)-C(8)	122(1)	C(24)-C(25)-C(26)	125(1)
C(7)-C(8)-C(9)	119(1)	C(25)-C(26)-C(27)	122(1)
C(8)-C(9)-C(10)	120(1)	N(6)-C(26)-C(25)	113(1)
N(2)-C(10)-C(9)	116(1)	N(6)-C(26)-C(27)	125(1)
C(11)-N(3)-C(15)	121(1)	C(26)-C(27)-C(28)	117(1)
N(3)-C(11)-C(12)	118(1)	C(27)-C(28)-C(29)	120(1)
C(11)-C(12)-C(13)	121(2)	C(28)-C(29)-C(30)	120(1)
C(12)-C(13)-C(14)	122(1)	N(6)-C(30)-C(29)	120(1)
C(13)-C(14)-C(15)	115(1)	C(26)-N(6)-C(30)	118(1)
N(3)-C(15)-C(14)	123(1)	O(1)-Cl(1)-O(2)	115(2)
N(3)-C(15)-C(16)	115(1)	O(1)-Cl(1)-O(3)	117(2)
C(14)-C(15)-C(16)	121(1)	O(1)-Cl(1)-O(4)	102(1)
N(4)-C(16)-C(15)	118(1)	O(2)-Cl(1)-O(3)	94(1)
C(15)-C(16)-C(17)	126(1)	O(2)-Cl(1)-O(4)	111(2)
N(4)-C(16)-C(17)	116(1)	O(3)-Cl(1)-O(4)	119(2)
C(16)-C(17)-C(18)	120(1)	O(5)-Cl(2)-O(6)	109.1(8)
C(17)-C(18)-C(19)	117(1)	O(5)-Cl(2)-O(7)	110.0(8)
C(18)-C(19)-C(20)	124(2)	O(5)-Cl(2)-O(8)	107.9(9)
N(4)-C(20)-C(19)	118(1)	O(6)-Cl(2)-O(7)	108.1(8)
C(16)-N(4)-C(20)	124(1)	O(6)-Cl(2)-O(8)	107.6(9)
C(21)-N(5)-C(25)	123(1)	O(7)-Cl(2)-O(8)	114(1)
N(5)-C(21)-C(22)	117(1)	O(9)-Cl(3)-O(10)	106.3(9)
C(21)-C(22)-C(23)	119(1)	O(9)-Cl(3)-O(11)	111.2(9)

O(9)-Cl(3)-O(12)	111.0(9)	O(10)-Cl(3)-O(12)	108.9(8)
O(10)-Cl(3)-O(11)	107.4(9)	O(11)-Cl(3)-O(12)	111.9(8)

Table 2.2

Equation of the plane	0.1556x + 0.2605y + 0.9528z = 7.0930					
Atoms	N(1)	C(1)	C(2)	C(3)	C(4)	C(5)
Deviation from the plane Å	-.013	.012	.014	-.012	.009	.010
Equation of the plane	0.1881x + 0.2831y + 0.9405z = 7.6140					
Atoms	N(2)	C(6)	C(7)	C(8)	C(9)	C(10)
Deviation from the plane Å	-.006	-.003	.011	-.010	.001	.006
Equation of the plane	-0.9837x + 0.0214y + 0.1785z = -2.3960					
Atoms	N(3)	C(11)	C(12)	C(13)	C(14)	C(15)
Deviation from the plane Å	.011	-.010	.006	-.002	.004	-.008

Equation of the plane	$-0.9722x - 0.0279y + 0.2321z = -2.8930$					
Atoms	N(4)	C(16)	C(17)	C(18)	C(19)	C(20)
Deviation from the plane °A	.008	-.011	-.004	.024	-.029	.011
Equation of the plane	$0.2215x - 0.9254y + 0.3070z = -12.710$					
Atoms	N(5)	C(21)	C(22)	C(23)	C(24)	C(25)
Deviation from the plane °A	.005	-.005	.004	-.002	.002	-.003
Equation of the plane	$0.2173x - 0.9128y + 0.3459z = -12.300$					
Atoms	N(6)	C(26)	C(27)	C(28)	C(29)	C(30)
Deviation from the plane °A	.012	-.020	.011	.004	-.012	.003

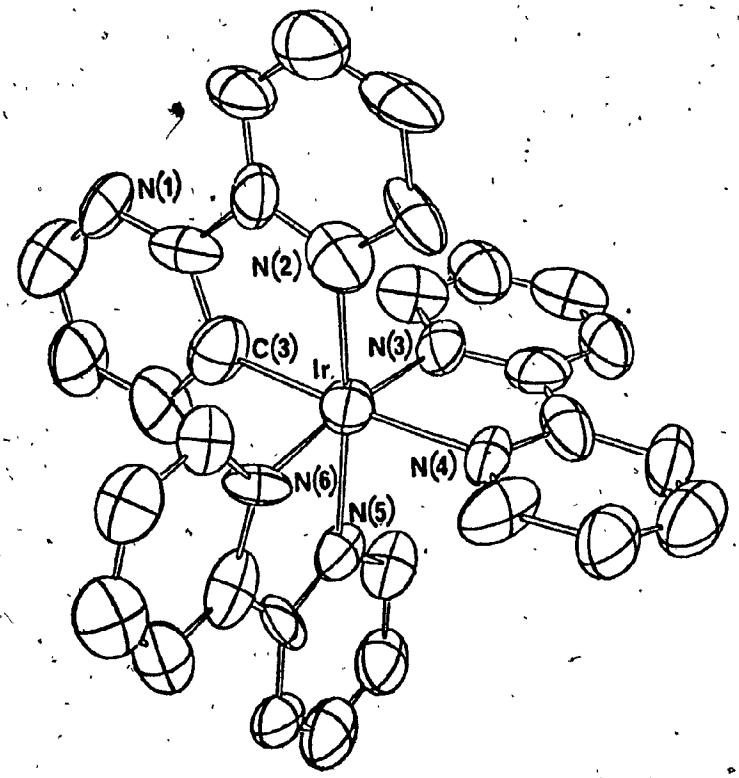

Figure 2.1. Geometry of the $[Ir(bpy)_2(bpy')]^{3+}$ cation

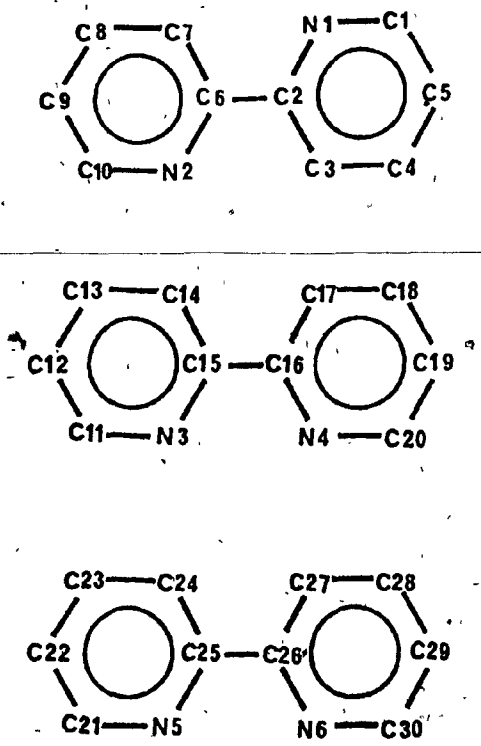

Figure 2.2. Molecular labelling system of $[Ir(bpy)_2(bpy')](ClO_4)_3 \cdot H_2O$

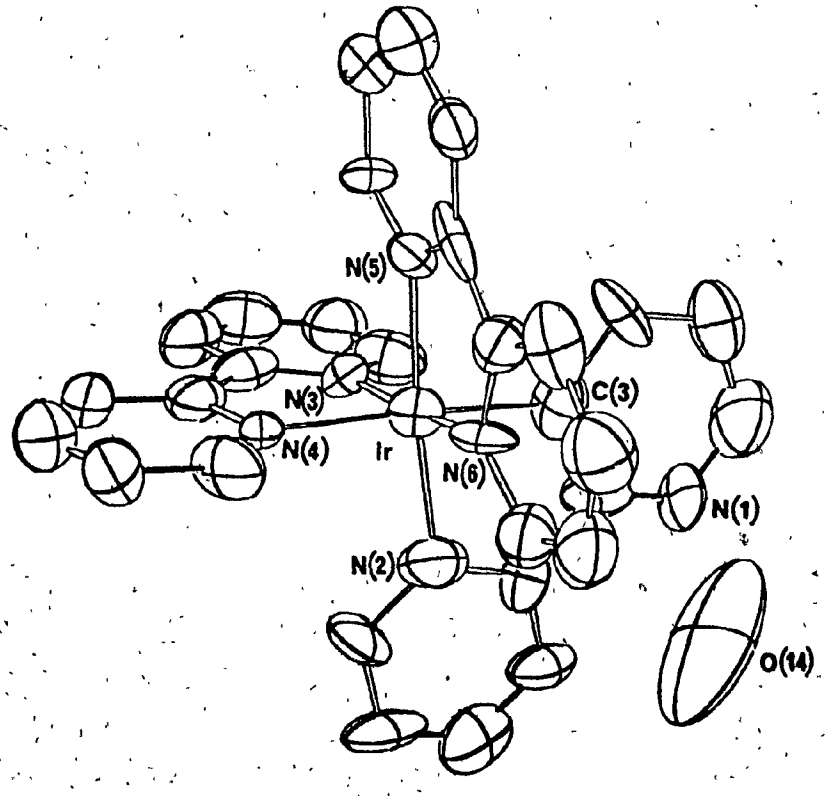

Figure 2.3. $[Ir(bpy)_2(bpy')]^{3+}$ cation with H-bonded water molecule

Figure 2.4. Stereoscopic view of the $[Ir(bpy)_2(bpy')]^{3+}$ cation with nearest 8 neighbours

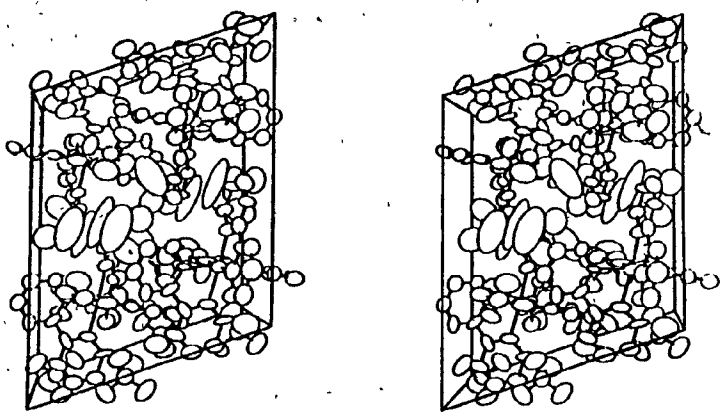

Figure 2.5. Unit cell packing diagram of $[Ir(bpy)_2(bpy')](ClO_4)_3.H_2O$ viewed approximately along the crystallographic b axis

2.3 MOLECULAR STRUCTURE OF "$[Cr(terpy)_2](ClO_4)_3.H_2O$"

2.3.1 Introduction

The excited state lifetimes of the polypyridyl complexes of chromium(III), especially those derived from bipyridine, 1,10-phenanthroline and their substituted derivatives are surprisingly long in aqueous media, when compared to other amine complexes [109-111]. Because of these longer excited state lifetimes, these polypyridyl complexes have been extensively studied for their photochemical and photophysical behaviour [59,112]. In fluid solution, an excited state which has a lifetime long enough to encounter other species, can undergo bimolecular electron and energy transfer processes. As said before, such processes have potential applicability in solar energy converting schemes [63,113].

Chromium(III) complexes possess a d^3 electronic configuration. The energy level diagram for a Cr(III) system with octahedral microsymmetry is shown in figure 2.6. The ground state is a quartet $^4A_2$ state. Typical absorption spectra of Cr(III) complexes with O_h microsymmetry have three weak spin allowed absorption bands (quartet → quartet) in the U.V and visible regions, and two very weak spin forbidden bands (quartet → doublet) in the near I.R region. The quartet → quartet bands correspond to

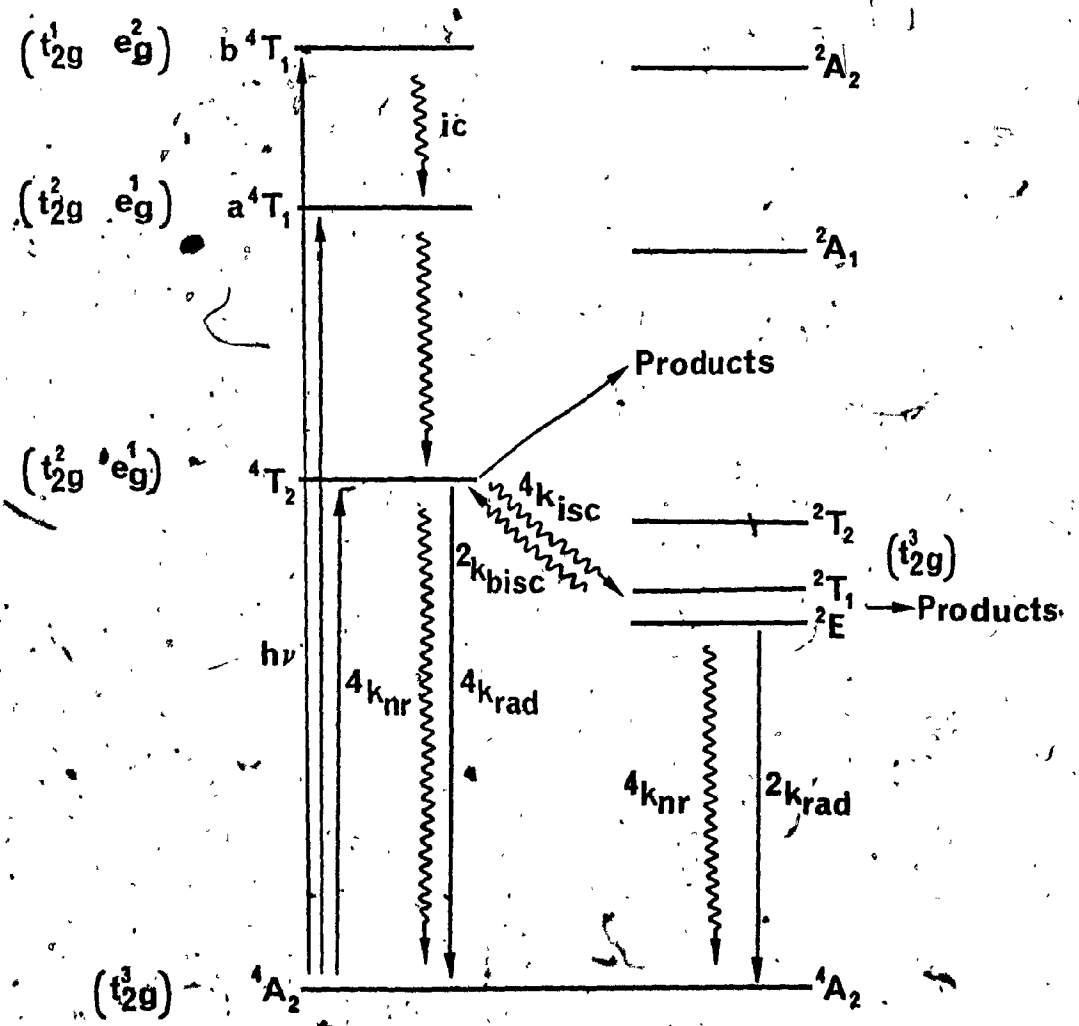
$(t_{2g}^1\ e_g^2)$ $b\,^4T_1$
$^2A_2$
ic
$(t_{2g}^2\ e_g^1)$ $a\,^4T_1$
$^2A_1$
Products
$(t_{2g}^2\ e_g^1)$ $^4T_2$
$^4k_{isc}$
$^2T_2$
(t_{2g}^3)
$^2k_{bisc}$
$^2T_1$
^2E
Products
hν
$^4k_{nr}$
$^4k_{rad}$
$^4k_{nr}$
$^2k_{rad}$
(t_{2g}^3) $^4A_2$
$^4A_2$

Figure 2.6

the spin allowed transitions from $^4A_2$ ground state to the excited quartet states $^4T_2$, a^4T_1 and b^4T_1. Even though the polypyridyl complexes of Cr(III) do not posses O_h symmetry, they are often discussed in this context because of the approximate octahedral arrangement of N atoms around Cr(III).

The energy level diagram which is shown in figure 2.6 has been constructed from the spectral analysis by Konig and Herzog [114] for $[Cr(bpy)_3]^{3+}$. The location of higher doublet states has been obtained from flash photolysis data [115]. With only minor modifications, this diagram could also be applied to other polypyridyl complexes of Cr(III), $[Cr(phen)_3]^{3+}$ and $[Cr(terpy)_2]^{3+}$.

In a typical photolysis experiment the following reaction sequence could take place. Upon irradiation the lowest excited quartet state $^4T_2$ is populated according to the reaction,

$$^4A_2 \quad Cr(NN)_3^{3+} \longrightarrow \quad ^4T_2 \qquad (2.1)$$

This $^4T_2$ state undergoes reactions 2.2 to 2.4 with a life time of 10 ps [116]. Thermally equilibrated ^2E and $^2T_1$ states are designated as ^2E. No fluoroscence emission from $^4T_2$ state has been observed [117]. Hence depopulation of

$^4T_2$ state takes place only through reactions 2.2 to 2.4.

$$^4T_2 \longrightarrow {}^4A_2 \qquad (2.2)$$

$$^4T_2 \longrightarrow \text{Products} \qquad (2.3)$$

$$^4T_2 \longrightarrow {}^2E \qquad (2.4)$$

To account for the photochemistry of Cr(III) complexes, two principal paths have been proposed: from the lowest spin forbidden doublet state [118-121] and the lowest spin allowed quartet state [122].

In support of reactions originating from the quartet $^4T_2$ state, Chen and Porter [123] have noted that only 50% of the photolysis reaction of trans $[Cr(NH_3)_2(NCS)_4]^-$ is quenched by the efficient doublet quencher $[Cr(CN)_6]^{3-}$. This was taken as evidence that 50% of the thiocyanate loss occurs from the quartet excited state before the intersystem crossing to the doublet ^2E state. Further, 40% of the photoreaction of $[Cr(en)_3]^{3+}$ in aqueous solution originates from the quartet $^4T_2$ state prior to intersystem crossing to the doublet ^2E state. Balzani and co-workers [124], have suggested that the quenchable portion of the photoreaction also comes from the quartet $^4T_2$ state by back intersystem crossing from the doublet ^2E state ($^2E \rightarrow {}^4T_2$).

The $^4T_2$ state is expected to be highly distorted with respect to the $^4A_2$ ground state. The distortion results from the promotion of an electron from a predominantly non-bonding $d\pi$ orbital to a σ^*anti-bonding orbital [58].

In contrast to the $^4T_2$ quartet state, the first excited doublet states ^2E and $^2T_1$ are not expected to be greatly distorted with respect to the $^4A_2$ ground state. Since $^4A_2 \rightarrow {}^2T_1/{}^2E$ transition involves no electron promotion to a σ^* antibonding orbital, rather electron spin pairing within the t_{2g} sub level, the bond lengths of this state are believed to be essentially the same as those of the ground state. As a further support, no Stokes shift has been observed [110] in the absorption $^4A_2 \rightarrow {}^2T_1/{}^2E$ and emission $^2T_1/{}^2E \rightarrow {}^4A_2$ spectra of Cr(III) amine complexes.

The observed lifetime of the ^2E state, $^2\tau_{obs}$, in the absence of any quenchers is the reciprocal sum of the rate constants which depopulate ^2E state. This is given by the equation,

$$^2\tau_{obs} = 1/(^2k_{nr} + {}^2k_{rx} + {}^2k_{rad} + {}^2k_{bisc})$$

where $^2k_{nr}$ is the rate constant for the non-radiative decay

$^2k_{nr}$ is the rate constant for the reaction (with

solvent).

$^2k_{rad}$ is the rate constant for the phosphorescence decay to the ground state.

$^2k_{bisc}$ is the rate constant for back intersystem crossing to the $^4T_2$ state..

The lifetimes of $(^2E)\ [Cr(bpy)_3]^{3+}$ and $(^2E)\ [Cr(phen)_3]^{3+}$ in deareated water at 22 C are 0.068 and 0.25 mS respectively [125]. With respect to other Cr(III) systems, the lifetime of these two complexes are surprisingly long.

The predominant factor which determines the lifetime of ^2E state is the nonradiative decay of ^2E to the $^4T_2$ ground state.

$$^2k_{nr} \gg {}^2k_{rx} + {}^2k_{rad} + {}^2k_{bisc}$$

Substituting D_2O in place of H_2O causes no change in lifetimes. This indicates the lack of direct vibrational coupling via H-bonds between the bulk solvent and the complex [111,126]. The nonradiative decay of ^2E state involves transformation of metal centered electronic energy into the ligand centered vibrational energy [111]. Here the ligand vibrational modes act as the energy acceptor as well

as the oscillation dipole perturbation that permits the energy transfer process to occur. Further, according to this model when the ligand becomes more vibrationally rigid, the ^2E life time is longer. Substitution of phenanthroline for bipyridine restricts the vibrational modes involving stretching, bending or rotation about the inter-ring C-C bond. This is because phenanthroline is a more rigid ligand than bipyridine. Since the restriction imposed on the vibrational freedom of the ligand affects the energy transfer process, thus reducing $^2k_{nr}$. This being the predominant factor which determines the lifetime of the ^2E state, $^2\tau_{obs}$ increases. This model holds well for $[Cr(bpy)_3]^{3+}$ and $[Cr(phen)_3]^{3+}$ systems. Phenanthroline, being a more rigid ligand than bipyridine, should show a longer excited state life-time when chelated to Cr(III). In fact this is found to be true. If the proposed model is true, then terpyridine complexes which are considered as more rigid than bipyridine complexes should also have a longer excited state lifetime. But the ^2E life time of $[Cr(terpy)_2]^{3+}$ in fact found to be very short, 0.05 μS [112], about one thousand times shorter than the bipyridine analogue. Interestingly, the metal to ligand charge transfer excited state of $[Ru(terpy)_2]^{2+}$ is also shorter lived than the bipyridine analogue [127-128].

Even though the terpyridyl ligand is vibrationally stiffer than the bipyridyl analogue, the shorter life time

is really not inconsistent with the proposed model. Terpyridine is a tridentate ligand. In principle, bis complexes of terpyridine could exist in either of two forms, meridional or facial forms as shown below.

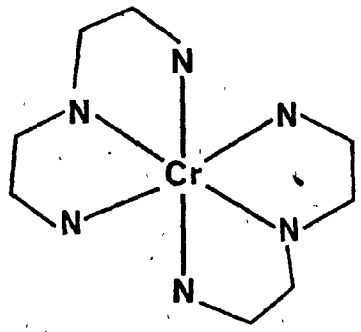

facial

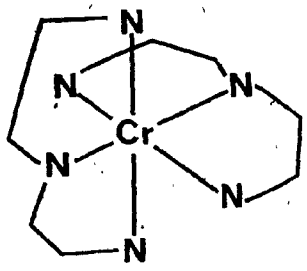

meridional

Of these two forms meridional form is much more thermodynamically stable than the facial form: in the facial form one of the pyridyl groups is forced to adopt a position perpendicular to the planes of the remaining two pyridyl rings. On the other hand, the meridional form, which is favourable on energy grounds, should be a highly distorted one, with distortions occuring in the terpyridyl planes (by analogy with other $[M(terpy)_2]^{n+}$ complexes) [129-132]. Here the Cr(III) core would be more exposed to the solvent perturbation so that direct vibrational coupling between the excited state metal core and the bulk solvent takes place. This will increase the rate of non-radiative decay, ie. $^2k_{nr}$, which is a major contributor to the ^2E

lifetimes. The more open structure of $[Ru(terpy)_2]^{2+}$ compared to $[Ru(bpy)_3]^{2+}$ has been postulated as the possible cause for the shorter living excited state of the former [127].

By studying the solvation of tris(1,10-phenanthroline)-Iron(11) cation, Van Meter and Newmann [133-134] have postulated the existence of two types of interligand pockets between the phenanthroline ligands. Three large V-shaped pockets and two smaller pockets have been defined. Approach to the central metal atom by a small molecule such as water, through the smaller pockets is hindered by the steric crowding, but approach via a larger pocket is possible. According to Van Meter and Neumann, small molecules could approach to at least 3 °A from the central metal ion.

The nature of the interligand pockets present in the title complex is different to those present in bipyridine and phenanthroline complexes. A detailed X-ray crystallographic study of the title complex was undertaken to investigate the qualitative nature of the interligand pockets present in this complex [105]. In addition we were interested to verify whether the one water of hydration and title complex form the covalent hydrate $[Cr(terpy)(terpy\ H\text{-}OH)^{3+}$ [135].

2.3.2 Experimental

Slow evaporation of an aqueous solution of the compound gave orange crystals. Preliminary Weissenberg and precession photographs indicated a monoclinic crystal with hkl; h+k odd absent, and h0l; l odd absent, thus limiting the possible space group to be C2/c (No. 15) or Cc (No. 9). Statistical tests favoured the non-centrosymmetric space group, hence the space group Cc was assumed. Subsequent successful refinement showed this to be correct.

Accurate cell dimensions were obtained by centering 12 reflections for both positive and negative 2θ. Appropriately averaged 2θ, ω, χ and ϕ values were used in a least-squares calculation to give the cell parameters with their estimated standard deviations. These cell parameters were used in subsequent calculations. A unique set of data were collected for $+h+k\pm l$ at $4.0 < 2\theta < 45$ by conventional θ-2θ scan techniques, using a Picker Nuclear FACS-1 four-circle diffractometer coupled to a PDP 8S minicomputer. Backgrounds were measured at each end of the peak for 20 seconds. Three standards were monitored at every 50 measurements. They varied in harmony by not more than 3%. The data were scaled and corrected for instrumental drift, Lorentz, and polarization effects. Of 2307 reflections collected, 2150 with $I > 3\sigma(I)$ were used in the subsequent calculations. The data reduction was carried out by a

locally written program PREP3 [136], on Concordia University CDC Cyber 170 computer.

The structure was solved by direct methods. The Cr atom position was also verified by the Patterson method. An electron density map phased by 232 reflections of $E \geq 1.5$ gave a three-dimensional map on which almost all the non hydrogen atoms could be found. The structure was refined by the full-matrix least-squares technique, with all the non hydrogen atoms refined anisotropically. In the last stages of the refinement, H atoms were included in their calculated positions 0.98 °A away from the C atom to which they were attached. Neither the position nor the isotropic thermal parameter, which was set for 5.0 , of these H atoms were refined.

The correct enantiomer was chosen by changing the sign of the imaginary term of the anomalous dispersion correction and rerefining the structure. For the chosen enantiomer the structure converged at R = 5.2% and R_w = 5.7%, and for the rejected enantiomer R = 5.3% and R_w = 5.9%. By applying Hamilton's significance test [103], the second enantiomer could be rejected at a significance level lower than 0.5%.

The following computer programs were employed: Fordap by Zalkin [138] to calculate Patterson, Fourier and difference Fourier maps, SFLS by Prewitt [138] to do least

squares and structure factor calculations, UTILITY by Bird [139] to calculate bond distances and angles, and to calculate least-squares planes through the selected atoms. Plots were made using Ortep by Johnson [57]. All the computations were done on Concordia University Cyber 170 computer.

2.3.3 Results and Discussion

The structure of the $[Cr(terpy)_2]^{3+}$ cation is depicted in figure 2.7. The molecular numbering scheme is given in figure 2.8, and the unit cell constants are given in table A.1. As expected, it possesses a highly distorted meridional configuration, the distortions occur in the two terpyridyl planes. The mean Cr-N distance is 2.03(4) °A, comparable to other known Cr-N distances reported in the literature [140-142]. Intraligand N-Cr-N bond angles vary from 78.2° to 79.0°. This value is comparable to those reported for the bis terpyridyl complexes of Co(II) and Cu(II) [129-132], bipyridyl complexes of Ru(II), Ni(II) and Cu(II) [89,96-97,107] and the phenanthroline complex of Cu(II) [108], but slightly smaller than those reported for $[Co(terpy)(CO_3)(OH)]$ [143], $[Co(bpy)_3]^{3+}$ [98] and $[Fe(phen)_3]^{3+}$ [144]. The mean N(terminal)-M-N(terminal) angle is 157.3°, comparable to those found in $[Co(terpy)_2]^{2+}$ [129,131] but slightly higher than that reported for $[Cu(terpy)_2]^{2+}$ [130,132].

In all the known terpyridyl complexes, the central N atom forms the shortest bond to the metal, but this N atom is the poorest donor atom among the three N atoms. This violates the general rule [145] of "the best donors make the shortest bond distances". The observed shorter bond distance to the poorest donor atom is purely a steric

effect. The two terminal N atoms cannot be brought closer to the metal atom without bringing the central N-atom even closer, thus the observed configuration represents a compromise between steric and electronic effects.

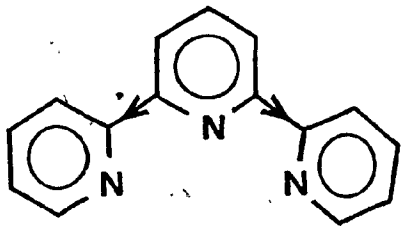

IX

The least square planes of the six pyridyl rings and the deviation of the atoms from their respective planes are tabulated in table 2.4. The individual pyridyl groups retain their planarity. The terminal pyridyl rings are tilted with respect to the central pyridyl group. The dihedral angles are 1.3° and 7.8° for the N(1)-N(2)-N(3) pyridyl group and 1.5° and 4.5° for the N(4)-N(5)-N(6) terpyridyl group. Similar dihedral angles are reported for other terpyridyl complexes [130]. Individual bond distances and angles are tabulated in table 2.3 with their estimated standard deviations.

The mean Cl-O distance and O-Cl-O bond angles of the ClO_4 anions are 1.40(4) and 109(3) respectively, comparable to those reported in the literature [74,106-108].

There are eight perchlorate units within 3.32 °A of a non-hydrogen atom of the cation. Three of these ClO_4 ions have oxygens wedged into the pockets described by the two terpyridyl planes. The water of hydration does not occupy a site in the intraligand pockets; rather it is hydrogen-bonded to two of the ClO_4 units. No covalent hydrate is evident.

The dihedral angle between the two terpyridyl planes is 83 , thus two types of intraligand pockets can be identified in the structure. This is evident from the stereo diagram shown in figure 2.10. Two larger pockets and two slightly smaller pockets are described by the two terpyridyl planes. Each of these pockets could easily hold at least two small molecules such as water. In aqueous solutions, the Cr(III) metal core may be regarded as being essentially hydrated.

A stereo packing diagram of the complex is shown in figure 2.11. The final positional parameters and the anisotropic thermal parameters are tabulated in table A.4.

Table 2.3

Bond Distances and Angles of $[Cr(terpy)_2](ClO_4)_3 \cdot H_2O$.

standard deviation is given in parenthesis

Bond Distances in Angstroms.

Cr-N(1)	2.049(5)	C(13)-C(14)	1.371(13)
Cr-N(2)	1.987(5)	C(14)-C(15)	1.395(11)
Cr-N(3)	2.070(5)	N(3)-C(11)	1.364(9)
Cr-N(4)	2.052(5)	N(3)-C(15)	1.366(9)
Cr-N(5)	1.964(5)	N(4)-C(16)	1.362(9)
Cr-N(6)	2.052(5)	N(4)-C(20)	1.359(8)
N(1)-C(1)	1.382(8)	C(16)-C(17)	1.376(11)
N(1)-C(5)	1.354(8)	C(17)-C(18)	1.376(12)
C(1)-C(2)	1.398(10)	C(18)-C(19)	1.426(11)
C(2)-C(3)	1.365(12)	C(19)-C(20)	1.379(10)
C(3)-C(4)	1.402(12)	C(20)-C(21)	1.461(10)
C(4)-C(5)	1.399(10)	C(21)-C(22)	1.389(10)
C(5)-C(6)	1.466(9)	C(22)-C(23)	1.405(12)
C(6)-C(7)	1.416(10)	C(23)-C(24)	1.392(10)
C(7)-C(8)	1.381(14)	C(24)-C(25)	1.364(10)
C(8)-C(9)	1.371(12)	N(5)-C(21)	1.343(8)
C(9)-C(10)	1.413(10)	N(5)-C(25)	1.375(9)
N(2)-C(6)	1.318(8)	C(25)-C(26)	1.479(9)
N(2)-C(10)	1.342(8)	C(26)-C(27)	1.383(10)
C(10)-C(11)	1.480(10)	C(27)-C(28)	1.413(12)
C(11)-C(12)	1.367(10)	C(28)-C(29)	1.318(13)
C(12)-C(13)	1.403(13)	C(29)-C(30)	1.456(11)

N(6)-C(26)	1.380(8)	Cl(2)-O(6)	1.398(8)
N(6)-C(30)	1.331(9)	Cl(2)-O(7)	1.470(12)
Cl(1)-O(1)	1.437(8)	Cl(2)-O(8)	1.409(9)
Cl(1)-O(2)	1.400(8)	Cl(3)-O(9)	1.397(12)
Cl(1)-O(3)	1.349(16)	Cl(3)-O(10)	1.415(7)
Cl(1)-O(4)	1.327(13)	Cl(3)-O(11)	1.401(12)
Cl(2)-O(5)	1.418(8)	Cl(3)-O(12)	1.399(8)

Bond Angles in Degrees.

N(1)-Cr-N(2)	78.5(2)	Cr-N(2)-C(6)	118.6(4)
N(1)-Cr-N(3)	157.5(2)	Cr-N(2)-C(10)	118.0(4)
N(1)-Cr-N(4)	89.2(2)	Cr-N(3)-C(11)	143.0(3)
N(1)-Cr-N(5)	104.0(2)	Cr-N(3)-C(15)	124.4(4)
N(1)-Cr-N(6)	94.8(2)	Cr-N(4)-C(16)	125.4(4)
N(2)-Cr-N(3)	79.0(2)	Cr-N(4)-C(20)	116.9(4)
N(2)-Cr-N(4)	103.0(2)	Cr-N(5)-C(21)	119.7(4)
N(2)-Cr-N(5)	177.3(2)	Cr-N(5)-C(25)	119.7(4)
N(2)-Cr-N(6)	99.9(2)	Cr-N(6)-C(26)	115.1(4)
N(3)-Cr-N(4)	96.1(2)	Cr-N(6)-C(30)	126.2(5)
N(3)-Cr-N(5)	98.5(2)	C(1)-N(1)-C(5)	119.9(6)
N(3)-Cr-N(6)	88.7(2)	N(1)-C(1)-C(2)	119.4(6)
N(4)-Cr-N(5)	78.2(2)	C(1)-C(2)-C(3)	121.1(7)
N(4)-Cr-N(6)	157.1(2)	C(2)-C(3)-C(4)	119.3(9)
N(5)-Cr-N(6)	79.0(2)	C(3)-C(4)-C(5)	118.7(7)
Cr-N(1)-C(1)	125.2(4)	C(4)-C(5)-N(1)	121.5(6)
Cr-N(1)-C(5)	114.9(4)	C(4)-C(5)-C(6)	124.4(6)

N(1)-C(5)-C(6)	114.1(5)	C(20)-C(21)-C(22)	125.3(6)
C(5)-C(6)-N(2)	113.9(5)	C(20)-C(21)-N(5)	112.8(6)
C(5)-C(6)-C(7)	127.2(6)	N(5)-C(21)-C(22)	121.8(7)
N(2)-C(6)-C(7)	118.9(6)	C(21)-C(22)-C(23)	116.8(7)
C(6)-C(7)-C(8)	118.6(7)	C(22)-C(23)-C(24)	121.5(7)
C(7)-C(8)-C(9)	121.8(8)	C(23)-C(24)-C(25)	118.4(7)
C(8)-C(9)-C(10)	117.1(7)	C(24)-C(25)-N(5)	120.9(6)
C(9)-C(10)-N(2)	120.2(6)	C(21)-N(5)-C(25)	120.5(6)
C(6)-N(2)-C(10)	123.4(6)	C(24)-C(25)-C(26)	127.2(6)
C(9)-C(10)-C(11)	125.3(6)	N(5)-C(25)-C(26)	111.9(6)
N(2)-C(10)-C(11)	114.5(6)	C(25)-C(26)-C(27)	122.2(6)
C(10)-C(11)-C(12)	124.2(7)	C(25)-C(26)-N(6)	114.1(6)
C(10)-C(11)-N(3)	113.5(6)	N(6)-C(26)-C(27)	123.7(6)
N(3)-C(11)-C(12)	122.2(7)	C(26)-C(27)-C(28)	115.9(7)
C(11)-C(12)-C(13)	116.9(8)	C(27)-C(28)-C(29)	122.2(8)
C(12)-C(13)-C(14)	121.8(8)	C(28)-C(29)-C(30)	119.1(8)
C(13)-C(14)-C(15)	119.0(8)	C(29)-C(30)-N(6)	120.3(7)
C(14)-C(15)-N(3)	119.5(7)	C(26)-N(6)-C(30)	118.6(6)
C(11)-N(3)-C(15)	120.5(6)	O(1)-Cl(1)-O(2)	112.4(5)
C(16)-N(4)-C(20)	119.2(6)	O(1)-Cl(1)-O(3)	103.0(7)
N(4)-C(16)-C(17)	121.7(7)	O(1)-Cl(1)-O(4)	110.6(7)
C(16)-C(17)-C(18)	119.3(7)	O(2)-Cl(1)-O(3)	107.4(8)
C(17)-C(18)-C(19)	120.0(7)	O(2)-Cl(1)-O(4)	112.4(7)
C(18)-C(19)-C(20)	117.4(7)	O(3)-Cl(1)-O(4)	110.5(9)
C(19)-C(20)-N(4)	122.3(7)	O(5)-Cl(2)-O(6)	112.1(5)
C(19)-C(20)-C(21)	123.8(6)	O(5)-Cl(2)-O(7)	111.1(6)
N(4)-C(20)-C(21)	113.9(6)	O(5)-Cl(2)-O(8)	111.6(5)

O(6)-Cl(2)-O(7)	106.5(6)	O(9)-Cl(3)-O(12)	110.7(6)
O(6)-Cl(2)-O(8)	110.0(6)	O(10)-Cl(3)-O(11)	108.2(7)
O(7)-Cl(2)-O(8)	105.1(6)	O(10)-Cl(3)-O(12)	108.7(5)
O(9)-Cl(3)-O(10)	106.1(5)	O(11)-Cl(3)-O(12)	109.6(6)
O(9)-Cl(3)-O(11)	113.3(8)		

Table 2.4

Equation of the plane	$-0.8815x - 0.3562y + 0.3099z = -0.4100$					
Atoms	N(1)	C(1)	C(2)	C(3)	C(4)	C(5)
Deviation from the plane °A	-.012	.005	.005	-.008	.002	.008
Equation of the plane	$-0.8873x - 0.3601y + 0.2881z = -0.5623$					
Atoms	N(2)	C(6)	C(7)	C(8)	C(9)	C(10)
Deviation from the plane °A	-.008	.006	.001	-.007	.005	.002
Equation of the plane	$-0.9329x - 0.2327y + 0.2748z = -0.9481$					
Atoms	N(3)	C(11)	C(12)	C(13)	C(14)	C(15)
Deviation from the plane °A	-.007	-.005	.011	-.005	-.007	.013

Equation of the plane	$-0.3305x + 0.8081y + 0.4875z = 1.4227$					
Atoms	N(4)	C(16)	C(17)	C(18)	C(19)	C(20)
Deviation from the plane °A	.001	-.002	.008	-.011	.009	-.004
Equation of the plane	$-0.3256x + 0.8470y + 0.4202z = 1.4566$					
Atoms	N(5)	C(21)	C(22)	C(23)	C(24)	C(25)
Deviation from the plane °A	-.004	.006	-.001	-.006	.008	-.003
Equation of the plane	$-0.3498x + 0.8360y + 0.4227z = 1.4376$					
Atoms	N(6)	C(26)	C(27)	C(28)	C(29)	C(30)
Deviation from the plane °A	.024	.025	-.006	-.006	.031	-.036

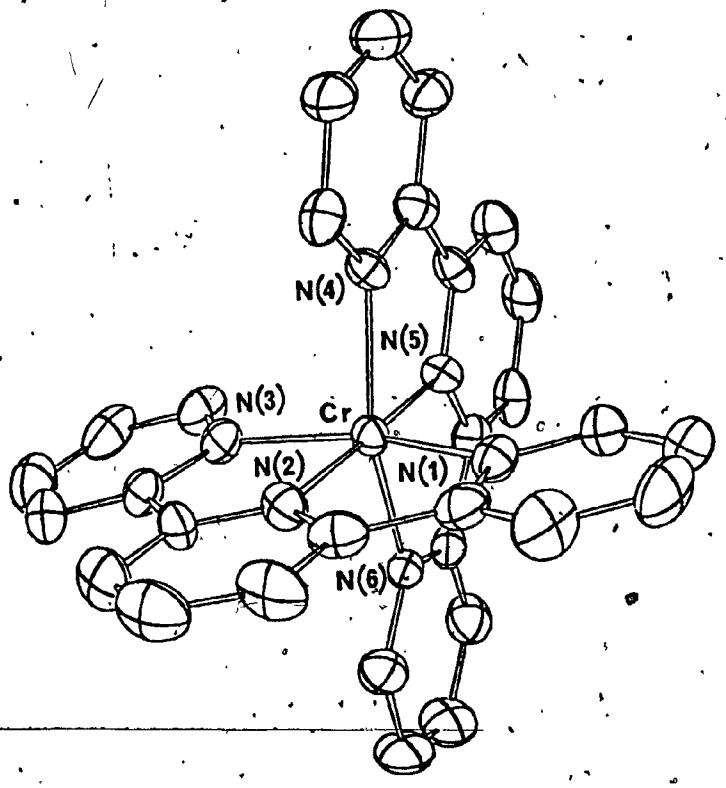

Figure 2.7. Geometry of the $[Cr(terpy)_2]^{3+}$ cation about the chromium metal core as viewed about the pseudo-threefold axis

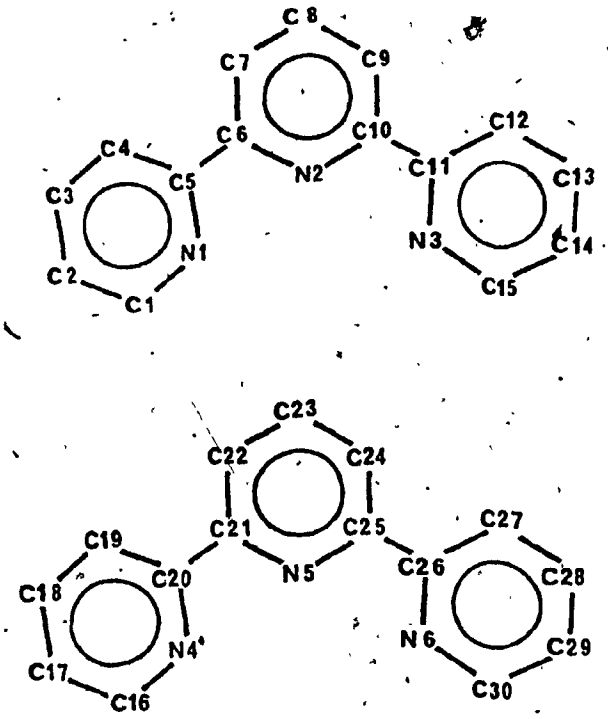

Figure 2.8. Molecular labelling system of $[Cr(terpy)_2](ClO_4)_3.H_2O$

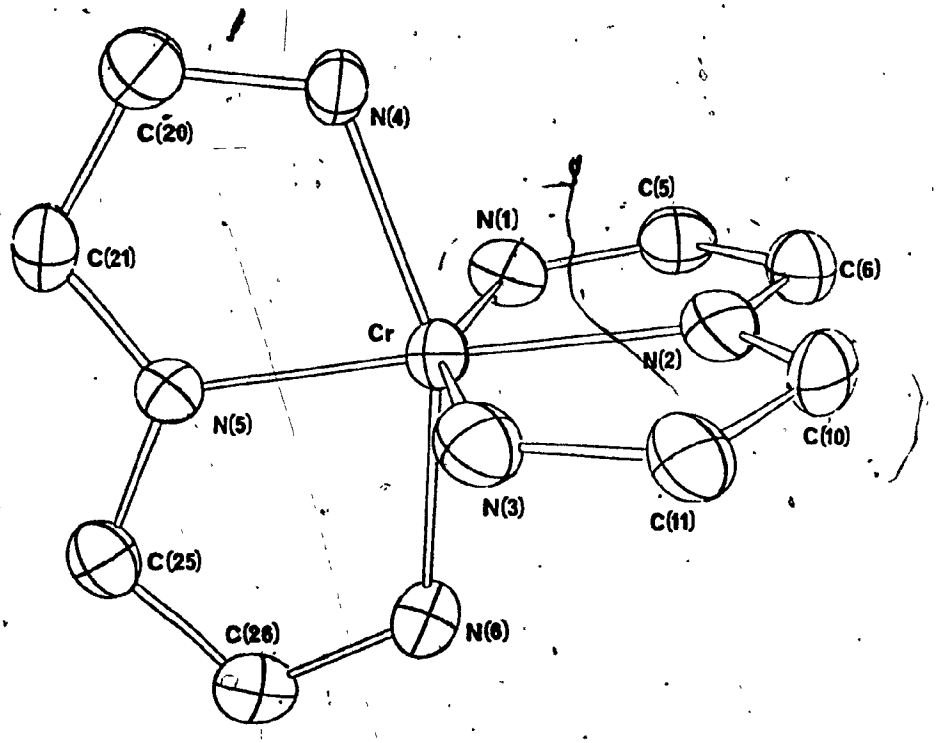

Figure 2.9. Skeletal view of the $[Cr(terpy)_2]^{3+}$ cation illustrating the distortions about the chromium core

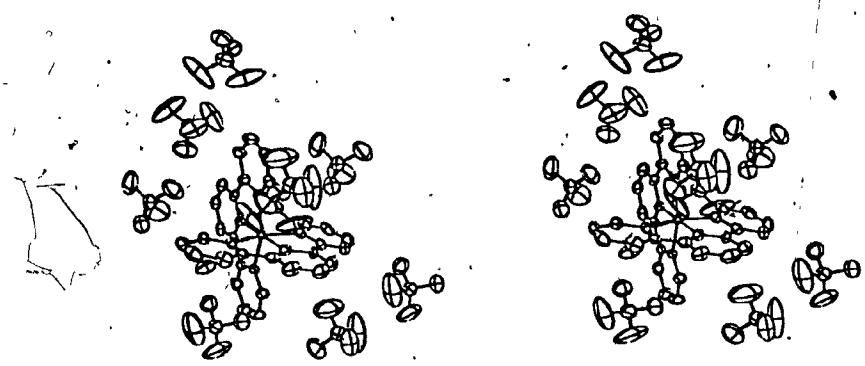

Figure 2.10. Stereoscopic view of the $[Cr(terpy)_2]^{3+}$ cation with nearest neighbours

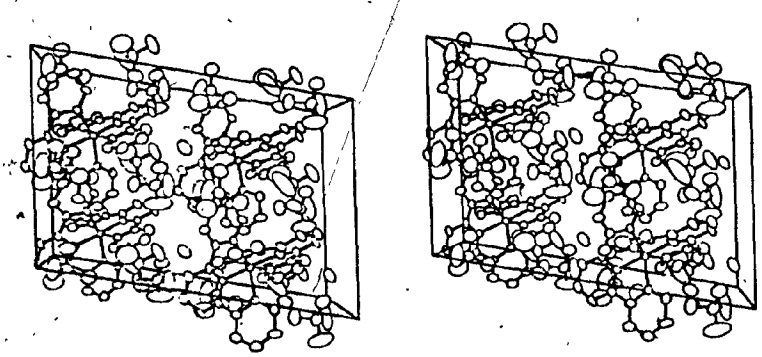

Figure 2.11. Unit cell packing diagram of $[Cr(terpy)_2](ClO_4)_3.H_2O$ viewed approximately along the crystallographic b axis

2.4 MOLECULAR STRUCTURE OF "$[Cr(bpy)_2(H_2O)Cl](ClO_4)_2.2H_2O$"

2.4.1 Introduction

The preparation of kinetically inert $[Cr(NN)_3]^{3+}$ complexes, where, NN is either bipyridine, phenanthroline or their substituted derivatives are usually carried out by the oxidation of a suspension of $[Cr(NN)_3]^{2+}$ by a suitable oxidizing agent in aqueous media [146].

$$Cr(H_2O)_6^{2+} + 3\,NN \longrightarrow Cr(NN)_3^{2+} + 6\,H_2O \qquad (2.5)$$

$$Cr(NN)_3^{2+} \xrightarrow{(O)} Cr(NN)_3^{3+} + e \qquad (2.6)$$

The direct reaction of $[Cr(H_2O)_6]^{3+}$ with NN does not yield the amine complex, because of hydroxide precipitation [147]. However instead of the free amine, if the acid salt of the amine is used, complex formation occurs [148]. Even then the tris(amine)chromium(III) complex has never been isolated in this manner.

According to Inskeep and Bjerrum [148], the addition of bipyridine to Cr(III) occur in two steps, producing trans diaquo species. This trans isomer cannot add another bipyridine without rearranging. The rate of trans → cis isomerization is a slow process, thus indicating a large

stability constant in favour of the trans isomer, hence only trans isomer can be isolated.

It was pointed out by McKenzie [149] that in an idealized trans $[M(bpy)_2X_2]^{n+}$ metal complex, with a metal to N distance of 2.0 Å, the H atoms of the C(6) carbon atoms have an intermolecular separation of only 1 Å.

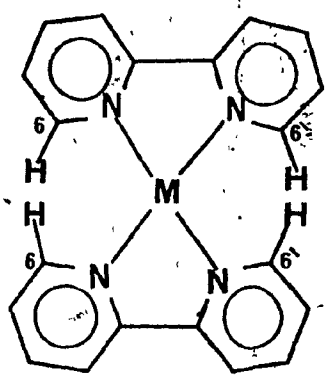

X

This means that the trans configuration must distort in some manner so as to relieve this steric strain. One obvious distortion would be to adopt a cis configuration rather than a trans configuration.

Not surprisingly, the species which were assumed to be trans bis(diamine)diaquo species were later shown to be dimeric μ-dihydroxo species as illustrated below (XI) [150-154].

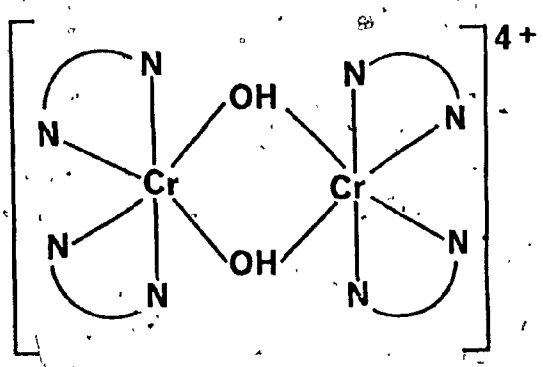

XI

Kraus has reported the isolation of trans-$[Ru(bpy)_2py_2](ClO_4)_2$ [152] and a mixture of cis and trans isomers of $[Ru(bpy)_2Cl_2]$ [153]. The resolution of $[Ru(bpy)_2Cl_2]$ in to pure cis and trans isomers had not been successful. In 1980 Meyer [154] and co-workers reported the first crystallographic characterization of a trans bis bipyridyl complex, trans $[Ru(bpy)_2(H_2O)(OH)](ClO_4)$ been isolated and characterized. As suggested by McKenzie [149], trans bipyridine groups had shown distortions to relieve the steric strain. Major ligand distortions were twisting of pyridyl groups around C(2)-C(2') axis.

In contrast to Cr(III) complexes, Cr(II) complexes in aqueous media are more labile: the former species, in octahedral coordination, is strongly stabilized because of the half filled t_{2g} sub level, figure 2.12.

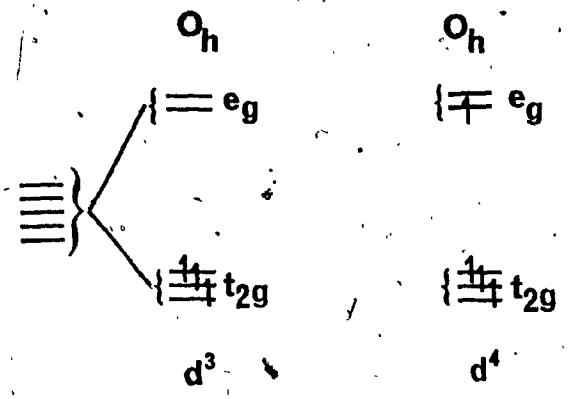

Figure 2.12

This lability of Cr(II) species is put to use in the preparation of tris chelated amine complexes of Cr(III).

In a typical preparation, for example preparation of $[Cr(bpy)_3]^{3+}$, a suspension of bipyridine is added to a deoxygenated aqueous perchloric acid solution of $CrCl_2$ to give a dark greenish black precipitate of $[Cr(bpy)_3]^{2+}$. This is then oxidized to Cr(III) by a suitable oxidizing agent. A large number of oxidizing agents have been employed, eg. $[Co(NH_3)_6]^{3+}$, Cl_2, Br_2, I_2, $K_2Cr_2O_7$ and even 30% H_2O_2 [146]. Depending upon the experimental conditions, a pink product has been obtained as a side product [155-156]. This was often taken to be $[Cr(bpy)_2(H_2O)_2]^{3+}$. Elemental analysis has shown a good approximation for $[Cr(bpy)_2(H_2O)_2](ClO_4)_3$. This compound, in aqueous acid media (0.01M HCl), shows a broad absorption at 520 nm in the visible absorption spectrum, and red shifts to 550 nm in aqueous basic media (0.01 M OH^-). The

corresponding absorption band of cis-$[Cr(bpy)_2(H_2O)_2]^{3+}$ which is obtained by the thermal or photolytic hydrolysis of $[Cr(bpy)_3]^{3+}$, occurs at 492 nm and red shifts to 518 nm in aqueous base for cis-$[Cr(bpy)_2(OH)_2]^{+}$ [157]. Thus the pink side product cannot be the cis isomer of the diaquo species. An X-ray crystallographic study of this compound was undertaken to establish its exact nature [146].

2.4.2 Experimental

The compound was recrystallized from aqueous methanol to give dark orange crystals. Preliminary Weissenberg and precession photographs indicated only $\bar{1}$ symmetry and no systematic absences, hence the crystal belongs to the primitive triclinic crystal system; space group either P1 or P$\bar{1}$. Statistical tests favoured the centrosymmetric space group, hence the latter space group was assumed. Subsequent refinements proved this to be correct.

Accurate cell dimensions were obtained on the four circle diffractometer by centering fifteen high angle reflections of $19 < 2\theta < 38$ and their Friedel equivalents. A unique set of data were collected for $\pm h+k+l$ between $3.5 < 2\theta < 45.0$ by the conventional $\theta-2\theta$ scan technique. The three standards measured showed random variation but not more than 4%. The data were scaled and corrected for Lorentz and polarization effects. Of 3319 reflections collected 2509 reflections with $I > 3\sigma(I)$ were used in the subsequent calculations.

The Patterson map was not easily interpretable, so the structure was solved by direct methods. In the initial phasing 224 reflections of $E \geq 1.8$ were used. An electron density map drawn based on the above model revealed the Cr and three Cl atom positions. Two cycles of refinement

followed by a difference Fourier map revealed the remaining non-hydrogen atom positions. One of the perchlorate units was found to be disorderd, probably with two or more orientations. Resolution of all four oxygen atoms was not possible. Two of the oxygens were resolved and their partial occupancies were treated as variables and included in the least-squares refinement. The partial occupancies added up to 1 in each case within experimental error. The structure was refined by the block-diagonal least-squares technique with all the non-hydrogen atoms refined anisotropically and all the ring hydrogens refined isotropically. Anomalous dispersion corrections were applied. The structure converged at $R = 5.82\%$ and $R_w = 7.57\%$. A final difference Fourier map was featureless.

2.4.3 Results and Discussion

The structure of the $[Cr(bpy)_2(H_2O)Cl]^{2+}$ cation is shown in figure 2.14. The molecular numbering scheme is given in figure 2.15, and the unit cell constants are given in table A.1. The structure is not the long assumed diaquo species, but it consists of two N-chelated bipyridyl groups, a Cl^-, and a water molecule attached to the central Cr(III) in a cis-manner.

The mean Cr-N distance is 2.042(11) °A, comparable to those found in $[Cr(terpy)_2]^{3+}$ [105,158]. The Cr-N bond trans to Cl is slightly longer than the other Cr-N bonds. This is probably due to the greater trans influence [90,159] of Cl^- than H_2O. Cr-O and Cr-Cl distances are 1.975(4) °A and 2.259(2) °A respectively, similar to those reported in literature [160-163]. The two N-Cr-N bond angles are 79.0(2) and 79.6(2), comparable to those found in other known bipyridyl complexes. [164-167] The observed C-H distances vary from 0.73 to 1.20 °A, typical of C-H distances obtained from x-ray diffraction studies [168-169]. The mean ring C-C and C-N distances are 1.367(18) °A and 1.339(12) °A respectively, comparable to the values reported for free bipyridine[[170]. The important bond distances and angles are tabulated in table 2.5.

The individual pyridyl groups retain planarity, the

equations of the least-squares planes calculated, and the deviation of the atoms from their respective planes are listed in table 2.6. Each pyridyl group is tilted with respect to the other slightly; dihedral angles are 3.8° and 4.9° degrees. The two bipyridyl groups are virtually perpendicular to each other, the dihedral angle is 89.6°.

The two water molecules were found to be hydrogen bonded to the bound water. The respective distances are 2.64 °A and 2.67 °A [99]. A stereo packing diagram of $[Cr(bpy)_2(H_2O)Cl]^{2+}$ with its nearest eight neighbours is shown in figure 2.16. There are six perchlorate units about the $[Cr(bpy)_2(H_2O)Cl]^{2+}$ cation within 3.3 °A of a non-hydrogen atom. One of these perchlorates has oxygens wedged into the intraligand pocket defined by the two bipyridyl planes.

The mean Cl-O distance is 1.38(4) °A, comparable to the values reported in the literature [105-108].

The observed single pK_a value of 4.6 is consistent with the structure [146] (figure 2.13). The difference in the energies of the visible absorption spectrum of the complexes, cis-$[Cr(bpy)_2(H_2O)Cl]^{2+}$ and cis-$[Cr(bpy)_2(H_2O)_2]^{3+}$ in aqueous media is also consistent with the structure. The d-d transitions of the latter complex occur at higher energies since H_2O affords a

stronger ligand field than Cl^- [90].

A stereo packing diagram of the complex is shown in figure 2.17. The final positional and thermal parameters are tabulated in table A.5.

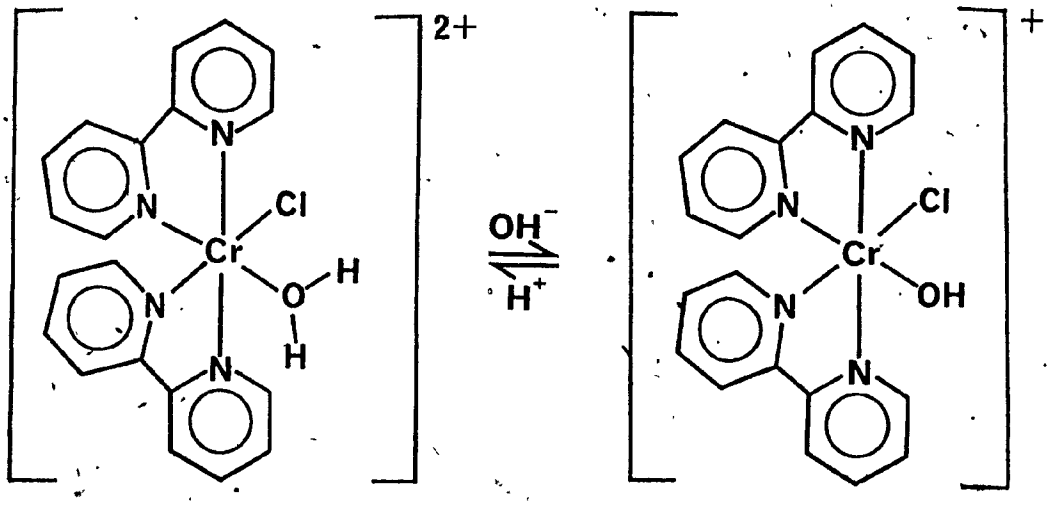

Figure 2.13

Table 2.5.

Bond Distances And Angles of $[Cr(bpy)_2(H_2O)Cl](ClO_4)_2.2H_2O$.

Standard Deviation is Given in Parenthesis.

Bond Distances in Angstroms.

Cr-Cl(1)	2.259(2)	C(11)-C(12)	1.370(10)
Cr-O(9)	1.975(4)	C(12)-C(13)	1.354(11)
Cr-N(1)	2.035(5)	C(13)-C(14)	1.352(11)
Cr-N(2)	2.059(5)	C(14)-C(15)	1.359(9)
Cr-N(3)	2.037(5)	C(15)-C(16)	1.448(9)
Cr-N(4)	2.039(5)	N(4)-C(16)	1.356(8)
N(1)-C(1)	1.339(8)	N(4)-C(20)	1.329(8)
N(1)-C(5)	1.338(8)	C(16)-C(17)	1.381(9)
C(1)-C(2)	1.399(10)	C(17)-C(18)	1.363(11)
C(2)-C(3)	1.354(11)	C(18)-C(19)	1.339(11)
C(3)-C(4)	1.369(10)	C(19)-C(20)	1.364(9)
C(4)-C(5)	1.403(9)	Cl(2)-O(1)	1.381(6)
C(5)-C(6)	1.470(9)	Cl(2)-O(2)	1.378(8)
N(2)-C(6)	1.332(8)	Cl(2)-O(3)	1.438(6)
N(2)-C(10)	1.340(8)	Cl(2)-O(4)	1.392(7)
C(6)-C(7)	1.385(10)	Cl(3)-O(5)	1.403(8)
C(7)-C(8)	1.349(10)	Cl(3)-O(6)	1.379(11)
C(8)-C(9)	1.363(10)	Cl(3)-O(7)	1.367(10)
C(9)-C(10)	1.368(10)	Cl(3)-O(8)	1.393(11)
N(3)-C(11)	1.335(9)	Cl(3)-O(A)	1.266(14)
N(3)-C(15)	1.367(8)	Cl(3)-O(B)	1.354(14)

Bond Angles in Degrees.

Cl(1)-Cr-O(9)	91.2(2)	C(1)-C(2)-C(3)	118.3(6)
Cl(1)-Cr-N(1)	95.0(2)	C(2)-C(3)-C(4)	120.8(6)
Cl(1)-Cr-N(2)	173.7(2)	C(3)-C(4)-C(5)	117.8(6)
Cl(1)-Cr-N(3)	92.5(2)	N(1)-C(5)-C(4)	122.4(6)
Cl(1)-Cr-N(4)	91.7(2)	N(1)-C(5)-C(6)	114.9(5)
O(9)-Cr-N(1)	91.1(2)	C(4)-C(5)-C(6)	122.7(6)
O(9)-Cr-N(2)	86.8(2)	C(5)-C(6)-N(2)	115.4(6)
O(9)-Cr-N(3)	94.2(2)	C(5)-C(6)-C(7)	123.6(6)
O(9)-Cr-N(4)	173.2(2)	N(2)-C(6)-C(7)	121.0(6)
N(1)-Cr-N(2)	79.0(2)	C(6)-N(2)-C(10)	118.4(5)
N(1)-Cr-N(3)	170.8(2)	C(6)-C(7)-C(8)	120.2(7)
N(1)-Cr-N(4)	94.8(2)	C(7)-C(8)-C(9)	118.8(6)
N(2)-Cr-N(3)	93.6(2)	C(8)-C(9)-C(10)	119.2(6)
N(2)-Cr-N(4)	91.0(2)	N(2)-C(10)-C(9)	122.2(6)
N(3)-Cr-N(4)	79.6(2)	C(11)-N(3)-C(15)	118.3(5)
Cr-N(1)-C(1)	126.1(4)	N(3)-C(11)-C(12)	121.4(6)
Cr-N(1)-C(5)	115.6(4)	C(11)-C(12)-C(13)	120.8(7)
Cr-N(2)-C(6)	114.8(4)	C(12)-C(13)-C(14)	117.6(6)
Cr-N(2)-C(10)	126.7(4)	C(13)-C(14)-C(15)	121.7(6)
Cr-N(3)-C(11)	126.6(4)	N(3)-C(15)-C(14)	120.2(6)
Cr-N(3)-C(15)	115.2(4)	N(3)-C(15)-C(16)	114.4(5)
Cr-N(4)-C(16)	114.6(4)	C(14)-C(15)-C(16)	125.4(6)
Cr-N(4)-C(20)	126.4(3)	C(15)-C(16)-N(4)	115.9(5)
C(1)-N(1)-C(5)	118.2(6)	C(15)-C(16)-C(17)	123.8(6)
N(1)-C(1)-C(2)	122.3(6)	N(4)-C(16)-C(17)	120.1(6)

C(16)-N(4)-C(20)	119.1(5)	O(5)-Cl(3)-O(A)	101.1(1)
C(16)-C(17)-C(18)	118.7(6)	O(5)-Cl(3)-O(B)	102(1)
C(17)-C(18)-C(19)	121.2(6)	O(6)-Cl(3)-O(7)	105.8(8)
C(18)-C(19)-C(20)	122.5(6)	O(6)-Cl(3)-O(8)	112.6(9)
O(1)-Cl(2)-O(2)	112.4(5)	O(6)-Cl(3)-O(A)	64(1)
O(1)-Cl(2)-O(3)	109.8(4)	O(6)-Cl(3)-O(B)	57(1)
O(1)-Cl(2)-O(4)	110.7(4)	O(7)-Cl(3)-O(8)	80(1)
O(2)-Cl(2)-O(3)	104.2(4)	O(7)-Cl(3)-O(A)	67(1)
O(2)-Cl(2)-O(4)	111.4(5)	O(7)-Cl(3)-O(B)	144(1)
O(3)-Cl(2)-O(4)	108.0(5)	O(8)-Cl(3)-O(A)	143(1)
O(5)-Cl(3)-O(6)	129.0(8)	O(8)-Cl(3)-O(B)	79(1)
O(5)-Cl(3)-O(7)	112.3(7)	O(A)-Cl(3)-O(B)	118(1)
O(5)-Cl(3)-O(8)	106.2(6)		

Table 2.6

Equation of the plane	$-0.1779x + 0.5963y + 0.7828z = 12.831$					
Atoms	N(1)	C(1)	C(2)	C(3)	C(4)	C(5)
Deviation from the plane °A	.008	.012	-.023	.015	.005	-.016
Equation of the plane	$-0.1682x + 0.5430y + 0.8227z = 12.834$					
Atoms	N(2)	C(6)	C(7)	C(8)	C(9)	C(10)
Deviation from the plane °A	-.006	.002	.006	-.011	.007	.001
Equation of the plane	$0.2437x - 0.7574y + 0.6057z = 0.8344$					
Atoms	N(3)	C(11)	C(12)	C(13)	C(14)	C(15)
Deviation from the plane °A	-.006	-.003	.006	.001	-.010	.013

Equation of the plane	$0.1717x - 0.7954y + 0.5813z = -1.7326$					
Atoms	N(4)	C(16)	C(17)	C(18)	C(19)	C(20)
Deviation from the plane Å	.009	.005	-.015	.018	-.007	-.007

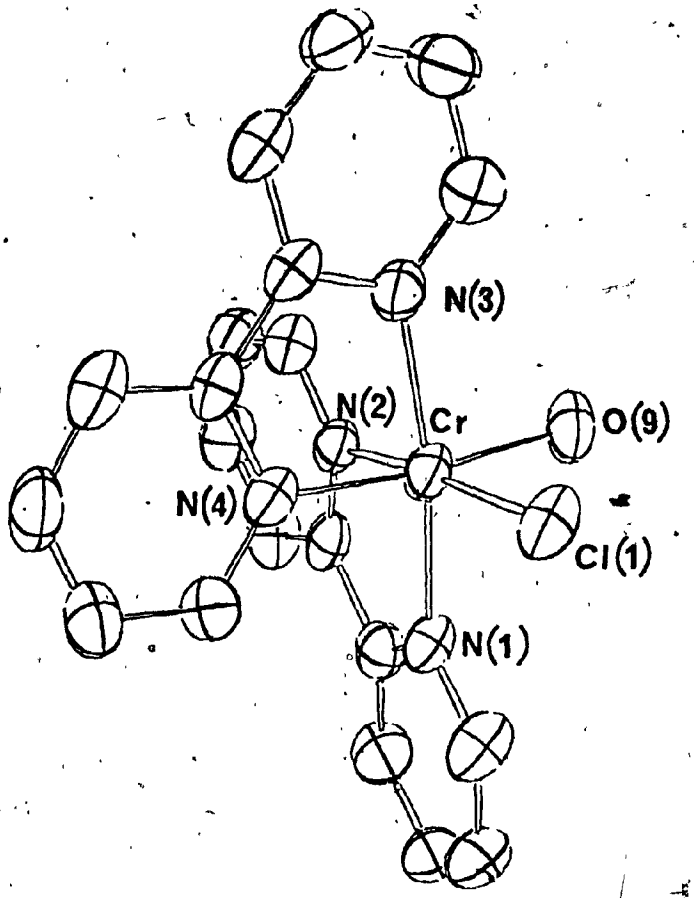

Figure 2.14. Geometry of the cis-$[Cr(bpy)_2(H_2O)Cl]^{2+}$ cation

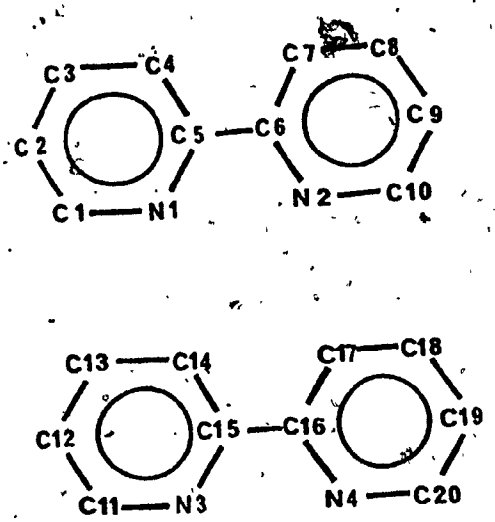

Figure 2.15. Molecular numbering scheme of $[Cr(bpy)_2(H_2O)Cl](ClO_4)_2.2H_2O$

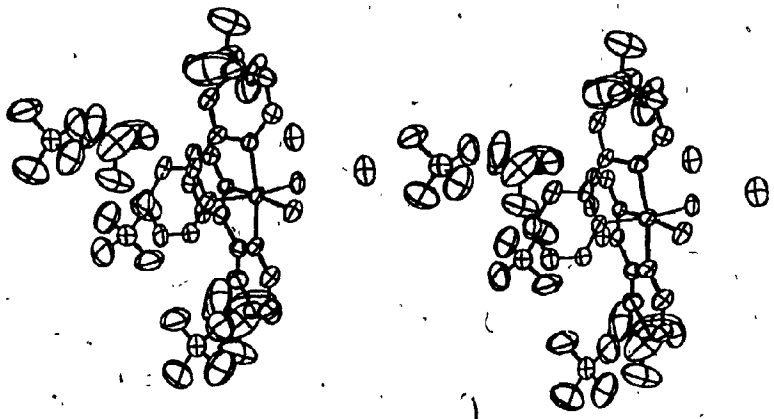

Figure 2.16. Stereoscopic view of the $[Cr(bpy)_2(H_2O)Cl](ClO_4)_2.H_2O$ complex

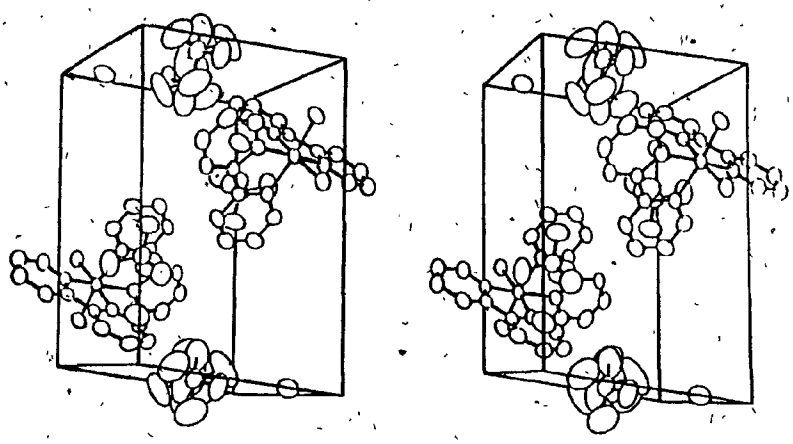

Figure 2.17. Unit cell packing of $[Cr(bpy)_2(H_2O)Cl](ClO_4)_2.2H_2O$ viewed approximately along the crystallographic c axis.

2.5 EPILOGUE

The study was not limited to the structures reported in this section. During this study, several polypyridyl complexes were attempted. To solve the mystery of the iridium-bipyridine complex [section-2.2], several anionic forms of the complex were tried, chloride, bromide, nitrate and perchlorate salts. Of these, the chloride salt was very poorly crystalline, we were unable to grow a single crystal suitable for diffraction studies. The bromide structure could not be completed. This compound crystallizes in monoclinic crystal form($\beta \simeq 90$), with probable space groups C2, Cm or C2/m. Iridium atom position was extracted from a three-dimensional Patterson map. A difference Fourier map phased on the Ir position gave two of the Br positions. Ir and both the Br atoms lie in special positions. From subsequent difference Fourier maps nothing could be identified. While this thesis was in preparation, the structure of the NO_3 salt was attempted; the work is in progress and seems promising.

Along with the $[Cr(terpy)_2](ClO_4)_3.H_2O$ (section-2.3), the structure of $[Cr(3,4,7,8\text{-}Me_4Phen)_2](ClO_4)_3.nH_2O$ was attempted. All attempts to crystallize this failed, hence it was not continued.

We were also interested in the structure of

$[Ru(bpy)_3]Cl_2.nH_2O$. This is because most of the photophysical and photochemical studies of Ru(II) complexes are centered on this chloride salt. This compound crystallizes in at least two different forms, monoclinic and hexagonal, neither form is very stable. The hexagonal form seems to be a little more stable than the monoclinic form. The monoclinic form transforms into the hexagonal form and the hexagonal form looses its crystallinity. Intensity data were collected for the hexagonal form. The ruthenium position was deduced from a three-dimensional Patterson synthesis. As in the case of the bromide salt of the iridium-bipyridyl complex, the difference Fourier maps were not interpretable. Due to the lack of time, further work on this and the bromide salt mentioned earlier, were not continued.

3.1 THE MOLECULAR STRUCTURES OF "$[Co_2LL_2(OH)_2]Br_4.9H_2O$" AND "$[Ni_2LL_2(H_2O)_2]Br_4.5H_2O$"

3.1.1 Introduction

Binuclear transition metal complexes with unpaired electrons are generally categorized into two main groups depending upon the strength of the metal-metal interaction [171]. In the strongly interacting type, the two metal atoms are in close proximity, usually with a metal-metal separation of less than 3.0 °A. Here relatively strong metal-metal bonds do occur, and the molecule as a whole displays simple diamagnetic behaviour for an even number of electrons, all paired. In the non-interacting type, the magnetic properties of the molecule are essentially unchanged from the paramagnetic monomer. Here the two metal atoms are fairly far apart, usually separated by a distance of greater than 6 °A. Between these two extreme groups another class of compounds can be defined. Here the two metal centers are separated by a distance of about 3 - 5 °A. No direct metal-metal bond exists, but weak coupling between the electrons of the two metal centers is possible. This leads to low-lying excited states. These states can be populated by thermal energies. The resulting magnetic behaviour of such a complex could be either anti-ferromagnetic or ferromagnetic, depending upon whether the spins are paired or parallel in the ground state, thus

these compounds show temperature dependent magnetic properties. A large number of such complexes have been studied, especially chromium and copper systems [140,172-179].

The magnetic interactions of this type of dimer have biological interest. The prosthetic group of hemocyanin, which is the oxygen carrier of certain animals such as arthropods and molluscs, incorporates a magnetically coupled Cu(II)·····Cu(II) system. Hemerythrin which is found in certain invertebrates, contains weakly interacting Fe(III)·····Fe(III) systems. To reach a better understanding about the magnetic interactions present in such systems, similar model compounds with different magnetic nuclei are being studied [180].

The magnetic properties of such binuclear transition metal complexes have also been shown to be dependent upon their structures. In the simplest case of Cu(II) complexes containing two hydroxo bridges the magnetic exchange parameter, J, has been found to be dependent upon the Cu-O-Cu bridging angle ϕ [181]. The value of J varies linearly with ϕ [182], decreasing with increasing ϕ. Attempts have been made to extend the above correlation to more complex systems, for eg. systems incorporating two Cr(III) centres [140,141,172,173]. Hodgson and co-workers have shown that in these systems, instead of a simple linear

relationship, a more complex dependance of J on ϕ exists. To establish such a relationship a large number of binuclear Cu(II) and Cr(III) systems have been characterized by x-ray crystallography.

While the detailed magnetic behaviour of many binuclear Cu(II) and Cr(III) systems have been studied, relatively few such studies on Co(II) and Ni(II) systems have been reported. In these systems also, exchange interactions may be expected to occur.

Attempts have also been made to design ligands which have a strong tendency to coordinate to two metal centres simultaneously, and to keep them in close proximity. Quadridentate amines [183] are suitable candidates for such work. The ligand 1,4-di(2'-pyridyl)aminophthalazine (I) was first reported in 1969 by Thompson and co-workers, [184].

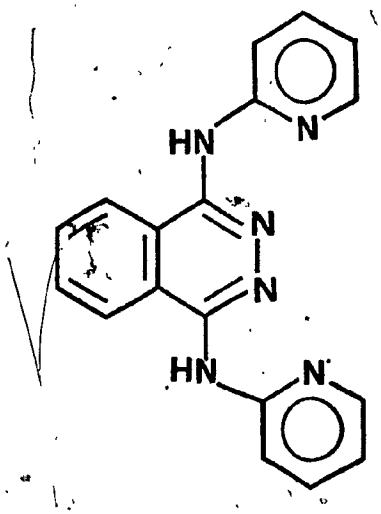

I

This could be conveniently prepared by condensing α-amino pyridine and iso-indoline in 2:1 molar ratio followed by the ring expansion of the resulting 1,3-di(2'-pyridyl)-iminoisoindoline with aqueous hydrazine. The reaction sequence is given in scheme 3.1.

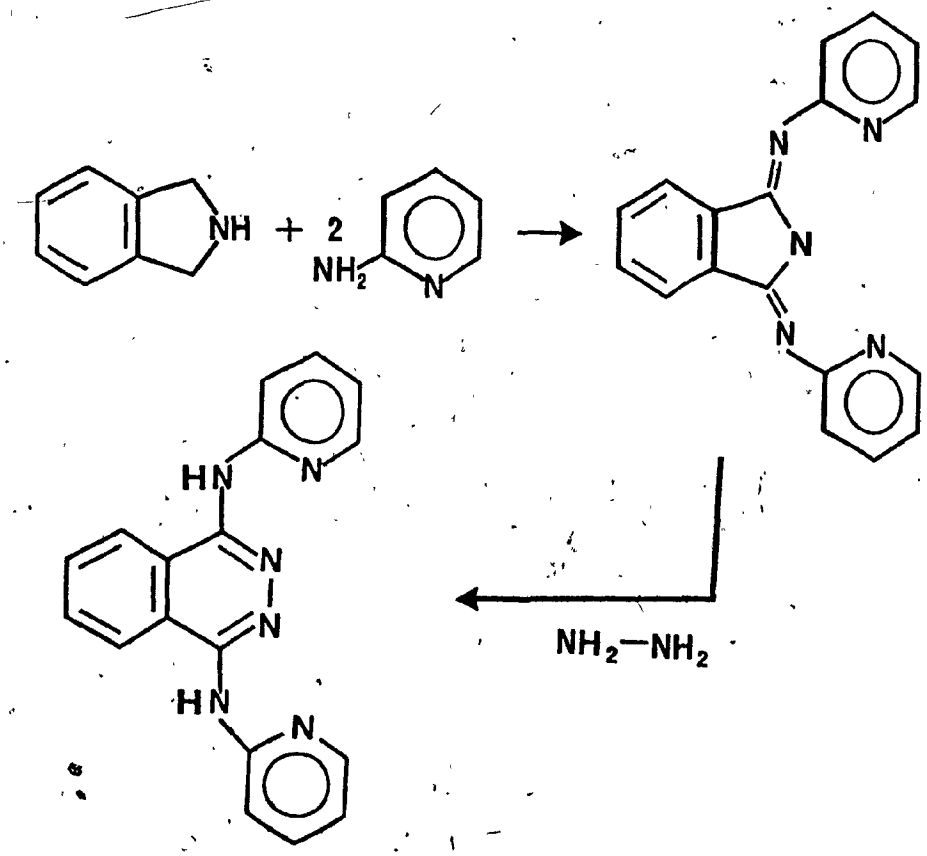

Scheme 3.1

The ligand might exist in at least 3 different tautomeric and 2 ionic forms as shown by figure 3.1.

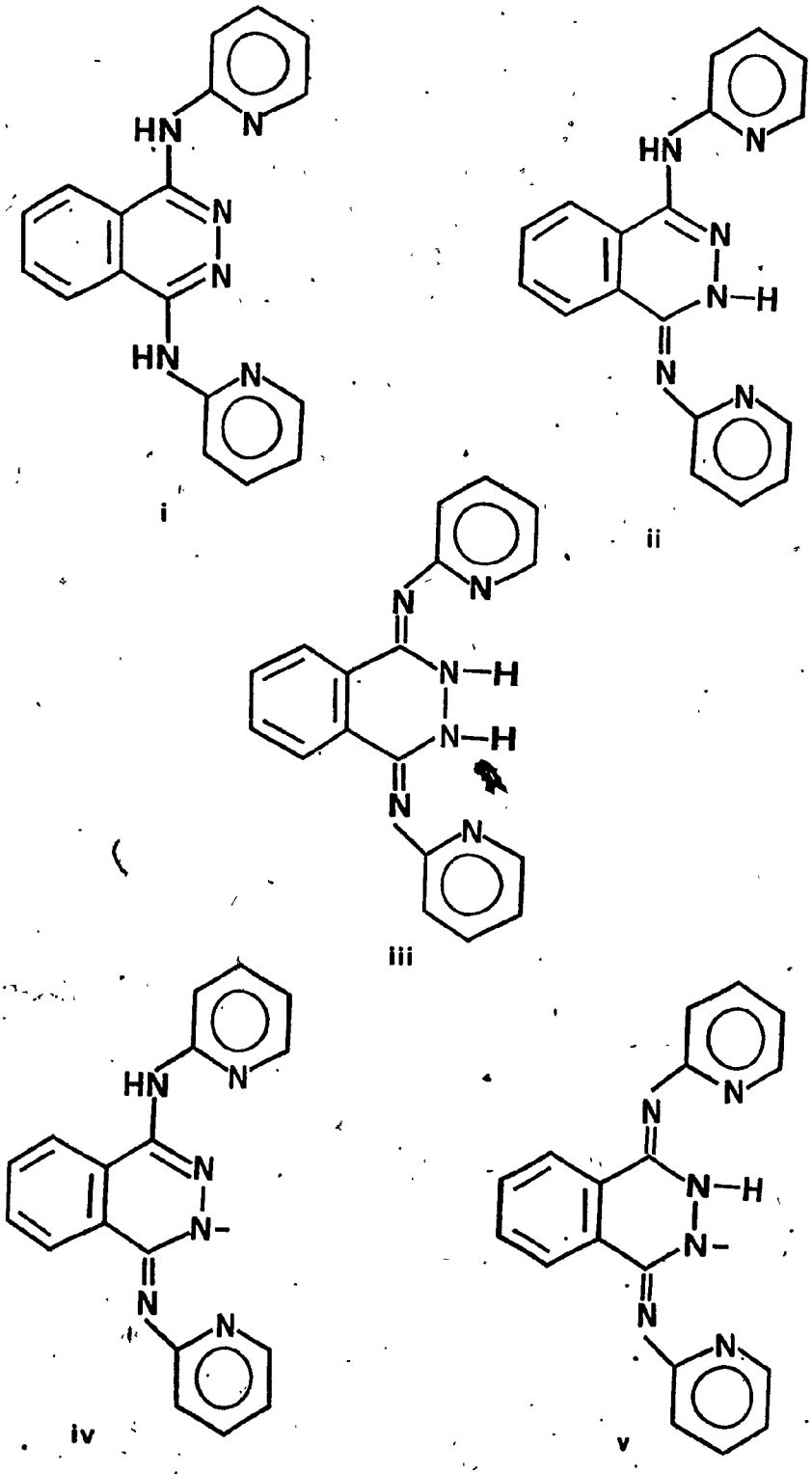

Figure 3.1

An x-ray structural investigation of a binuclear Cu complex containing L has revealed that the ligand exists in the tautomeric form (i), with both hydrogen atoms on exocyclic nitrogen atoms, rather than the tautomeric forms (ii) and (iii) [185]. Complexes containing the monoanionic ligand are not unknown [184]. In these complexes the anionic form (iv) rather than (v) is believed to be involved. Neutral and anionic ligand residues can be identified by their U.V spectra [184]. The lowest energy peak in the U.V spectrum of the neutral ligand species had been observed between 27 400 and 29 600 cm^{-1}, whilst in the anionic ligand complexes this occurs between 24 000 and 25 600 cm^{-1}.

The binuclear complex Co_2LBr_3 (II) was first reported by Lever, Thompson and Reiff in 1972 [183]. It consists of tetrahedrally coordinated binuclear Co(II) with a bridging bromide ion. The detailed magnetic behaviour of this compound has been reported, and consists of antiferromagnetically coupled Co(II) ions. When an aqueous solution of this complex upon standing in air for about two days, the colour changes from orange to dark brown. Dark brownish black crystals have been isolated, and show diamagnetic behaviour. Elemental analysis and detailed spectroscopic investigations have not indicated a definite structure but an octahedrally coordinated hydroxo-bridged binuclear Co(III) species consisting two 1,4-di(2'-pyridyl)

aminophthalazine (L) ligands has been proposed (III).

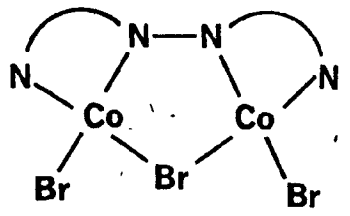

II

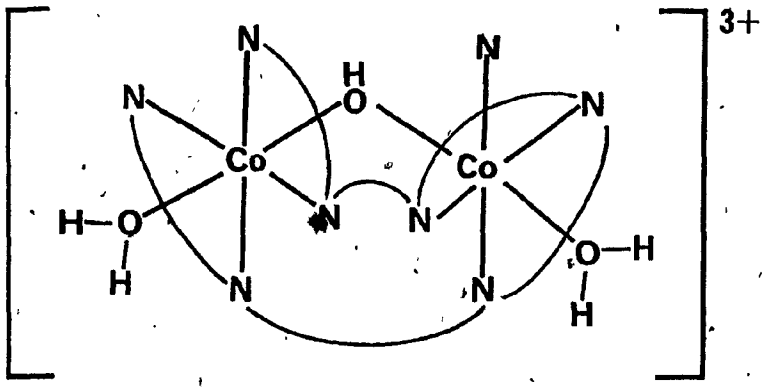

III

A paramagnetic binuclear Ni(II) complex, isolated from the direct reaction between the ligand and $NiBr_2$ has been characterized by spectroscopic methods to consist of two bridging diazine residues. The proposed structure is given below (IV).

No complex consisting two bridging diazine residues

derived from the ligand L has been characterized by X-ray crystallography [183-185], therefore the two crystal structure determinations described here were undertaken.

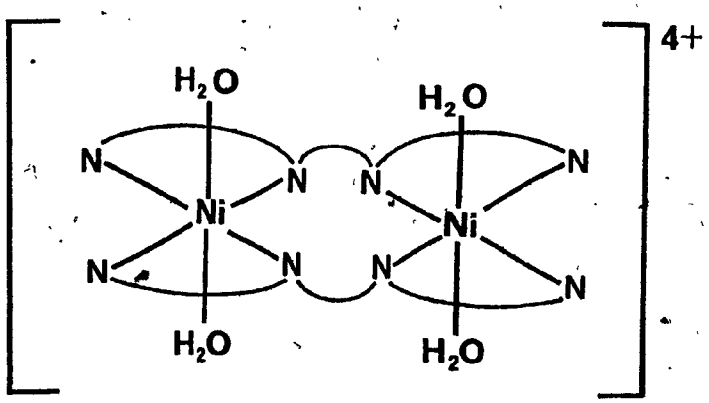

IV

3.1.1 Experimental

The Co Dimer

Preliminary Weissenberg and precession photographs showed orthorhombic symmetry with hkl; h+k = odd absent, and on 001; l odd absent. These data uniquely established the space group to be $C222_1$. Accurate cell dimensions were obtained on the diffractometer by centering 15 high angle reflections ($16 < 2\theta < 27$) and their Friedel equivalents in the detector aperture. Three sets of reflections of h k l, h-k-l and -h-k-l were collected for $3.5 < 2\theta < 40.0$. Three standards monitored showed random variation not more than 2%. The intensities were appropriately averaged and corrected for Lorentz and polarization effects. Out of 2843 independent reflections, 2029 with $I > 2\sigma(I)$ were used in the subsequent calculations. The structure was solved by direct methods: 129 reflections with $E \geq 1.60$ gave a Fourier synthesis from which positions of the Co and Br atoms could be determined. The remaining non-hydrogen atoms were subsequently found by a series of difference Fourier maps. All the non-hydrogen atoms were refined anisotropically by block-diagonal least-squares techniques to a final R = 5.01% and R_w = 6.10%. The signs of the anomalous dispersion correction were changed and the refinement continued. This gave a better discrepancy index. The enantiomer implied by this sign change was chosen as the

correct enantiomer on the basis of the Hamilton's test [103]. The refinement converged at R = 4.36% and R_w = 5.48%. A hydrogen atom on the bridging oxygen O(1), was clearly visible in a final difference Fourier map. No attempt was made to locate the other hydrogen atoms.

The Ni Dimer

Preliminary photographs indicated monoclinic crystal system with; on h0l; l = odd absent, and on 0k0; k odd absent. These data uniquely established the space group to be $P2_1/c$. Accurate cell dimensions were obtained on the four circle diffractometer by centering 15 reflections and their Friedel equivelents ($19 < 2\theta < 30$). Data were collected for $\pm h+k+l$. Three standards monitored after every 50 reflections showed a random variation of not more than 4%. The data were corrected for Lorentz and polarization effects. Of 5674 reflections collected, 2916 with $I > 2\sigma(I)$ were used in the subsequent calculations. The structure was solved by the direct method. The two Ni and three Br^- positions were obtained from a Fourier synthesis based on 364 reflections with $E \geq 1.85$. These positions were refined by the full-matrix least-squares technique. Structure factor calculations followed by difference Fourier syntheses yielded most of the non-hydrogen atoms. The 4th Br^- was found to be disordered between two sites. The occupancy was refined to a total of 0.99. Due to memory

restrictions the whole structure could not be refined anisotropically at the same time, hence the refinement was done in parts. The refinement converged at $R = 7.28\%$ and $R_w = 9.42\%$. A final difference Fourier map was featureless.

3.1.3 Results and Discussion

The structures of the two dimers are depicted in figures 3.2 and 3.3, and the molecular numbering schemes are given in figures 3.4 and 3.5. The unit cell constants are tabulated in table A.2. The density measurements of the Co dimer indicated 4 molecular formula units per unit cell. Since the general positions in space group $C222_1$ are 8 fold, with only 4 molecules per unit cell, the dimer is required to lie on a 2-fold axis. The structure consists of two crystallographically equivalent Co(III) atoms linked by two symmetrically bridging hydroxy groups and by the two adjacent nitrogen atoms of a diazine ring. The phthalazine moiety containing this diazine residue acts in its full capacity; ie. as a quadridentate ligand. In addition each cobalt atom is linked to another phthalazine group which acts in a bidentate fashion. The geometry around each cobalt atom is approximately octahedral, the two octahedra share a single face. A closer view of the coordination around Co atoms is shown in figure 3.6.

The bonding in the Ni dimer is virtually identical to that of the Co complex, except for the two oxygen bridges. The two oxygen bridges present in the Ni complex cannot be clearly identified as either aquo or hydroxo bridges, but a di-aquo bridge is more favoured. As in the case of the Co complex, the geometry around each Ni is approximately

octahedral. A closer view of the coordination around Ni atoms is shown in figure 3.7.

The mean Co-N distance is 1.92(4) A. Assuming a covalent radius of 0.70 °A for N , covalent radius Co(III) could be calculated as 1.22 °A. If a Co-Co single bond is present the Co····Co distance should be close to 2.4 °A. The observed Co····Co distance of 2.795(3) °A and the approximately octahedral geometry around each Co atom suggests no direct bonding interaction between the two metal atoms. The mean Ni-N distance is 2.07(2) °A. By a similar procedure a covalent radius of 1.37 °A could be deduced for Ni(II). If a Ni-Ni single bond is present, the Ni····Ni distance should be close to 2.74 °A, but the observed Ni····Ni distance of 3.152(1) °A and the approximate octahedral coordination around each Ni atom suggests no direct bonding interaction between the two Ni atoms.

The mean Co-N and Ni-N distances observed are comparable to the other known Co-N and Ni-N distances found in similar dimers, which average to 1.93(2) °A and 2.06(3) °A [186-191], respectively.

The mean ring C-C, C-N and N-N distances are 1.40(4), 1.36(4) and 1.37(4), °A respectively. They show excellent agreement with the values reported by Morongue and Lingafelter [185] for the same ligand.

The M-O-M bridging angles are 93.7° for the Co complex and 94.0° for the Ni complex. These are slightly smaller than the other known doubly bridging M-O-M angles reported in the literature [140,142,173,175,188,192].

The observed structures are very much different from those formulated by spectroscopic and elemental analysis. In retrospect, it seems improbable that there would be two planar ligand residues coordinated to both metal centres, as proposed, because of steric crowding.

The ligand is markedly non-planar. The least-squares planes calculated for the individual pyridyl groups and phthalazine residues are tabulated in tables 3.3 and 3.4. The dihedral angles between the phthalazines and the adjacent pyridyl groups vary from 7.4° to 34.1°. The greatest deviation is observed when the pyridyl group takes part in bonding to the metal atom along with the adjacent diazine nitrogen atom. In such cases the dihedral angles vary from 24.6° to 34.1° : in non-bonding cases this show minor variation from 7.4° to 11.4°.

There is an extensive intramolecular H-bonding network present in both structures. This is depicted in figures 3.8 and 3.9. Non-ligating N atoms of the diazine and pyridyl residues along with the H atoms of the bridging oxygens take part in this H-bonding scheme. In the Co complex,

O(1)·····N(6) and O(1)·····N(2) distances are 2.94 and 2.61 °A, respectively. In the Ni dimer O(1)·····N(3C), O(1)·····N(7C), O(2)·····N(2A) and O(2)·····N(6A) distances are 2.64, 2.78, 2.64 and 2.78 °A, respectively.

The important bond lengths and angles are tabulated in tables 3.1 and 3.2. A stereo view of the dimers and stereo packing diagrams of the molecules are depicted in figures 3.10-3.13. Final positional and thermal parameters are listed in tables A·6-A·7.

Table 3.1

Bond Distances and Angles of $[Co_2LL'_2(OH)_2]Br_4.9H_2O$,

standard deviation is given in parenthesis.

Bond Distances in Angstroms.

Co-O(1)	1.902(7)	C(13)-C(14)	1.430(22)
Co-O(1)	1.929(6)	C(14)-C(15)	1.348(19)
Co-N(3)	1.885(9)	C(15)-N(6)	1.338(15)
Co-N(7)	1.951(8)	N(6)-C(11)	1.318(16)
Co-N(8)	1.880(8)	N(5)-C(16)	1.402(13)
Co-N(10)	1.956(7)	C(16)-C(17)	1.373(14)
C(1)-N(2)	1.282(13)	C(17)-C(18)	1.328(15)
C(1)-C(10)	1.447(16)	C(18)-C(19)	1.435(17)
C(1)-N(4)	1.378(14)	C(19)-C(20)	1.353(15)
N(2)-N(3)	1.316(11)	C(20)-N(7)	1.376(14)
N(3)-C(4)	1.317(13)	N(8)-N(8')	1.377(15)
C(4)-C(9)	1.423(15)	N(8)-C(21)	1.298(12)
C(4)-N(5)	1.345(13)	C(22)-C(22')	1.428(23)
C(5)-C(9)	1.417(16)	C(22)-C(23)	1.361(15)
C(5)-C(6)	1.389(18)	C(23)-C(24)	1.420(14)
C(6)-C(7)	1.369(20)	C(24)-C(24')	1.432(19)
C(7)-C(8)	1.468(20)	C(21)-C(24)	1.428(13)
C(8)-C(10)	1.408(16)	C(21)-N(9)	1.351(12)
C(9)-C(10)	1.405(17)	N(9)-C(25)	1.419(13)
N(4)-C(11)	1.403(16)	C(25)-C(26)	1.413(15)
C(11)-C(12)	1.440(17)	C(26)-C(27)	1.418(18)
C(12)-C(13)	1.432(19)	C(27)-C(28)	1.434(18)

C(28)-C(29)	1.353(19)	C(29)-N(10)	1.435(14)

Bond Angles in Degrees.

N(3)-Co-N(7)	90.1(4)	Co-O(1)-Co	93.7(3)
N(3)-Co-N(8)	177.4(4)	N(2)-C(1)-C(10)	121.1(10)
N(3)-Co-N(10)	91.8(4)	N(2)-C(1)-N(4)	121.3(10)
N(3)-Co-O(1)	93.5(3)	N(4)-C(1)-C(10)	117.5(10)
N(3)-Co-O(1')	93.1(3)	C(1)-N(2)-N(3)	123.4(9)
N(7)-Co-N(8)	92.4(4)	N(2)-N(3)-C(4)	120.7(8)
N(7)-Co-N(10)	91.8(4)	N(3)-C(4)-C(9)	120.2(10)
N(7)-Co-O(1)	172.3(3)	N(5)-C(4)-C(9)	117.7(10)
N(7)-Co-O(1')	92.4(3)	C(4)-C(9)-C(10)	118.1(10)
N(8)-Co-N(10)	87.3(3)	C(5)-C(9)-C(10)	118.7(10)
N(8)-Co-O(1)	84.1(3)	C(9)-C(5)-C(6)	119.8(11)
N(8)-Co-O(1')	87.6(3)	C(5)-C(6)-C(7)	122.3(12)
N(10)-Co-O(1)	94.9(3)	C(6)-C(7)-C(8)	119.6(11)
N(10)-Co-O(1')	173.5(3)	C(7)-C(8)-C(10)	116.9(12)
O(1)-Co-O(1')	80.6(3)	C(8)-C(10)-C(9)	122.4(12)
Co-N(3)-N(2)	112.8(6)	C(1)-C(10)-C(9)	115.4(10)
Co-N(3)-C(4)	126.1(7)	C(1)-N(4)-C(11)	123.6(10)
Co-N(8)-N(8')	111.7(6)	N(4)-C(11)-C(12)	111.6(11)
Co-N(8)-C(21)	128.5(6)	N(4)-C(11)-N(6)	123.7(10)
Co-N(10)-C(29)	116.4(7)	N(6)-C(11)-C(12)	124.6(12)
Co-N(10)-C(25)	122.6(7)	C(11)-C(12)-C(13)	112.8(13)
Co-N(7)-C(16)	124.6(7)	C(12)-C(13)-C(14)	120.4(12)
Co-N(7)-C(20)	117.2(7)	C(13)-C(14)-C(15)	119.7(12)

C(14)-C(15)-N(6)	121.4(12)	C(22')-C(22)-C(23)	121.7(10)
C(4)-N(5)-C(16)	127.3(9)	C(22)-C(23)-C(24)	118.1(10)
N(5)-C(16)-N(7)	117.8(9)	C(23)-C(24)-C(24')	120.0(9)
N(5)-C(16)-C(17)	119.2(9)	C(21)-C(24)-C(24')	116.0(9)
N(7)-C(16)-C(17)	122.9(10)	C(21)-N(9)-C(25)	122.4(8)
C(16)-C(17)-C(18)	118.4(10)	N(9)-C(25)-N(10)	120.7(9)
C(17)-C(18)-C(19)	121.4(10)	N(9)-C(25)-C(26)	114.6(9)
C(18)-C(19)-C(20)	115.7(10)	N(10)-C(25)-C(26)	124.6(10)
C(19)-C(20)-N(7)	123.0(10)	C(25)-C(26)-C(27)	114.4(11)
C(16)-N(7)-C(20)	117.5(9)	C(26)-C(27)-C(28)	121.4(10)
N(8)-C(21)-C(24)	123.3(9)	C(27)-C(28)-C(29)	120.1(11)
N(8)-C(21)-N(9)	118.8(9)	C(28)-C(29)-N(10)	118.2(11)
C(24)-C(21)-N(9)	117.8(9)	C(25)-N(10)-C(29)	121.0(8)
C(21)-N(8)-N(8')	119.8(8)		

Table 3.2

Bond Distances and Angles of $[Ni_2LL'_2(H_2O)_2]Br_4.5H_2O$,

standard deviation is given in parenthesis.

Bond Distances in Angstroms.

Ni(1)-O(1)	2.139(10)	C(7)-C(8)	1.444(30)
Ni(1)-O(2)	2.166(11)	C(8)-C(10)	1.458(27)
Ni(1)-N(3B)	2.075(13)	C(1)-C(10)	1.405(26)
Ni(1)-N(7B)	2.070(15)	C(1)-N(4)	1.392(23)
Ni(1)-N(2C)	2.056(14)	N(4)-C(11)	1.417(25)
Ni(1)-N(6C)	2.119(13)	C(11)-C(12)	1.428(28)
Ni(2)-O(1)	2.173(11)	C(12)-C(13)	1.413(33)
Ni(2)-O(2)	2.143(10)	C(13)-C(14)	1.346(31)
Ni(2)-N(3A)	2.014(14)	C(14)-C(15)	1.444(29)
Ni(2)-N(7A)	2.084(13)	C(15)-N(6)	1.337(24)
Ni(2)-N(2B)	2.085(14)	N(6)-C(11)	1.288(25)
Ni(2)-N(6B)	2.082(14)	C(4)-N(5)	1.382(23)
Molecule A		N(5)-C(16)	1.359(24)
C(1)-N(2)	1.294(23)	C(16)-C(17)	1.480(27)
N(2)-N(3)	1.420(19)	C(17)-C(18)	1.360(30)
N(3)-C(4)	1.331(22)	C(18)-C(19)	1.488(30)
C(4)-N(5)	1.382(23)	C(19)-C(20)	1.395(26)
C(4)-C(9)	1.416(26)	C(20)-N(7)	1.392(24)
C(9)-C(10)	1.450(27)	N(7)-C(16)	1.372(24)
C(5)-C(9)	1.375(26)	Molecule B	
C(5)-C(6)	1.390(27)	C(1)-N(2)	1.303(22)
C(6)-C(7)	1.478(33)	N(2)-N(3)	1.408(19)

N(3)-C(4)	1.285(20)
C(4)-N(5)	1.388(22)
C(4)-C(9)	1.423(23)
C(9)-C(10)	1.499(25)
C(5)-C(9)	1.451(26)
C(5)-C(6)	1.444(27)
C(6)-C(7)	1.367(28)
C(7)-C(8)	1.408(26)
C(8)-C(10)	1.436(24)
C(1)-C(10)	1.454(25)
C(1)-N(4)	1.377(23)
N(4)-C(11)	1.436(24)
C(11)-C(12)	1.439(26)
C(12)-C(13)	1.425(29)
C(13)-C(14)	1.374(28)
C(14)-C(15)	1.380(27)
C(15)-N(6)	1.357(24)
N(6)-C(11)	1.340(23)
C(4)-N(5)	1.388(22)
N(5)-C(16)	1.449(24)
C(16)-C(17)	1.446(26)
C(17)-C(18)	1.358(28)
C(18)-C(19)	1.412(28)
C(19)-C(20)	1.402(28)
C(20)-N(7)	1.360(24)
N(7)-C(16)	1.338(24)

Molecule C

C(1)-N(2)	1.318(20)
N(2)-N(3)	1.340(18)
N(3)-C(4)	1.319(22)
C(4)-N(5)	1.371(21)
C(4)-C(9)	1.447(23)
C(9)-C(10)	1.406(25)
C(5)-C(9)	1.465(26)
C(5)-C(6)	1.379(30)
C(6)-C(7)	1.442(31)
C(7)-C(8)	1.400(28)
C(8)-C(10)	1.416(26)
C(1)-C(10)	1.401(23)
C(1)-N(4)	1.371(21)
N(4)-C(11)	1.377(24)
C(11)-C(12)	1.416(24)
C(12)-C(13)	1.383(26)
C(13)-C(14)	1.417(28)
C(14)-C(15)	1.377(26)
C(15)-N(6)	1.331(21)
N(6)-C(11)	1.370(21)
C(4)-N(5)	1.371(21)
N(5)-C(16)	1.410(24)
C(16)-C(17)	1.411(26)
C(17)-C(18)	1.410(28)
C(18)-C(19)	1.308(32)
C(19)-C(20)	1.369(30)

C(20)-N(7)	1.385(24)	N(7)-C(16)	1.380(27)

Bond Angles in Degrees.

O(1)-Ni(1)-O(2)	79.0(4)	N(2B)-Ni(2)-N(3A)	172.0(5)
O(1)-Ni(1)-N(3B)	82.7(5)	N(6B)-Ni(2)-N(7A)	96.5(6)
O(1)-Ni(1)-N(6C)	170.8(5)	N(6B)-Ni(2)-N(3A)	95.2(6)
O(1)-Ni(1)-N(7B)	93.4(5)	N(7A)-Ni(2)-N(3A)	88.0(6)
O(1)-Ni(1)-N(2C)	90.3(5)	Ni(1)-O(1)-Ni(2)	94.0(4)
O(2)-Ni(1)-N(3B)	87.7(5)	Ni(1)-O(2)-Ni(2)	94.0(4)
O(2)-Ni(1)-N(6C)	92.1(5)	Ni(1)-N(2C)-C(1C)	129.6(11)
O(2)-Ni(1)-N(7B)	170.1(4)	Ni(1)-N(2C)-N(3C)	108.1(10)
O(2)-Ni(1)-N(2C)	90.2(5)	Ni(1)-N(7B)-C(16B)	122.9(12)
N(3B)-Ni(1)-N(6C)	99.1(5)	Ni(1)-N(7B)-C(20B)	117.8(12)
N(3B)-Ni(1)-N(7B)	85.2(5)	Ni(1)-N(6C)-C(11C)	121.9(11)
N(3B)-Ni(1)-N(2C)	172.9(5)	Ni(1)-N(6C)-C(15C)	116.1(11)
N(6C)-Ni(1)-N(7B)	95.7(6)	Ni(1)-N(3B)-C(4B)	126.6(11)
N(6C)-Ni(1)-N(2C)	87.8(5)	Ni(1)-N(3B)-N(2B)	112.7(9)
N(7B)-Ni(1)-N(2C)	96.1(6)	Ni(2)-N(3A)-N(2A)	109.5(10)
O(1)-Ni(2)-O(2)	78.7(4)	Ni(2)-N(3A)-C(4A)	132.6(12)N
O(1)-Ni(2)-N(2B)	87.5(5)	Ni(2)-N(7A)-C(16A)	123.2(12)
O(1)-Ni(2)-N(6B)	171.1(5)	Ni(2)-N(7A)-C(20A)	115.8(11)
O(1)-Ni(2)-N(7A)	91.0(5)	Ni(2)-N(6B)-C(15B)	120.4(12)
O(2)-Ni(2)-N(2B)	81.2(4)	Ni(2)-N(6B)-C(11B)	122.0(12)
O(2)-Ni(2)-N(7A)	169.6(5)	Ni(2)-N(2B)-N(3B)	114.0(9)
O(2)-Ni(2)-N(3A)	90.8(5)	Ni(2)-N(2B)-C(1B)	126.2(12)
N(2B)-Ni(2)-N(7A)	99.6(6)	Molecule A	

N(2)-C(1)-N(4)	117.6(16)	N(5)-C(16)-C(17)	115.4(16)
C(10)-C(1)-N(4)	119.4(16)	N(7)-C(16)-C(17)	119.1(17)
C(10)-C(1)-N(2)	122.9(17)	C(16)-C(17)-C(18)	119.0(18)
C(1)-N(2)-N(3)	120.5(14)	C(17)-C(18)-C(19)	121.8(18)
N(2)-N(3)-C(4)	117.8(14)	C(18)-C(19)-C(20)	115.7(19)
N(3)-C(4)-C(9)	125.3(17)	C(19)-C(20)-N(7)	123.2(18)
N(3)-C(4)-N(5)	118.3(16)	C(16)-N(7)-C(20)	121.0(14)
N(5)-C(4)-C(9)	116.4(16)	Molecule B	
C(4)-C(9)-C(10)	113.8(16)	N(2)-C(1)-N(4)	119.7(16)
C(5)-C(9)-C(10)	122.5(17)	C(10)-C(1)-N(4)	116.9(15)
C(9)-C(5)-C(6)	117.2(19)	C(10)-C(1)-N(2)	123.4(16)
C(5)-C(6)-C(7)	124.7(18)	C(1)-N(2)-N(3)	119.5(14)
C(6)-C(7)-C(8)	117.3(20)	N(2)-N(3)-C(4)	119.8(13)
C(7)-C(8)-C(10)	117.3(20)	N(3)-C(4)-C(9)	123.3(15)
C(1)-C(10)-C(9)	118.8(16)	N(3)-C(4)-N(5)	119.3(14)
C(8)-C(10)-C(9)	120.7(17)	N(5)-C(4)-C(9)	117.3(14)
C(1)-N(4)-C(11)	127.2(15)	C(4)-C(9)-C(10)	118.3(15)
N(4)-C(11)-C(12)	113.6(18)	C(5)-C(9)-C(10)	119.5(16)
N(4)-C(11)-N(6)	123.5(16)	C(9)-C(5)-C(6)	114.6(18)
N(6)-C(11)-C(12)	122.8(19)	C(5)-C(6)-C(7)	123.9(18)
C(11)-C(12)-C(13)	116.4(20)	C(6)-C(7)-C(8)	122.6(17)
C(12)-C(13)-C(14)	121.9(21)	C(7)-C(8)-C(10)	114.5(16)
C(13)-C(14)-C(15)	116.3(20)	C(1)-C(10)-C(9)	115.2(15)
C(14)-C(15)-N(6)	122.4(19)	C(8)-C(10)-C(9)	124.6(16)
C(11)-N(6)-C(15)	120.2(16)	C(1)-N(4)-C(11)	124.9(15)
C(4)-N(5)-C(16)	129.5(15)	N(4)-C(11)-C(12)	114.8(16)
N(5)-C(16)-N(7)	125.4(16)	N(4)-C(11)-N(6)	122.6(16)

N(6)-C(11)-C(12)	122.5(17)	C(5)-C(9)-C(10)	120.9(16)
C(11)-C(12)-C(13)	118.2(18)	C(9)-C(5)-C(6)	119.2(18)
C(12)-C(13)-C(14)	117.1(18)	C(5)-C(6)-C(7)	118.4(19)
C(13)-C(14)-C(15)	121.4(18)	C(6)-C(7)-C(8)	123.0(19)
C(14)-C(15)-N(6)	123.1(17)	C(7)-C(8)-C(10)	118.5(17)
C(11)-N(6)-C(15)	117.6(15)	C(1)-C(10)-C(9)	118.4(15)
C(4)-N(5)-C(16)	124.8(15)	C(8)-C(10)-C(9)	119.7(15)
N(5)-C(16)-N(7)	122.0(16)	C(1)-N(4)-C(11)	131.3(14)
N(5)-C(16)-C(17)	116.2(16)	N(4)-C(11)-C(12)	118.4(15)
N(7)-C(16)-C(17)	121.7(17)	N(4)-C(11)-N(6)	122.3(14)
C(16)-C(17)-C(18)	119.2(17)	N(6)-C(11)-C(12)	119.2(15)
C(17)-C(18)-C(19)	118.7(18)	C(11)-C(12)-C(13)	12.1(17)
C(18)-C(19)-C(20)	120.0(17)	C(12)-C(13)-C(14)	115.0(18)
C(19)-C(20)-N(7)	121.1(17)	C(13)-C(14)-C(15)	122.3(18)
C(16)-N(7)-C(20)	119.3(16)	C(14)-C(15)-N(6)	120.8(16)
Molecule C		C(11)-N(6)-C(15)	120.6(14)
N(2)-C(1)-N(4)	118.3(14)	C(4)-N(5)-C(16)	127.2(15)
C(10)-C(1)-N(4)	120.6(14)	N(5)-C(16)-N(7)	119.2(15)
C(10)-C(1)-N(2)	121.0(15)	N(5)-C(16)-C(17)	116.7(18)
C(1)-N(2)-N(3)	121.5(14)	N(7)-C(16)-C(17)	124.0(18)
N(2)-N(3)-C(4)	122.1(14)	C(16)-C(17)-C(18)	115.3(20)
N(3)-C(4)-C(9)	119.6(15)	C(17)-C(18)-C(19)	121.7(18)
N(3)-C(4)-N(5)	122.1(15)	C(18)-C(19)-C(20)	121.3(19)
N(5)-C(4)-C(9)	118.3(15)	C(19)-C(20)-N(7)	122.2(19)
C(4)-C(9)-C(10)	117.1(15)	C(16)-N(7)-C(20)	115.0(16)

Table 3.3

Equation of the plane	$0.0040x - 0.1204y + 0.9927z = 5.4155$					
Atoms	C11	C12	C13	C14	C15	N5
Deviation from the plane °A	.012	.007	-.007	.014	-.013	.002
Equation of the plane	$0.5957x - 0.2984y + 0.7458z = 7.9918$					
Atoms	C16	C17	C18	C19	C20	N7
Deviation from the plane °A	.040	.016	-.062	.053	-.002	-.046
Equation of the plane	$0.2932x - 0.9554y + 0.0358z = -4.2701$					
Atoms	C25	C26	C27	C28	C29	N10
Deviation from the plane °A	-.022	.017	-.012	.011	.014	.020
Equation of the plane	$-0.0445x - 0.8887y + 0.4564z = -3.282$					
Atoms	C21	C22	C23	C24	N8	
Deviation from the plane °A	.028	.021	-.025	-.017	-.007	

Equation of the plane	$0.1433x - 0.1598y + 0.9767z = 6.6681$									
Atoms	C1	N2	N3	C4	C5	C6	C7	C8	C9	C10
Deviation from the Plane °A	-.023	.098	.090	-.102	-.012	.113	.038	-.054	-.075	-.072

Table 3.4

Equation of the plane	$-0.0380x - 0.9966y + 0.0734z = -6.0399$									
Atoms	C1A	N2A	N3A	C4A	C5A	C6A	C7A	C8A	C9A	C10A
Deviation from the Plane A	-.048	-.072	.083	.075	-.098	-.014	.070	.033	-.028	.001
Equation of the plane	$-0.6290x + 0.5703y + 0.5284z = 12.006$									
Atoms	C1B	N2B	N3B	C4B	C5B	C6B	C7B	C8B	C9B	C10B
Deviation from the Plane A	-.037	-.011	.089	-.004	-.042	.033	.025	.033	-.047	-.037
Equation of the plane	$-0.0371x + 0.9992y + 0.0061z = 2.857$									
Atoms	C1C	N2C	N3C	C4C	C5C	C6C	C7C	C8C	C9C	C10C
Deviation from the Plane A	-.072	-.007	.098	.034	-.080	.001	.097	.028	-.042	-.057

Equation of the plane	$0.0475x - 0.9845y + 0.1688z = -4.422$					
Atoms	C11A	C12A	C13A	C14A	C15A	N6A
Deviation from the plane A	.012	-.007	-.007	.015	-.011	-.002

Equation of the plane	$0.8756x + 0.0410y + 0.4812z = 11.420$					
Atoms	C11B	C12B	C13B	C14B	C15B	N6B
Deviation from the plane A	.006	.012	-.019	.008	.012	-.018

Equation of the plane	$-0.1696x + 0.9014y + 0.3984z = 3.260$					
Atoms	C11C	C12C	C13C	C14C	C15C	N6C
Deviation from the plane A	.009	.019	-.023	-.001	-.013	.009

Equation of the plane	$-0.1271x - 0.8940y + 0.4297z = -4.925$					
Atoms	C16A	C17A	C18A	C19A	C20A	N7A
Deviation from the plane A	.025	-.026	.003	.024	-.027	.002
Equation of the plane	$0.7610x + 0.0605y + 0.6459z = 13.05$					
Atoms	C16B	C17B	C18B	C19B	C20B	N7B
Deviation from the plane A	.003	-.009	.002	.010	-.016	.009
Equation of the plane	$-0.0230x - 0.9830y + 0.1824z = -1.976$					
Atoms	C16C	C17C	C18C	C19C	C20C	N7C
Deviation from the plane A	.020	.013	-.028	.007	.027	-.040

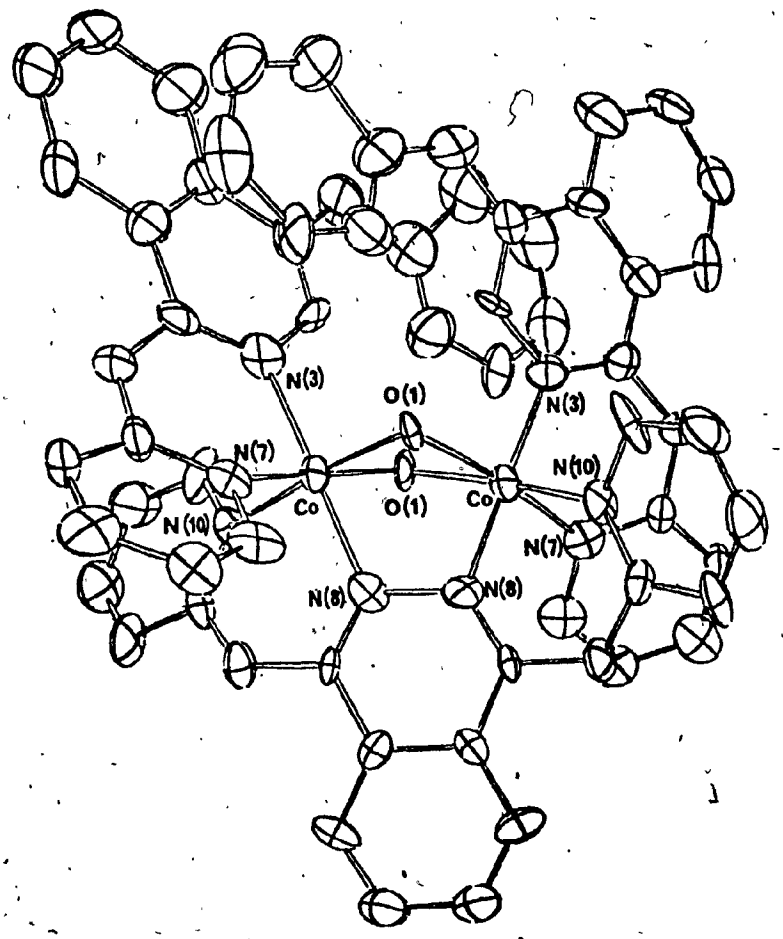

Figure 3.2. Geometry of the $[Co_2LL'_2(\mu\text{-}OH)_2]^{4+}$ cation

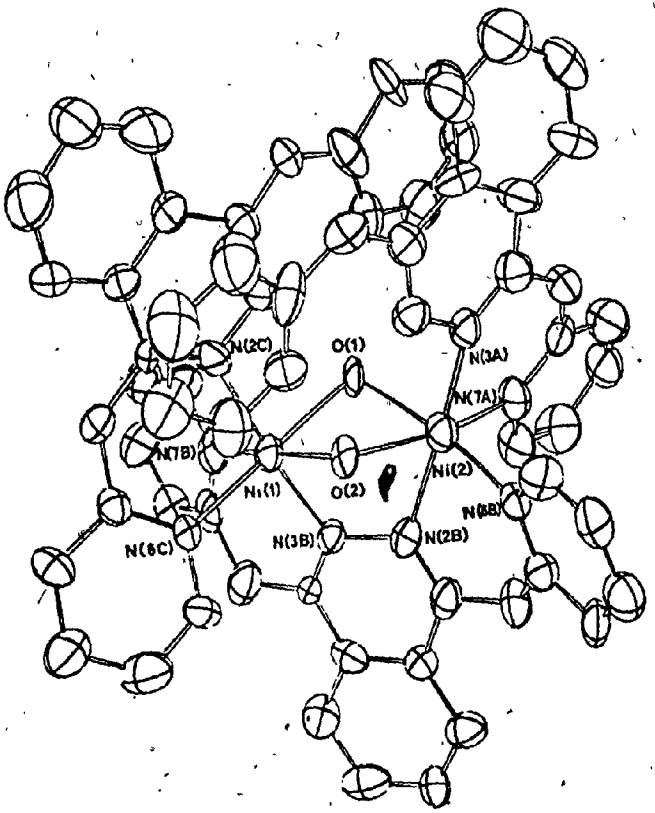

Figure 3.3. Geometry of the $[Ni_2LL'_2(\mu\text{-}H_2O)_2]^{4+}$ cation

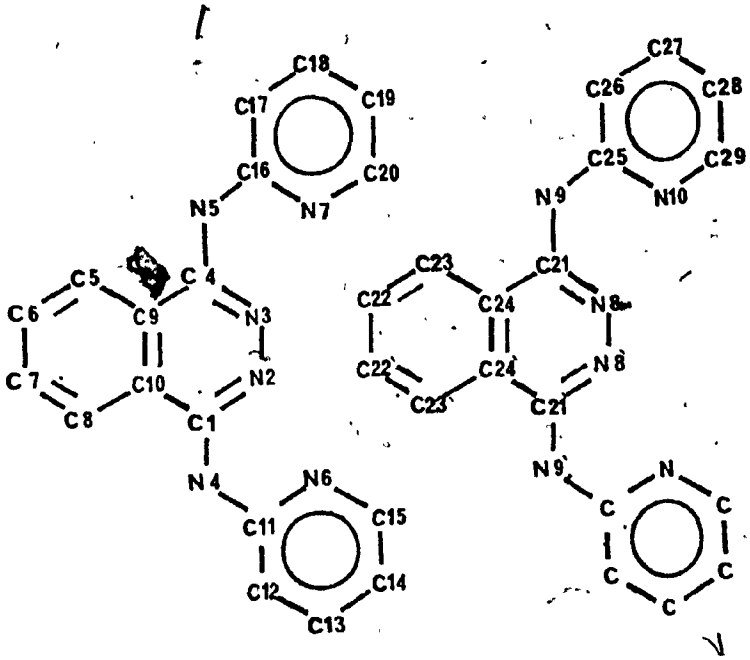

Figure 3.4. Molecular numbering scheme of the $[Co_2LL'_2(\mu\text{-}OH)_2]^{4+}$ cation

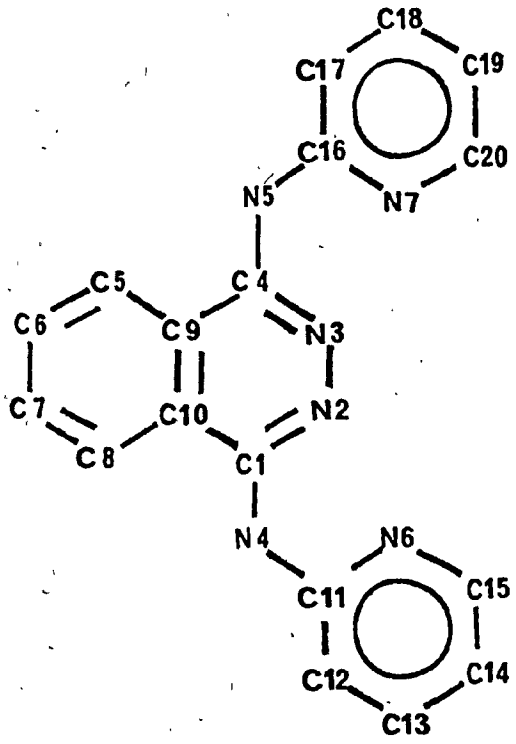

Figure 3.5. Molecular numbering scheme of the $[Ni_2LL'_2(\mu\text{-}H_2O)_2]^{4+}$ cation

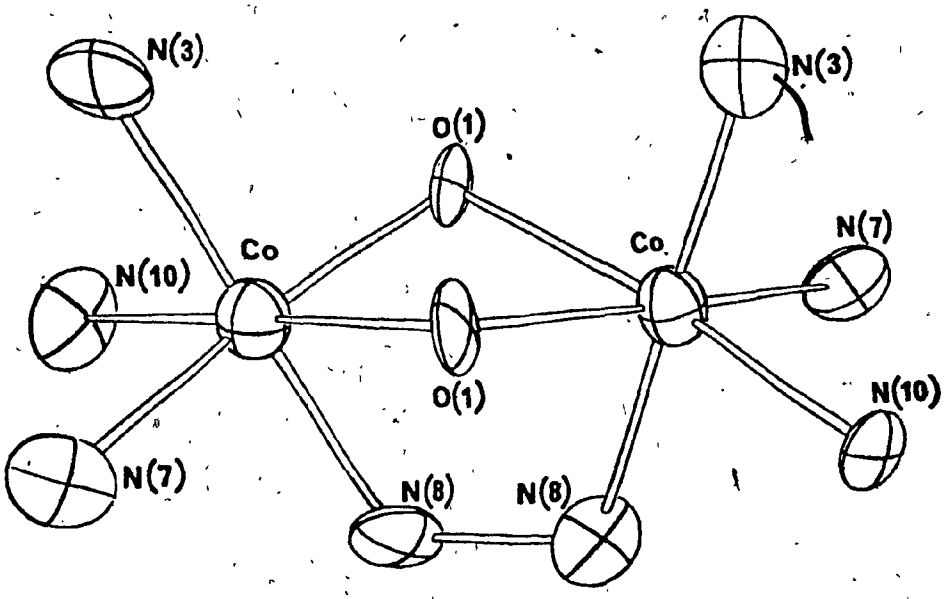

Figure 3.6. Skeletal view of the $[Co_2LL'_2(\mu\text{-}OH)_2]^{4+}$ cation illustrating the geometry around the two Co(III) atoms

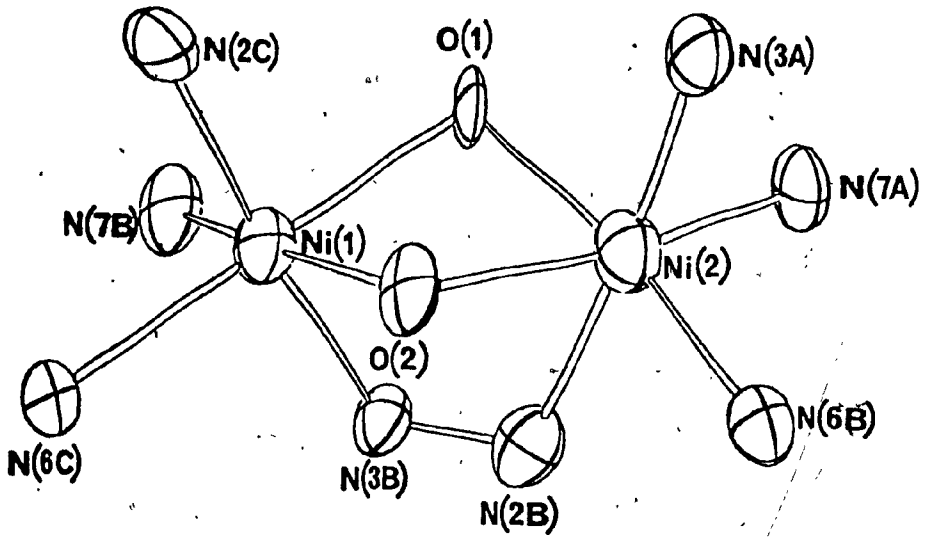

Figure 3.7. Skeletal view of the $[Ni_2LL'_2(\mu\text{-}H_2O)_2]^{4+}$ cation illustrating the geometry around the two Ni(II) atoms

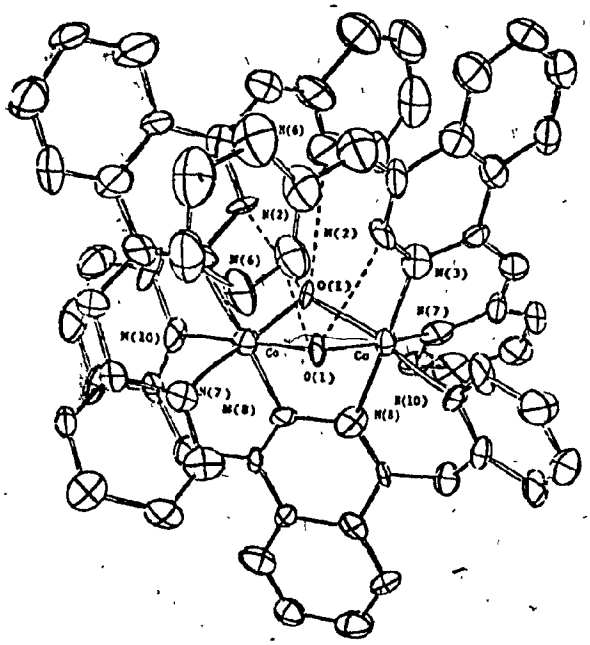

Figure 3.8. $[Co_2LL'_2(\mu\text{-}OH)_2]^{4+}$ cation, illustrating the intra-ligand H-bonds(dashed lines)

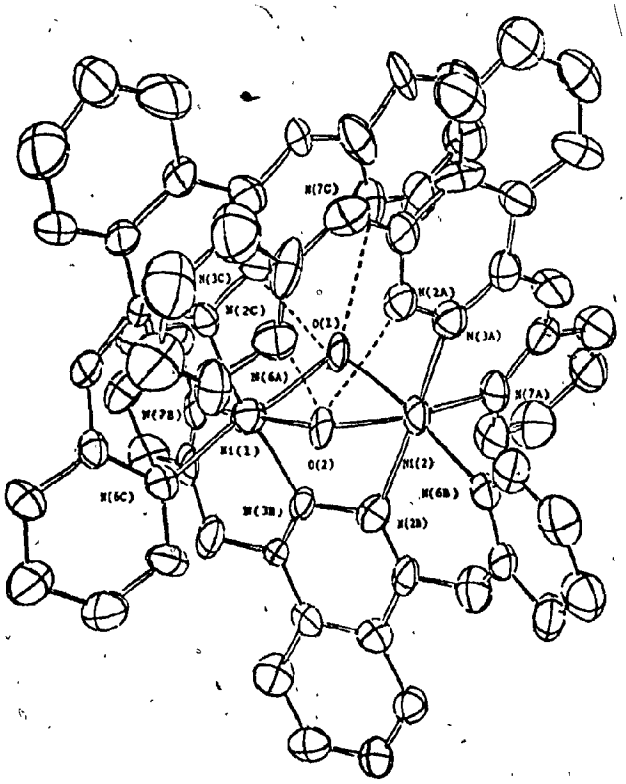

Figure 3.9. $[Ni_2LL'_2(\mu-H_2O)_2]^{4+}$ cation, illustrating the intra-ligand H-bonds(dashed lines)

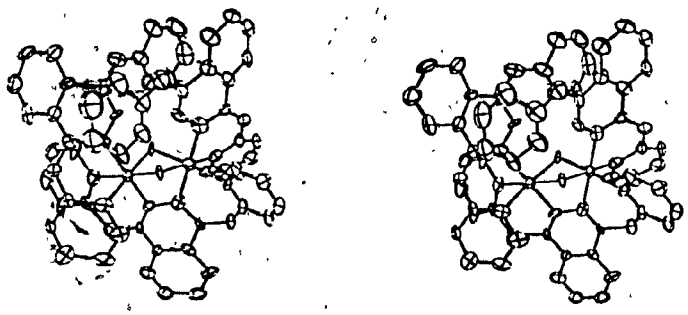

Figure 3.10. Stereoscopic view of the $[Co_2LL'_2(\mu\text{-}OH)_2]^{4+}$ cation

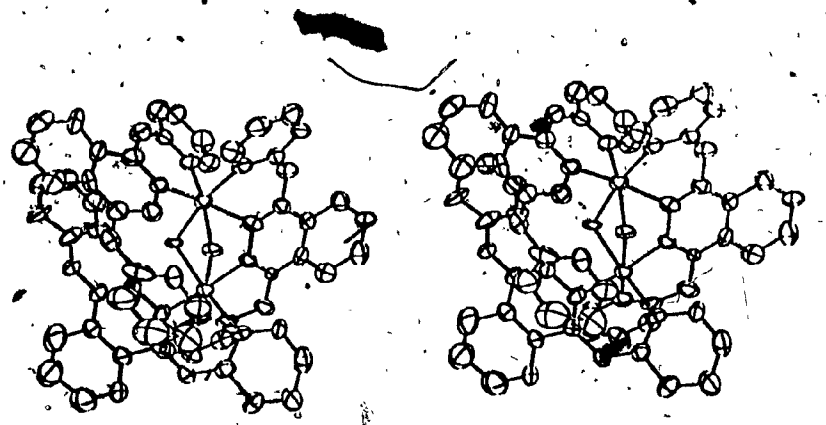

Figure 3.11. Stereoscopic view of the $[Ni_2LL'_2(\mu\text{-}H_2O)_2]^{4+}$ cation

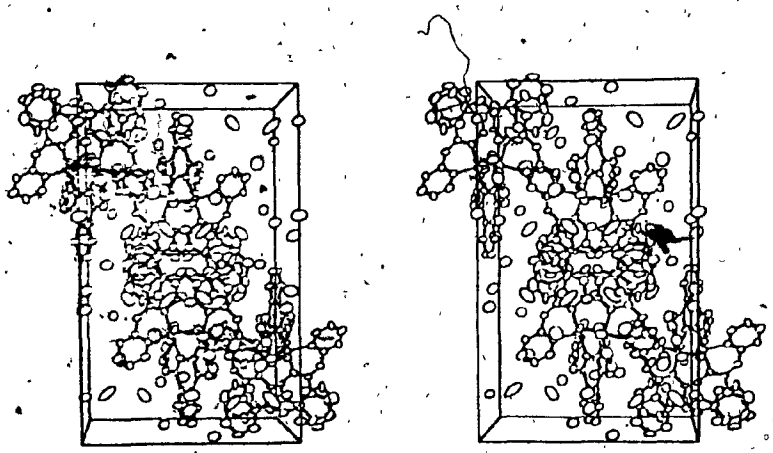

Figure 3.12. Unit cell packing diagram of $[Co_2LL'_2(\mu\text{-}OH)_2]Br_4 \cdot 9H_2O$ viewed approximately along the crystallographic c axis

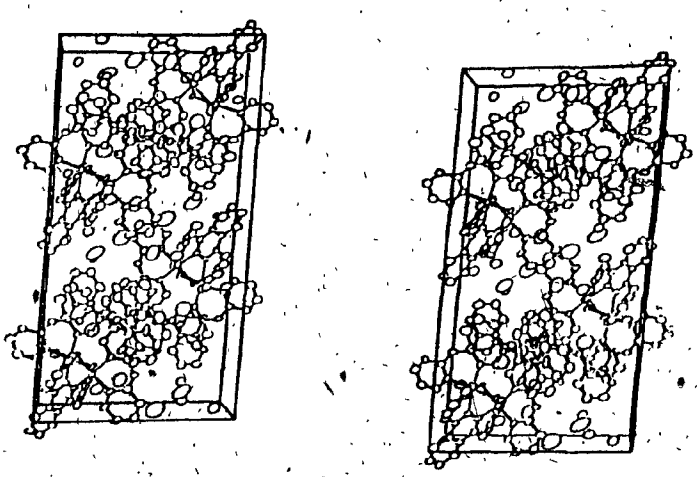

Figure 3.13. Unit cell packing diagram of $[Ni_2LL'_2(\mu\text{-}H_2O)_2]Br_4.5H_2O$ viewed approximately along the crystallographic b axis

REFERENCES

(1) E.S.Fedorov, Imperial St. Petersburg Mineralogical Soc., 23, 99 (1887)

(2) E.S.Fedorov, Imperial St. Petersburg Mineralogical Soc., 26, 345 (1890)

(3) A.Schoenflies, Krystallsysteme und Krystallstructur, B.G.Teubner, Leipzig,1891

(4) E.S.Fedorow, Z.Krist., 21,679 (1893)

(5) W.Barlow, Z.Krist., 23, 1 (1894)

(6) E. Von Fedorow, Z. Krist., 24, 209 (1895)

(7) W.Barlow, Z. Krist., 25, 86 (1896)

(8) E. von Fedorow, Z. Krist., 25, 113(1896)

(9) W.Barlow, Mineral. Mag., 11, 119 (1896)

(10) W.Barlow, Z. Krist., 29, 433 (1898)

(11) Max Von Laue, Physic. Z., 14, 1075 (1913)

(12) W.L.Bragg, Proc. Cambridge Phil. Soc., 17, 43 (1913)

(13) W.H.Bragg and W.L.Bragg Proc. Roy. Soc., (London) (A), 89, 248 (1913)

(14) W.L.Bragg, Proc. Roy. Soc., (London) (A), 89, 468 (1914)

(15) Modern X-ray Analysis on Single Crystals, P.Luger, Walter de Gruyter, 1979

(16) Structure Determination by X-ray Crystallography, M.F.C.Ladd and R.A.Palmer, Plenum Press, 1977

(17) Crystals, X-rays and Proteins, D.Sherwood, Longman 1972

(18) D.T.Cromer and J.T.Waber, Acta. Cryst., 18, 104 (1965)

(19) International Tables for X-ray Crystallography, Vol.III, The Kynoch Press, Birmingham, England, 1962

(20) Crystal Structure Analysis, M.J.Buerger, John Wiley, 1960

(21) X-ray Structure Determination, A Practical Guide, G.H.Stout and L.H.Jensen, The Macmillan, 1968

(22) A.J.C.Wilson, Nature, 150, 152 (1942)

(23) M.J.Burger and G.E.Klein, J. Appl. Phys., 16, 408 (1945)

(24) M.J.Burger and G.E.Klein, J. Appl. Phys., 17, 285 (1946)

(25) C.W.Burnam, Am. Mineral., 51, 159 (1966)

(26) Introduction to Crystallography, D.E.Sands, W.A.Benjamin, 1965

(27) Elements of X-ray Crystallography, L.V.Azaroff, Mc-Growhill, 1968

(28) Principles of Crystal Structure Determination, G.B.Carpenter, W.A.Benjamin, 1969

(29) Crystal Structure Analysis, J.P.Glusker and K.N.Trueblood, Oxford Univ. Press, 1972

(30) A.L.Patterson, Phys. Rev., 46, 372 (1934)

(31) A.L.Patterson, Z. Krysst., A90, 517 (1935)

(32) Theory and Practice of Direct Methods in Crystallography, M.F.C.Ladd and R.A.Palmer, Plenum Press, 1980

(33) Direct Methods in Crystallography, M.M.Woolfson, Oxford Univ. Press, 1961

(34) Fourier Methods in Crystallography, G.N.Ramachandran and R.Srinivasan, Wiley-Interscience, 1970

(35) D.Sayre, Acta. Cryst., 5, 60 (1952)

(36) D.Harker and J.S.Kasper, Acta. Cryst., 3, 374 (1948)

(37) J.Karle and I.Karle, Acta. Cryst., 21, 849 (1966)

(38) E.W.Hughes, Acta. Cryst., 6, 871 (1953)

(39) J.Karle and H.Hauptman, Acta. Cryst., 9, 635 (1956)

(40) G.Germain, P.Main and M.M.Woolfson, Acta. Cryst., B26, 274 (1970)

(41) M.M.Woolfson, Acta. Cryst., 7, 61 (1954)

(42) W.Cochran and M.M.Woolfson, Acta. Cryst., 8, 1 (1955)

(43) G.Germain, P.Main and M.M.Woolfson, Acta. Cryst., A27, 368 (1971)

(44) X-ray Crystallography, M.M.Woolfson, University Press, 1970

(45) K.Weissenberg, Z. Physik., 23, 229 (1924)

(46) X-ray Diffraction Methods, E.W.Nuffield, Wiley, 1966

(47) X-ray Crystallography, M.J.Buerger, Wiley, 1942

(48) The Precession Method, M.J.Buerger, Wiley, 1964

(49) NRC Program "DIFFRAC", Written at NRC by E.J.Gabe etal.

(50) D.F.Grant and E.J.Gabe, J. Appl. Cryst., 11, 114 (1978)

(51) NRC Program "DATRD2", Written at NRC by E.J.Gabe etal.

(52) NRC Program "FOURR", Written at NRC by E.J.Gabe etal.

(53) "MULTAN" Written by P.Main, M.M.Woolfson and G.Germain

(54) International Tables for x-ray Crystallography, Vol.IV, The Kynoch Press, Birmingham, England, 1974

(55) NRC Program "LSTSQ", Written at NRC by E.J.Gabe etal.

(56) NRC Program "DISPOW", Written at NRC by E.J.Gabe etal.

(57) "ORTEP" Written by Johnson

(58) M.A.Jamieson, N.Serpone and M.Z.Hoffman, Coord. Chem. Rev., in press

(59) N.Serpone, M.A.Jamieson, M.S.Henry, M.Z.Hoffman, F.Bolletta and M.Maestri, J. Am. Chem. Soc., 101, 2907 (1979)

(60) N.Sutin and C.Creutz, Adv. Chem. Ser., 168, 1 (1978)

(61) W.D.A.Clark and N.Sutin, J. Am. Chem. Soc., 99, 4676 (1977)

(62) P.J.Delaive, J-T.Lee, H.Abruna, H.W.Sprintschnik, T.J.Meyer and D.G.Whitten, Adv. Chem. Ser., 168, 28 (1978)

(63) V.Balzani, F.Bolletta, M.T.Gandolifi and M.Maestri, Topics Curr. Chem., 75, 1 (1978)

(64) V.Balzani, L.Moggi, M.F.Manfrin and F.Bolletta, Coord. Chem. Rev. 15, 321 (1975)

(65) C.M.Flynn, Jr., and J.N.Demas, J. Am. Chem. Soc., 96, 1959 (1974)

(66) C.M.Flynn, Jr., and J.N.Demas, J. Am. Chem. Soc., 97, 1988 (1975)

(67) B.Martin and G.Waind, J. Chem. Soc., 4284 (1958)

(68) R.E.Desimone and R.S.Drago, Inorg. Chem., 8, 2517 (1969)

(69) S.Castellano, H.Gunther and S.Ebersole, J. Phys. Chem., 69, 4166 (1965)

(70) D.H.W.Carstens and G.A.Crosby, J. Mol. Spect., 34, 113 (1970)

(71) R.J.Watts, J.S.Harrington and J. Van Houten, J. Am. Chem. Soc., 99, 2179 (1977)

(72) R.D.Gillard, R.J.Lancashire and P.A.Williams, J.C.S. Dalton, 190 (1979)

(73) P.J.Spellane and R.J.Watts, Inorg. Chem., 20, 3561 (1981)

(74) W.A.Wickramasinghe, P.H.Bird and N.Serpone, J.C.S. Chem. Comm., 1284 (1981)

(75) R.F.Childers, Jr., K.G.Vander Zyl, Jr., D.A.House, R.G.Hughes and C.S.Garner, Inorg. Chem., 7, 749 (1968)

(76) M.J.Carter and J.K.Beattie, Inorg. Chem., 9, 1233 (1970)

(77) M.D.Alexander and C.A.Spillert, Inorg. Chem., 9, 2344 (1970)

(78) G.W.Bushnell, K.R.Dixon and M.A.Khan, Can. J. Chem., 52, 1367 (1974)

(79) R.D.Gillard, Coord. Chem. Rev., 16, 67 (1975)

(80) W.S.Walters, R.D.Gillard and P.A.Williams, Aust. J. Chem., 31, 1959 (1978)

(81) R.D.Gillard and R.J.Wademan, J.C.S. Chem. Comm., 448 (1981)

(82) J.L.Khal, K.Hanck and K. De Armond, J. Inorg. Nucl. Chem., 41, 495 (1979)

(83) U.Ewers, H.Gunther and L.Jaenicke, Angew. Chem., Int. Ed. Eng., 14, 354 (1975)

(84) J.P.Geerts, A.Nagel and Van der Plas, Org. Mag. Res., 8, 607 (1976)

(85) Standard Deviation Calculation, $\sigma = \sqrt{\frac{\Sigma x^2 - (\Sigma x)^2/n}{n-1}}$

(86) P.Diversi and G.Ingrosso, J. Org. Met. Chem., 125, 253 (1977)

(87) M.J.Nolte, E.Singleton and E. Van der Stock, J.C.S. Chem. Comm., 973 (1978)

(88) T.A.B.M.Bolsman and J.A. Van Doorn, J. Org. Met. Chem., 178, 381 (1979)

(89) P.Rillema and D.S.Jones, J.C.S. Chem. Comm., 849 (1979)

(90) Inorganic Chemistry, K.F.Purcell and J.C.Koltz, W.B.Saunders, 1977

(91) J.Mueller, H.Menig, G.Huttner and A.Frank, J. Org. Met. Chem., 185, 251 (1980)

(92) S.A.Bezman, P.H.Bird, A.R.Fraser and J.A.Osborn, Inorg. Chem., 19, 3755 (1980)

(93) G.R.Clark, M.A.Mazid, D.R.Russell, P.W.Clark and A.J.Jones, J. Org. Met. Chem., 166, 109 (1979)

(94) P.F.Heveldt, B.F.G.Johnson, J.Lewis, P.R.Raithby and G.M.Sheldrick, J.C.S. Chem. Comm., 340 (1978)

(95) G.Bombieri, F.Faraone, G.Bruno and G.Faraone, J. Org. Met. Chem., 188, 379 (1980)

(96) A.Wada, N.Sakabe and J.Tanaka, Acta. Cryst., B32, 1121 (1976)

(97) A.Wada, C.Katayama and J.Tanaka, Acta. Cryst., B32, 3194 (1976)

(98) Y.Ohashi, K.Yanagi, Y.Mitsuhashi, K.Nagata, Y.Kaizu, Y.Sasada and H.Kobayashi, J. Am. Chem. Soc., 101, 4739 (1979)

(99) Hydrogen Bonding, S.N.Vinogradov and R.H.Linnell, Van Nostrand Reinhold, 1971

(100) M.Nonayama, Bull. Chem. Soc. Jap., 47, 767 (1974)

(101) B.N.Cockhurn, D.V.Howe, T.Keating, B.F.G.Johnson and J.Lewis, J.C.S. Dalton, 404 (1973)

(102) M.Nonayama and K.Yamasaki, Inorg. Nucl. Chem., 7, 943 (1971)

(103) W.C.Hamilton, Acta. Cryst., 18, 502 (1965)

(104) R.J.Watts and S.F.Bergeron, J.Phys. Chem., 1979

(105) W.A.Wickramasinghe, P.H.Bird, M.A.Jamieson and N.Serpone, J.C.S. Chem. Comm., 798 (1979)

(106) Tables of Interatomic Distances and Configurations in Molecules and Ions, Chem. Soc., Special Publ., No.18, 1965

(107) O.P.Anderson, J.C.S. Dalton, 2597 (1972)

(108) O.P.Anderson, J.C.S. Dalton, 1237 (1973)

(109) A.W.Adamson, A.R.Gutierrez, R.E.Wright and R.T.Walters, Informal Conf. Photochem., 122 National Bureau of Standards, Washington, D.C., June, 1976

(110) D.Sandrini, M.T.Gandolfi, L.Moggi and V.Balzani, J. Am. Chem. Soc., 100, 1463 (1978)

(111) M.S.Henry and M.Z.Hoffman, Adv. Chem. Ser., 168, 91 (1978)

(112) B.Brunschwig and N.Sutin, J.Am. Chem, Soc., 100, 7568 (1978)

(113) N.Sutin, J. Photochem., 10, 19 (1979)

(114) E.Konig and S. Herzog, J. Inorg. Nucl. Chem., 32, 585 (1970)

(115) M.Maestri, F.Bolletta, L.Moggi, V.Balzani, M.S.Henry and M.Z.Hoffman, J. Am. Chem. Soc., 100, 2694 (1978)

(116) D.Nicollin, P.Bertels and J.A.Koniugstein, Can. J. Chem., 58, 1334 (1980)

(117) M.Maestri, F.Bolletta, L.Moggi, V.Balzani, M.S.Henry and M.Z.Hoffman, J.C.S. Chem. Comm., 491 (1977)

(118) H.L.Schlafer, J. Phys. Chem., 69, 2201 (1965)

(119) R.A.Plane and J.P.Hunt, J. Am. Chem. Soc., 79, 3343 (1957)

(120) R.L.Plane and M.R.Edelson, J. Phys. Chem., 63, 327 (1959)

(121) M.R.Edelson and R.A.Plane, Inorg. Chem., 3, 231 (1964)

(122) A.W.Adomson, J. Phys. Chem., 71, 798 (1967)

(123) S.Chen and G.B.Porter, Chem. Phys. Lett., 6, 41 (1971)

(124) R.Ballardini, G.Varani, F.Wasgestian, L.Moggi and V.Balzani, J. Phys. Chem., 77, 2947 (1973)

(125) R.Sriram, M.Z.Hoffman, M.A.Jamieson and N.Serpone, J. Am. Chem. Soc., 102, 1754 (1980)

(126) M.S.Henry, J. Am. Chem. Soc., 99, 6138 (1977)

(127) R.C.Young, J.K.Nagle, T.J.Meyer and D.G.Whitten, J. Am. Chem. Soc., 100, 4773 (1978)

(128) C.T.Lin, W.Battcher, M.Chou, C.Creutz and N.Sutin, J. Am. Chem. Soc., 98, 6536 (1976)

(129) C.R.Raston and A.H.White, J.C.S. Dalton, 7 (1976)

(130) M.Mathew and G.J.Palenik, J. Coord. Chem., 1, 243 (1971)

(131) E.N.Maslen, C.L.Raston and A.H.White, J.C.S. Dalton, 1803 (1974)

(132) R.Allmann, W.Henke and D.Reinen, Inorg. Chem., 17, 348 (1978)

(133) F.M. Van Meter and H.M.Neumann, J. Am. Chem. Soc., 98, 1388 (1976)

(134) F.M. Van Meter and H.M.Neumann, J. Am. Chem. Soc., 98, 1382 (1976)

(135) See Page 47 of this Thesis

(136) "PREP3" Written by P.H.Bird

(137) "FORDAP" Written by A.L.Zalkin

(138) "SFLS" Written by C.T.Prewitt

(139) "UTILITY" Written by P.H.Bird

(140) S.J.Cline, R.P.Scaringe, W.E.Hatfield and D.J.Hodgson, J.C.S. Dalton, 1662 (1977)

(141) R.P.Scaringe, P.Singh, R.P.EcKberg, W.E.Hatfield and D.J.Hodgson, Inorg. Chem., 14, 1127 (1975)

(142) K.Kass, Acta. Cryst., B32, 2021 (1976)

(143) E.S.Kucharski, B.W.Skelton and A.H.White, Aust. J. Chem., 31, 47 (1978)

(144) J.Baker, L.M.Engelhardt, B.N.Figgis and A.H.White, J.C.S. Dalton, 530 (1975)

(145) M.Bartlett and G.J.Palenik, J.C.S. Chem. Comm., 416 (1970)

(146) W.A.Wickramasinghe, P.H.Bird, M.A.Jameison, N.Serpone and M.Maestri, Inorg. Chim. Acta. Lett., in press

(147) P.Pfeiffer and B.Werdelmann, Z. Anorg. Chem., 263, 31 (1950)

(148) R.G.Inskeep and J.Bjerrum, Acta. Chem. Scand., 15, 62 (1961)

(149) E.D.McKenzie, Coord. Chem. Rev., 6,187 (1971)

(150) R.G.Inskeep and M.Benson, J. Inorg. Nucl. Chem., 20, 290 (1961)

(151) D.Wolcott, Sr., and J.B.Hunt, Inorg. Chem., 7, 755 (1968)

(152) R.A.Krause, Inorg. Chim. Acta. 22, 209 (1977)

(153) R.A.Krause, Inorg. Chim. Acta., 31, 241 (1978)

(154) B.Durham, S.R.Wilson, D.J.Hodgson and T.J.Meyer, J. Am. Chem. Soc., 102, 600 (1980)

(155) B.R.Baker and B.D.Mehta, Inorg. Chem., 4, 848 (1965)

(156) M.Maestri and N.Serpone, Unpublished Observations, 1975

(157) M.Maestri, F.Bolletta, N.Serpone, L.Moggi and V.Balzani, Inorg. Chem., 15, 2048 (1976)

(158) W.A.Wickramasinghe, P.H.Bird and N.Serpone, Inorg. Chem., (1982) in press

(159) N.Serpone, P.H.Bird, D.G.Bickley and D.W.Thompson, J.C.S. Chem. Comm., 217 (1972)

(160) F.A.Cotton, W.H.Ilsley and W.Kaim, J. Am. Chem. Soc., 102, 3464 (1980)

(161) T.J.Greenhough, B.W.S.Kolthammer, P.Legdzins and J.Trotter, Acta. Cryst., 36B, 795 (1980)

(162) B.M.Foxman, Inorg. Chem., 17, 1932 (1978)

(163) M.H.Chisholm, F.A.Cotton, M.W.Extine and D.C.Rideout, Inorg. Chem., 17, 3536 (1978)

(164) A.Walsh, B.Walsh, B.Murphy and B.J.Hathaway, Acta. Cryst., B37, 1512 (1981)

(165) R.J.Fereday, P.Hodgson, S.Tyagi and B.J.Hathaway, J.C.S. Dalton, 2070 (1981)

(166) W.Fitzgerald and G.J.Hathaway, J.C.S. Dalton, 567 (1981)

(167) M.V.Veidis, B.Dockum, F.F.Charron, Jr., and W.M.Reiff, Inorg. Chim. Acta., 53, L197 (1981)

(168) I.D.Brown, M.C.Brown and F.C.Hawthorne, BIDICS-1980

(169) R.G.Teller and R.Bau, Structure and Bonding, 44, 1 (1981)

(170) L.L.Merritt, Jr., and E.D.Schroeder, Acta. Cryst., 9, 801 (1956)

(171) P.J.Hay, J.C.Thibeault and R.Hoffman, J. Am. Chem. Soc., 97, 4884 (1975)

(172) J.Josephsen and E.Pedersen, Inorg. Chem., 16, 2534 (1977)

(173) R.P.Scaringe, W.E.Hatfield and D.J.Hodgson, Inorg. Chem., 16, 1600 (1977)

(174) E.D.Estes, R.P.Scaringe, W.E.Hatfield and D.J.Hodgson, Inorg. Chem., 16, 1605 (1977)

(175) M.R.Churchill, G.M.Harris, R.A.Lashewycz, T.P.Dasgupta and K.Koshy, Inorg. Chem., 18, 2290 (1979)

(176) S.J.Cline, S.Kallesoe, E.Pederson and D,J.Hodgson, Inorg. Chem., 18, 796 (1979)

(177) M.F.Charlot, S.Jeannin, Y.Jeannin, O.Khan, J. Lucrece-Abaul and J.Martin-Frere, Inorg. Chem., 18, 1675 (1979)

(178) D.J.Hodgson and E.Pederson, Inorg. Chem., 19, 3116 (1980)

(179) M.S.Haddad, S.R.Wilson, D.J.Hodgson and D.N.Hendrickson, J. Am. Chem. Soc., 103, 384 (1981)

(180) Bioinorganic Chemistry, Ei-Ichiro Ochiai, Allyn and Bacon Inc., 1977

(181) D.J.Hodgson, Inorg. Chem., 19, 173 (1975)

(182) V.H.Crawford, H.W.Richardson, J.R.Watson, D.J.Hodgson and W.E.Hatfield, Inorg. Chem., 15, 2107 (1976)

(183) A.B.P.Lever, L.K.Thompson and W.M.Reiff, Inorg. Chem., 11, 104 (1972)

(184) L.K.Thompson, V.T.Chacko, J.A.E.Elvidge, A.B.P.Lever and R.V.Parish, Can. J. Chem., 47, 4141 (1969)

(185) G.Marongiu and E.C.Lingafelter, A Preprint

(186) J.E.Andrew and A.B.Blake, J.Chem. Soc. (A), 1408 (1969)

(187) R.J.Butcher, J.Jasinski, G.M.Mockler and E.Sinn, J.C.S. Dalton, 1099 (1976)

(188) G.S.Mandel, R.E.Marsh, W.P.Schaefor, N.S.Mandel and B.C.Wang, Acta. Cryst., B33, 3185 (1977)

(189) G.S.Mandel, N.S.Mandel, R.E.Marsh and W.P.Schaefer, Acta. Cryst., B33, 700 (1977).

(190) M.G.Kurilla and W.P.Schaefer, Act. Cryst., B35, 3008 (1979)

(191) E.D.McKenzie and F.S.Stephens, Inorg. Chim. Acta., 32, 253 (1979)

(192) Chia-Chin Ou, W.J.Bomowski, J.A.Potenza and H.J.Schugar, Acta. Cryst., B33, 3246 (1977)

(193) NRC program Delny

APPENDIX

Table A.1 and A.2. Unit Cell Constants at 20°C

Table A.3 Final Positional and Thermal Parameters of $[Ir(bpy)_2(bpy')](ClO_4)_3.H_2O$

Table A.4 Final Positional and Thermal Parameters of $[Cr(terpy)_2](ClO_4)_3.H_2O$

Table A.5 Final Positional and Thermal Parameters of $[Cr(bpy)_2(H_2O)Cl](ClO_4)_2.2H_2O$

Table A.6 Final Positional and Thermal Parameters of $[Co_2LL'_2(\mu\text{-}OH)_2]Br_4.9H_2O$

Table A.7 Final Positional and Thermal Parameters of $[Ni_2LL'_2(\mu\text{-}H_2O)_2]Br_4.5H_2O$

The Estimated Standard Deviations in Paranthesis are Right Justified to the Least Significant Digit.

Anisotropic Thermal Parameters were Applied as

$$\exp[-2\pi^2(U_{11}h^2a^{*2}+U_{22}k^2b^{*2}+U_{33}l^2c^{*2}+2U_{12}hka^*b^* +2U_{13}hla^*c^*+2U_{23}klb^*c^*)]$$

Table A.1

	I	II	III	
a °A	16.619(10)	12.937(13)	8.723(4)	16.410
b °A	16.200(6)	13.606(20)	11.371(4)	11.371
c °A	13.550(6)	19.441(22)	13.876(7)	13.876
α Deg.	90	90	84.58(4)	95.53
β Deg.	108.74(4)	100.63(7)	81.30(4)	134.47
γ Deg.	90	90	108.28(3)	116.60
V $°A^3$	3456.6	3257	1277.0	
Space Group	$P2_1/c$	Cc	$P\bar{1}$	
Mol. Wt.	977.0	834.9	650.7	
Z	4	4	2	
ρ_{cal} g cm^{-3}	1.88	1.67	1.69	
ρ_{obs} g cm^{-3} (flotation)	1.86	1.65	1.67	
Crystal Dimensions mm	0.3X0.2X0.2	0.6X0.4X0.3	0.5X0.4X0.3	
Radiation	Mo $K_{\bar{\alpha}}$ (0.7107 Angs.)			
Monochromator	Highly Oriented Graphite $2\theta_{002}$ = 12.1			
Crystal-Detector Distance	25.0 cm			
Detector	Scintillation Counter and Pulse Height Analyzer set for 100% Mo K_α			
Attenuators	Ni foil for intensities 10^4 cps			
Take off Angle Deg.	3.0			
Detector Aperture	4 X 4 mm			
Scan Type	Coupled θ(Crystal)-2θ(Detector) 2.0 deg. min^{-1}			
Scan Base Width Deg.	1.8	2.5	2.0	

Scan Length	(base width + 0.692 tan θ) deg.			
Rotation Axis	c	c		a
Reflections Measured	$\pm h+k+l$	$+h+k\pm l$		$\pm h+k\pm l$
Min. Max. 2θ	3.5–40.0	4.0–45.0		3.5–45.0
Standards		every 50 cycles		
Variation of Standards	2%	3%		4%
Linear Abs. Coef. cm^{-1}	6.8	44.1		8.5
No. of Reflections Collected	3218	2307		3319
Reflections with $I > 3\sigma$	2376	2150		2509
R	4.39	5.20	5.30**	5.02
R_w	5.09	5.70	5.90	7.57
GOF	3.30	2.19	2.28	2.79

I = $[Ir(bpy)_2(bpy')](ClO_4)_3.H_2O$

II = $[Cr(terpy)_2](ClO_4)_3.H_2O$

III = $[Cr(bpy)_2(H_2O)Cl](ClO_4)_2.2H_2O$

* = Reduced Cell [193]

** = Rejected Enantiomer

Table A.2

	I	II
a °A	24.667(5)	16.056(6)
b °A	15.435(5)	12.757(5)
c °A	16.029(3)	29.820(13)
α Deg.	90	90
β Deg.	90	95.18(4)
γ Deg.	90	90
V $°A^3$	6102.8	6083.2
Space Group	$C222_1$	$P2_1/c$
Mol. Wt.	1576.9	1506.2
Z	4	4
ρ_{cal} g cm^{-3}	1.72	1.64
ρ_{obs} g cm^{-3}	1.73	1.64
Crystal Dimensions	0.15X0.1X0.15	0.3X0.25X0.2 mm
Radiation	Mo K_{α} (0.7107 Angs.)	
Monochromator	Highly Oriented Graphite $2\theta_{002}$ = 12.1	
Crystal-Detector Distance	25.0 cm	
Detector	Scintillation Counter and Pulse Height Analyzer set for 100% Mo K_{α}	
Attenuators	Ni foil for intensities 10^4 cps	
Take off Angle Deg.	3.0	
Detector Aperture	4 X 4 mm	
Scan Type	Coupled θ(crystal)-2θ(Detector) 2.0 deg. min^{-1}	
Scan Base Width Deg.	1.8	1.36

Scan Length	(base width + 0.692 tan θ) deg		
Rotation Axis	b		b
Reflections Measured	+h+k+l;	+h-k-l;-h-k-l	±h+k+l
Min. Max. 2θ	3.5-40.0		3.5-40.0
Standards	Every 50 Cycles		
Linear Abs. Coef. cm^{-1}	32.1		32.9
No. of Reflections Collected	4703		5674
Reflections with $I > 2\sigma$	2029		2916
R	4.36	5.01*	7.28
R_w	5.48	6.10	9.42
GOF	1.10	1.19	2.25

I = $[Co_2LL'_2(OH)_2]Br_4 \cdot 9H_2O$

II = $[Ni_2LL'_2(H_2O)_2]Br_4 \cdot 5H_2O$

* = Rejected Enantiomer

Table A.3

ATOM	x	y	z	U_{11}	U_{22}	U_{33}	U_{12}	U_{13}	U_{23}
Ir	0.24295(3)	-.05303(4)	0.21563(5)	0.0476(3)	0.0525(3)	0.0696(4)	-.0010(4)	0.0229(3)	-.0040(4)
Cl(1)	0.4657(3)	-.3156(3)	0.1269(4)	0.133(5)	0.125(5)	0.134(5)	0.028(4)	0.026(4)	0.018(4)
O(1)	0.4870(16)	0.2183(12)	0.2894(17)	0.53(4)	0.185(20)	0.246(22)	0.145(24)	-.216(25)	-.067(17)
O(2)	0.5192(12)	0.2062(25)	0.4598(16)	0.171(18)	0.95(7)	0.168(19)	-.04(3)	0.025(15)	-.22(3)
O(3)	0.6111(13)	0.2095(16)	0.4045(16)	0.240(22)	0.46(4)	0.233(22)	-.150(25)	0.108(18)	-.039(24)
O(4)	0.5212(18)	0.1064(13)	0.3537(19)	0.52(4)	0.150(18)	0.32(3)	-.159(24)	-.074(28)	0.050(18)
Cl(2)	-.0179(3)	-.3410(3)	0.0954(3)	0.086(3)	0.096(3)	0.086(3)	-.024(3)	0.0266(25)	-.0007(27)
O(5)	0.0827(7)	0.3727(8)	-.0076(10)	0.104(10)	0.116(11)	0.132(11)	-.037(8)	-.014(8)	-.006(8)
O(6)	0.9464(8)	0.1044(9)	0.3790(10)	0.096(9)	0.150(12)	0.146(12)	-.014(9)	0.010(8)	-.013(10)
O(7)	-.0083(8)	0.2352(8)	0.4279(12)	0.157(13)	0.098(11)	0.228(16)	0.056(10)	0.073(12)	0.000(10)
O(8)	0.0486(9)	0.1601(13)	0.3204(10)	0.137(12)	0.367(25)	0.107(11)	-.016(15)	0.071(10)	0.012(14)
Cl(3)	-.26398(26)	-.08390(27)	0.1675(3)	0.0718(28)	0.093(3)	0.100(3)	-.0065(25)	0.0325(25)	-.0119(26)
O(9)	0.3186(9)	0.3577(9)	0.3109(12)	0.143(12)	0.151(14)	0.231(17)	0.054(11)	0.096(12)	-.003(12)
O(10)	0.3159(8)	0.4774(8)	0.3947(10)	0.138(12)	0.126(12)	0.136(12)	-.019(9)	0.020(9)	-.008(9)

ATOM	x	y	z	U_{11}	U_{22}	U_{33}	U_{12}	U_{13}	U_{23}
O(11)	0.2168(8)	0.3808(9)	0.3910(10)	0.116(10)	0.204(16)	0.143(12)	-.006(10)	0.074(9)	0.067(11)
O(12)	0.2105(8)	0.4533(8)	0.2395(9)	0.116(8)	0.178(14)	0.087(9)	-.010(10)	0.003(8)	0.037(9)
O(14)	0.3964(19)	0.2576(14)	0.5108(18)	0.56(4)	0.239(24)	0.312(28)	0.196(26)	0.263(30)	-.006(20)
N(1)	0.2234(7)	0.0669(6)	0.1736(9)	0.088(9)	0.050(8)	0.063(8)	0.001(7)	0.013(7)	0.007(6)
N(2)	0.6473(7)	0.4729(7)	0.3186(9)	0.057(8)	0.089(10)	0.083(9)	0.013(7)	0.024(7)	0.020(7)
C(1)	0.1514(9)	0.1144(9)	0.1737(12)	0.077(11)	0.061(11)	0.107(13)	0.036(9)	0.031(10)	0.001(10)
C(2)	0.1472(10)	0.1978(9)	0.1428(13)	0.106(14)	0.065(11)	0.110(14)	0.025(10)	0.042(11)	0.017(10)
C(3)	0.2150(11)	0.2342(10)	0.1156(14)	0.125(16)	0.068(12)	0.139(18)	0.001(12)	0.038(13)	0.017(12)
C(4)	0.2844(9)	0.1861(8)	0.1156(11)	0.081(11)	0.050(10)	0.080(14)	-.003(8)	0.022(9)	0.018(8)
C(5)	0.2882(8)	0.1066(10)	0.1466(10)	0.056(10)	0.089(12)	0.056(10)	-.007(9)	0.030(8)	-.010(9)
C(6)	0.3586(9)	0.0523(8)	0.1480(10)	0.080(10)	0.052(9)	0.056(9)	-.013(9)	0.017(8)	-.010(8)
C(7)	0.4259(8)	0.0762(9)	0.1209(11)	0.050(9)	0.091(13)	0.073(10)	-.018(8)	0.029(8)	-.011(9)
C(8)	0.4885(11)	0.0249(11)	0.1225(13)	0.103(14)	0.115(16)	0.098(14)	-.034(12)	0.046(12)	-.028(11)
C(9)	0.5134(9)	0.4416(12)	0.3423(12)	0.048(10)	0.166(18)	0.090(12)	0.025(11)	0.028(9)	0.050(13)
C(10)	0.5838(8)	0.4139(10)	0.3109(11)	0.046(9)	0.094(12)	0.084(12)	-.022(8)	0.020(8)	0.024(9)
N(3)	0.8072(6)	0.3980(7)	0.4308(9)	0.045(7)	0.060(8)	0.092(9)	0.012(6)	0.028(6)	0.015(7)

ATOM	x	y	z	U_{11}	U_{22}	U_{33}	U_{12}	U_{13}	U_{23}
N(4)	0.7321(6)	0.3223(6)	0.2482(9)	0.056(8)	0.038(7)	0.120(11)	0.000(6)	0.046(7)	0.010(6)
C(11)	0.8403(9)	0.0564(10)	0.0185(11)	0.061(10)	0.100(13)	0.074(11)	0.002(10)	0.018(8)	0.016(10)
C(12)	0.8798(10)	0.0984(11)	0.1118(13)	0.075(12)	0.109(14)	0.091(13)	-.009(11)	0.022(10)	-.015(11)
C(13)	0.8821(10)	0.1823(11)	0.1149(13)	0.083(12)	0.132(17)	0.091(13)	-.008(12)	0.035(10)	-.016(12)
C(14)	0.8472(9)	0.2299(9)	0.0241(12)	0.080(12)	0.062(11)	0.099(13)	-.016(9)	0.021(10)	-.037(10)
C(15)	0.8090(8)	0.3136(9)	0.4337(11)	0.053(9)	0.074(11)	0.076(11)	0.008(8)	0.028(8)	0.005(8)
C(16)	0.7686(9)	0.2735(8)	0.3363(12)	0.063(10)	0.054(10)	0.099(12)	0.012(8)	0.034(9)	0.027(9)
C(17)	0.7600(10)	0.1854(9)	0.3210(14)	0.086(12)	0.055(11)	0.159(18)	0.012(9)	0.063(12)	0.021(10)
C(18)	0.7155(10)	0.1520(10)	0.2200(13)	0.088(12)	0.088(13)	0.107(14)	-.007(10)	0.025(11)	-.021(11)
C(19)	0.6790(10)	0.2063(9)	0.1416(13)	0.082(12)	0.065(11)	0.134(15)	-.014(9)	0.060(11)	-.015(11)
C(20)	0.6881(9)	0.2919(10)	0.1512(12)	0.068(11)	0.081(12)	0.110(14)	-.022(10)	0.032(10)	-.048(11)
N(5)	0.8656(6)	0.4317(6)	0.2423(9)	0.044(7)	0.042(8)	0.114(10)	0.002(6)	0.036(7)	-.010(7)
N(6)	0.7174(6)	0.4860(6)	0.1357(8)	0.031(6)	0.076(8)	0.057(7)	-.008(6)	0.022(6)	-.011(6)
C(21)	0.9389(8)	0.4004(9)	0.31209(12)	0.040(9)	0.062(10)	0.121(14)	0.004(8)	0.026(9)	0.001(10)
C(22)	1.0106(9)	0.3897(9)	0.2751(13)	0.064(11)	0.068(12)	0.125(15)	-.002(9)	0.036(10)	0.007(10)
C(23)	1.0031(9)	0.4117(10)	0.1750(14)	0.064(11)	0.070(11)	0.141(16)	-.008(9)	0.040(10)	0.006(11)

ATOM	x	y	z	U_{11}	U_{22}	U_{33}	U_{12}	U_{13}	U_{23}
C(24)	0.9273(9)	0.4437(8)	0.1064(12)	0.072(10)	0.050(9)	0.110(12)	-.015(9)	0.055(9)	-.015(9)
C(25)	0.8585(9)	0.4539(8)	0.1426(10)	0.096(11)	0.048(9)	0.059(9)	-.029(9)	0.044(8)	-.009(8)
C(26)	0.7754(8)	0.4868(8)	0.0813(11)	0.041(9)	0.042(9)	0.095(12)	-.008(7)	0.004(8)	0.005(8)
C(27)	0.2413(10)	0.4874(9)	0.0198(10)	0.100(13)	0.066(10)	0.051(9)	-.017(10)	0.015(9)	-.003(8)
C(28)	0.3224(10)	0.4554(10)	0.0704(12)	0.098(13)	0.087(13)	0.090(13)	-.016(11)	0.027(10)	-.004(10)
C(29)	0.3823(10)	0.4521(10)	0.0170(13)	0.089(12)	0.077(12)	0.104(14)	0.001(10)	0.027(10)	0.007(11)
C(30)	0.3616(9)	0.0176(9)	0.4134(11)	0.074(11)	0.061(10)	0.070(11)	-.003(8)	0.015(9)	-.005(8)

Table A.4

ATOM	x	y	z	U_{11}	U_{22}	U_{33}	U_{12}	U_{13}	U_{23}
Cr	-.154	-.04482(6)	-.160	0.0249(5)	0.0244(5)	0.0237(5)	0.0027(4)	0.0024(4)	0.0027(4)
Cl(1)	-.07041(18)	-.65682(15)	-.30839(10)	0.0608(13)	0.0578(13)	0.0421(11)	-.0014(11)	0.0026(10)	-.0060(10)
Cl(2)	-.47053(17)	-.91219(15)	-.06171(12)	0.0533(12)	0.0502(11)	0.0622(13)	0.0098(10)	0.0105(10)	0.0061(10)
Cl(3)	0.04005(19)	-.10264(16)	-.37069(12)	0.0632(14)	0.0696(14)	0.0671(14)	0.0250(12)	0.0288(11)	0.0304(12)
O(1)	0.0312(6)	-.6945(7)	-3446(4)	0.060(4)	0.132(6)	0.099(6)	0.013(4)	0.005(4)	-.004(5)
O(2)	-.1381(7)	-.6497(6)	-.3734(4)	0.120(6)	0.124(6)	0.069(5)	0.050(5)	-.033(4)	-.030(4)
O(3)	-.1089(11)	-.7272(12)	-.2711(8)	0.142(9)	0.233(14)	0.229(13)	-.052(10)	0.053(9)	0.102(12)
O(4)	-.0610(10)	-.5723(9)	-.2736(7)	0.204(12)	0.145(8)	0.178(9)	0.092(8)	-.101(9)	-.113(8)
O(5)	-.4442(6)	-.9225(5)	-.1291(4)	0.101(5)	0.084(4)	0.092(5)	0.022(4)	0.034(4)	0.011(4)
O(6)	-.5684(6)	-.8673(7)	-.0645(4)	0.077(5)	0.136(7)	0.100(6)	0.037(5)	0.025(4)	0.010(5)
O(7)	-.3934(8)	-.8504(8)	-.0161(6)	0.126(8)	0.154(9)	0.176(10)	-.067(7)	0.041(7)	-.066(8)
O(8)	-.4681(100	-1.0032(6)	-.0268(4)	0.245(12)	0.077(5)	0.092(6)	0.052(7)	0.057(7)	0.006(5)
O(9)	0.0294(11)	-.1880(9)	-.4114(4)	0.246(13)	0.215(12)	0.053(4)	0.151(11)	0.003(6)	-.028(6)
O(10)	0.0508(6)	-.1341(5)	-.3002(3)	0.109(5)	0.068(4)	0.057(4)	0.018(4)	0.020(3)	0.011(3)

ATOM	x	y	z	U_{11}	U_{22}	U_{33}	U_{12}	U_{13}	U_{23}
O(11)	0.1289(8)	-.0470(10)	-.3772(8)	0.093(7)	0.245(15)	0.345(19)	0.038(8)	0.088(9)	0.240(15)
O(12)	-.0500(6)	-.0441(5)	-.3870(4)	0.072(4)	0.090(5)	0.107(5)	0.033(4)	0.032(4)	0.037(4)
O(14)	-.1515(5)	-.4678(5)	-.4581(3)	0.074(4)	0.083(4)	0.062(4)	0.034(3)	-.010(3)	-.015(3)
N(1)	-.1517(4)	-.1580(4)	-.22935(27)	0.030(3)	0.033(3)	0.035(3)	-.001(2)	-.007(2)	-.006(2)
N(2)	-.2400(4)	0.0102(4)	-.24679(26)	0.026(3)	0.031(3)	0.036(3)	-.001(2)	0.000(2)	0.005(2)
N(3)	-.1906(4)	0.0925(4)	-.12526(27)	0.027(3)	0.037(3)	0.033(3)	0.001(2)	0.005(2)	-.001(2)
C(1)	-.1003(6)	-.2465(5)	-.2139(4)	0.047(4)	0.028(4)	0.052(4)	0.002(3)	0.019(3)	-.003(3)
C(2)	-.1099(7)	-.3198(5)	-.2652(4)	0.063(5)	0.042(4)	0.059(5)	0.004(4)	0.031(4)	-.005(4)
C(3)	-.1689(6)	-.3053(6)	-.3303(4)	0.060(5)	0.057(5)	0.059(5)	-.006(4)	0.021(4)	-.028(4)
C(4)	-.2192(6)	-.2147(6)	-.3463(4)	0.057(5)	0.055(5)	0.050(4)	-.015(4)	0.006(4)	-.023(4)
C(5)	-.2083(5)	-.1421(5)	-.2944(3)	0.028(3)	0.045(4)	0.039(4)	-.001(3)	0.011(3)	0.002(3)
C(6)	-.2580(5)	-.0450(5)	-.3036(3)	0.033(4)	0.048(4)	0.025(3)	-.005(3)	0.002(3)	0.003(3)
C(7)	-.3211(6)	-.0069(7)	-.3652(4)	0.044(5)	0.067(6)	0.031(4)	-.002(4)	-.013(3)	0.020(4)
C(8)	-.3606(7)	0.0872(7)	-.3634(4)	0.048(6)	0.070(6)	0.043(5)	-.005(5)	-.008(4)	0.021(4)
C(9)	-.3394(6)	0.1443(6)	-.3043(4)	0.039(5)	0.052(4)	0.043(5)	0.010(4)	-.008(4)	0.012(4)
C(10)	-.2766(5)	0.1022(5)	-.2444(4)	0.031(4)	0.025(4)	0.037(4)	0.008(3)	0.004(3)	0.009(3)

ATOM	x	y	z	U_{11}	U_{22}	U_{33}	U_{12}	U_{13}	U_{23}
C(11)	-.2439(5)	0.1522(5)	-.1761(4)	0.024(4)	0.036(4)	0.035(4)	0.005(3)	0.003(3)	0.001(3)
C(12)	-.2611(7)	0.2494(6)	-.1646(5)	0.057(5)	0.035(5)	0.059(6)	0.015(4)	0.022(4)	0.006(4)
C(13)	-.2216(7)	0.2859(6)	-.0973(5)	0.056(5)	0.038(5)	0.075(7)	0.005(4)	0.016(5)	-.010(5)
C(14)	-.1702(7)	0.2266(6)	-.0448(5)	0.044(5)	0.060(5)	0.057(6)	-.001(4)	0.020(4)	-.021(4)
C(15)	-.1548(6)	0.1279(5)	-.0593(4)	0.043(4)	0.041(4)	0.036(4)	-.006(4)	0.012(4)	-.018(4)
N(4)	-.2622(4)	-.1211(4)	-.1158(3)	0.032(3)	0.024(3)	0.021(3)	-.002(2)	0.001(2)	0.002(2)
N(5)	-.0676(4)	-.0930(4)	-.0726(3)	0.026(3)	0.026(3)	0.024(3)	-.002(2)	0.002(2)	0.001(2)
N(6)	-.0088(4)	0.0085(4)	-.1694(3)	0.031(3)	0.028(3)	0.027(3)	0.006(2)	0.009(2)	0.003(2)
C(16)	-.3654(5)	-.1331(5)	-.1451(4)	0.027(4)	0.036(4)	0.038(4)	0.002(3)	-.001(4)	-.006(3)
C(17)	-.4316(6)	-.1898(5)	-.1136(4)	0.040(5)	0.037(4)	0.060(5)	-.007(4)	0.020(4)	-.004(4)
C(18)	-.3934(7)	-.2336(6)	-.0502(4)	0.052(5)	0.049(5)	0.052(5)	-.013(4)	0.022(4)	-.006(4)
C(19)	-.2853(6)	-.2231(5)	-.0190(4)	0.038(4)	0.036(4)	0.056(5)	-.010(4)	0.018(4)	-.010(4)
C(20)	-.2238(6)	-.1651(5)	-.0535(4)	0.040(4)	0.028(3)	0.030(4)	-.005(3)	0.007(3)	-.004(3)
C(21)	-.1123(6)	-.1460(4)	-.0276(3)	0.046(4)	0.021(4)	0.021(4)	0.001(3)	0.000(3)	0.000(3)
C(22)	-.0561(6)	-.1762(6)	0.0369(4)	0.047(5)	0.042(4)	0.032(4)	0.009(4)	-.003(3)	0.010(3)
C(23)	0.0505(6)	-.1494(5)	0.0527(4)	0.047(5)	0.038(4)	0.032(4)	0.016(4)	-.003(4)	0.007(3)

ATOM	x	y	z	U_{11}	U_{22}	U_{33}	U_{12}	U_{13}	U_{23}
C(24)	0.0975(6)	-.0959(5)	0.0056(4)	0.033(4)	0.040(4)	0.035(4)	0.019(4)	-.013(3)	0.000(3)
C(25)	0.0370(5)	-.0677(5)	-.0564(3)	0.033(4)	0.030(3)	0.027(4)	0.001(3)	0.002(3)	-.008(3)
C(26)	0.0697(5)	-.0072(5)	-.1119(3)	0.027(4)	0.024(3)	0.040(4)	0.003(3)	0.007(3)	-.003(3)
C(27)	0.1706(6)	0.0295(5)	-.1061(4)	0.038(4)	0.034(4)	0.056(5)	-.002(3)	0.008(4)	-.002(4)
C(28)	0.1917(6)	0.0826(6)	-.1646(5)	0.039(5)	0.046(5)	0.063(6)	-.016(4)	0.010(4)	0.002(4)
C(29)	0.1182(6)	0.1018(6)	-.2195(5)	0.034(5)	0.059(5)	0.074(6)	-.011(4)	0.021(5)	0.017(4)
C(30)	0.0135(6)	0.0608(5)	-.2228(4)	0.043(4)	0.045(4)	0.030(4)	0.005(3)	0.008(3)	0.008(3)

Table A.5

ATOM	x	y	z	U_{11}	U_{22}	U_{33}	U_{12}	U_{13}	U_{23}
Cr	0.14133(12)	0.81692(10)	0.71732(8)	0.0319(6)	0.0414(6)	0.0463(6)	0.0162(5)	-.0008(5)	-.0064(5)
Cl(1)	0.08916(21)	0.97143(17)	0.62763(14)	0.0460(10)	0.0525(11)	0.0639(12)	0.0249(9)	0.0000(9)	0.0033(9)
Cl(2)	0.17174(23)	0.36386(18)	0.64406(15)	0.0611(12)	0.0624(12)	0.0697(13)	0.0269(10)	-.0145(10)	-.0213(10)
Cl(3)	0.37974(25)	0.19482(19)	0.00765(16)	0.0643(13)	0.0694(14)	0.0808(15)	0.0247(11)	-.0218(11)	-.0135(11)
N(1)	-.0841(6)	0.6872(5)	0.7248(4)	0.032(3)	0.044(3)	0.046(3)	0.0156(26)	-.0013(25)	-.0021(26)
N(2)	0.1611(6)	0.6666(4)	0.8034(4)	0.034(3)	0.039(3)	0.042(3)	0.015(2)	-.0025(25)	-.0079(25)
N(3)	0.3808(6)	0.9232(5)	0.7085(4)	0.039(3)	0.037(3)	0.050(3)	0.0153(26)	-.0034(26)	-.0059(26)
N(4)	0.2485(6)	0.7680(5)	0.5934(4)	0.032(3)	0.038(3)	0.049(3)	0.0148(25)	-.0017(26)	-.0010(26)
C(1)	-.2043(8)	0.7033(7)	0.6811(5)	0.043(4)	0.061(5)	0.063(5)	0.022(4)	-.003(4)	0.002(4)
C(2)	0.3577(8)	-.6097(7)	-.6923(6)	0.038(4)	0.076(6)	0.072(5)	0.019(4)	-.009(4)	-.020(4)
C(3)	0.3875(8)	-.5021(7)	-.7541(6)	0.031(4)	0.063(5)	0.073(5)	0.010(4)	-.006(4)	-.022(4)
C(4)	0.2672(8)	-.4822(6)	-.7997(5)	0.046(4)	0.049(4)	0.054(5)	0.007(4)	0.002(4)	-.006(4)
C(5)	0.1139(8)	-.5779(6)	-.7820(5)	0.042(4)	0.047(4)	0.039(4)	0.016(3)	0.000(3)	-.012(3)
C(6)	-.0259(8)	-.5658(6)	-.8245(4)	0.040(4)	0.052(4)	0.039(4)	0.022(3)	0.002(3)	-.009(3)

ATOM	x	y	z	U_{11}	U_{22}	U_{33}	U_{12}	U_{13}	U_{23}
C(7)	-.0217(9)	-.4581(7)	-.8820(5)	0.066(5)	0.052(5)	0.049(4)	0.028(4)	-.002(4)	-.006(4)
C(8)	-.1561(9)	-.4532(7)	-.9170(5)	0.067(5)	0.058(5)	0.047(4)	0.033(4)	-.009(4)	-.003(4)
C(9)	-.2935(9)	-.5571(7)	-.8971(5)	0.056(5)	0.066(5)	0.054(5)	0.034(4)	-.017(4)	-.017(4)
C(10)	-.2931(8)	-.6618(6)	-.8399(5)	0.046(4)	0.052(4)	0.055(5)	0.023(4)	-.010(3)	-.014(4)
C(11)	-.4389(8)	-1.0065(7)	-.7670(5)	0.052(4)	0.055(5)	0.059(5)	0.019(4)	-.009(4)	-.011(4)
C(12)	-.6034(9)	-1.0725(7)	-.7542(6)	0.062(5)	0.056(5)	0.083(6)	0.012(4)	-.030(4)	-.021(4)
C(13)	-.7122(8)	-1.0560(7)	-.6806(6)	0.036(4)	0.062(5)	0.075(5)	0.010(4)	-.009(4)	-.006(4)
C(14)	0.6524(8)	0.9732(7)	0.6204(5)	0.038(4)	0.0625)	0.058(5)	0.025(4)	0.001(3)	-.001(4)
C(15)	0.4892(7)	0.9081(6)	0.6326(5)	0.034(4)	0.048(4)	0.046(4)	0.020(3)	-.004(3)	-.001(3)
C(16)	0.4150(8)	0.8176(6)	0.5719(5)	0.042(4)	0.043(4)	0.043(4)	0.025(3)	-.002(3)	0.000(3)
C(17)	0.5022(8)	0.7891(7)	0.4911(5)	0.047(4)	0.063(5)	0.058(5)	0.030(4)	0.005(4)	-.004(4)
C(18)	0.4180(10)	0.7076(7)	0.4361(5)	0.069(5)	0.080(6)	0.057(5)	0.044(4)	-.004(4)	-.024(4)
C(19)	0.2535(9)	0.6608(7)	0.4559(5)	0.067(5)	0.068(5)	0.055(5)	0.035(4)	-.010(4)	-.028(4)
C(20)	0.1714(8)	0.6924(6)	0.5356(5)	0.050(4)	0.045(4)	0.057(5)	0.019(4)	-.014(4)	-.013(4)
O(1)	0.1901(9)	0.3448(7)	0.5468(4)	0.128(6)	0.185(7)	0.077(4)	0.084(6)	-.028(4)	-.066(5)
O(2)	0.2612(9)	0.4837(6)	0.6552(5)	0.128(6)	0.074(4)	0.118(6)	0.010(4)	-.038(5)	-.017(4)

ATOM	x	y	z	U_{11}	U_{22}	U_{33}	U_{12}	U_{13}	U_{23}
O(3)	0.2381(8)	0.2850(6)	0.6998(5)	0.117(6)	0.116(5)	0.107(5)	0.066(4)	-.008(4)	0.013(4)
O(4)	0.0062(8)	0.3337(10)	0.6858(6)	0.060(4)	0.287(11)	0.172(8)	0.057(6)	-.040(5)	-.141(8)
O(5)	0.2339(12)	0.1165(8)	-.0148(7)	0.179(9)	0.129(7)	0.197(9)	0.003(6)	-.097(7)	-.040(6)
O(6)	0.5403(16)	0.2155(12)	-.0366(11)	0.134(11)	0.134(10)	0.216(14)	0.041(9)	0.085(10)	-.010(10)
O(7)	0.3714(15)	0.3100(10)	0.0225(12)	0.[illegible]1(10)	0.092(8)	0.316(18)	0.071(8)	-.094(11)	-.107(10)
O(8)	0.3572(14)	0.1802(14)	0.1102(8)	0.175(10)	0.397(19)	0.147(9)	0.027(11)	-.065(8)	-.023(10)
O(9)	0.0634(6)	0.8700(4)	0.8416(3)	0.056(3)	0.051(3)	0.058(3)	0.026(2)	0.004(2)	-.016(2)
O(10)	0.0336(7)	0.0959(5)	0.8508(4)	0.1053(5)	0.067(4)	0.078(4)	0.040(4)	0.004(3)	-.008(3)
O(11)	0.171[illegible]	0.8322(5)	0.0054(4)	0.108(5)	0.068(4)	0.067(4)	0.043(3)	-.004(3)	-.006(3)
O(A)	0.4345(24)	0.2758(19)	-.0694(16)	0.116(16)	0.137(17)	0.155(19)	0.039(13)	0.038(14)	0.136(16)
O(B)	0.4609(24)	0.1134(18)	0.0247(16)	0.110(15)	0.110(15)	0.148(18)	0.091(13)	-.039(13)	-.004(13)
H(1)	-.171(8)	0.774(6)	0.633(5)	0.07(2)					
H(2)	-.459(8)	0.640(6)	0.650(5)	0.07(2)					
H(3)	-.477(8)	0.444(6)	0.756(5)	0.09(2)					
H(4)	-.292(8)	0.409(6)	0.860(5)	0.08(2)					
H(7)	-.077(8)	0.388(6)	0.904(5)	0.07(2)					

ATOM	x	y	z	U
H(8)	0.166(7)	0.394(6)	0.969(4)	0.07(2)
H(9)	0.365(9)	0.554(7)	0.938(5)	0.09(2)
H(10)	0.390(7)	0.743(5)	0.830(4)	0.05(2)
H(11)	0.346(8)	1.011(6)	0.813(4)	0.07(2)
H(12)	0.620(7)	1.106(6)	0.786(4)	0.06(2)
H(13)	0.826(6)	1.112(5)	0.669(4)	0.04(2)
H(14)	0.704(6)	0.960(5)	0.580(4)	0.04(2)
H(17)	0.615(7)	0.833(5)	0.473(4)	0.06(2)
H(18)	0.462(9)	0.689(7)	0.394(5)	0.09(2)
H(19)	0.206(9)	0.626(7)	0.417(5)	0.09(2)
H(20)	0.040(8)	0.645(6)	0.553(5)	0.08(2)

Table A.6

ATOM	x	y	z	U_{11}	U_{22}	U_{33}	U_{12}	U_{13}	U_{23}
Co	-.28691(6)	-.43288(9)	-.44149(8)	0.0349(8)	0.0297(8)	0.0224(8)	0.0000(7)	0.0017(7)	-.0029(8)
Br(1)	-.39613(8)	-.500	-.000	0.0480(12)	0.0669(13)	0.1116(18)	0.000	0.000	0.0196(15)
Br(2)	-.13493(9)	-.500	-.000	0.0702(14)	0.1130(19)	0.0740(16)	0.000	0.000	0.0216(16)
Br(3)	-.34231(6)	-.13234(8)	-.20622(8)	0.0703(9)	0.0557(8)	0.0430(7)	-.0050(8)	-.0018(8)	-.0068(8)
O(1)	-.30422(25)	-.5530(4)	-.4420(4)	0.0404(4)	0.039(4)	0.017(4)	-.001(3)	0.010(3)	-.018(4)
O(2)	-.2929(4)	-.6599(7)	-.2957(8)	0.120(10)	0.110(9)	0.133(11)	0.005(7)	-.036(9)	0.001(8)
O(3)	-.0803(3)	-.5013(8)	-.1864(6)	0.076(6)	0.094(7)	0.075(7)	-.014(6)	0.002(5)	-.021(6)
O(4)	-.000	-.3927(8)	-.250	0.059(8)	0.083(10)	0.053(8)	0.000	-.025(7)	0.000
O(5)	-.1039(5)	-.0974(8)	-.2958(6)	0.157(11)	0.173(12)	0.059(7)	0.116(10)	0.052(8)	0.034(8)
O(6)	-.0959(4)	-.2882(7)	-.3015(6)	0.120(9)	0.119(9)	0.071(8)	-.067(7)	-.028(7)	0.003(7)
C(1)	-.4429(4)	-.4567(7)	-.3964(7)	0.0548)	0.047(8)	0.039(7)	-.004(6)	0.008(7)	-.025(6)
C(4)	-.3731(4)	-.3225(7)	-.3860(6)	0.031(7)	0.039(7)	0.025(7)	0.002(6)	-.013(6)	0.004(6)
C(5)	-.4490(5)	-.2194(7)	-.3583(7)	0.084(10)	0.032(7)	0.031(8)	0.011(7)	-.010(7)	-.008(6)
C(6)	-.5046(6)	-.2058(9)	-.3516(8)	0.050(8)	0.090(10)	0.055(9)	0.006(8)	0.005(7)	-.029(8)

ATOM	x	y	z	U_{11}	U_{22}	U_{33}	U_{12}	U_{13}	U_{23}
C(7)	-.5409(4)	-.2727(9)	-.3492(8)	0.026(7)	0.097(11)	0.055(9)	0.001(7)	0.016(7)	-.017(8)
C(8)	-.5218(5)	-.3619(10)	-.3616(8)	0.053(9)	0.086(10)	0.056(9)	0.000(8)	0.016(7)	-.015(9)
C(9)	-.4289(5)	-.3042(8)	-.3722(8)	0.039(7)	0.056(8)	0.044(8)	0.001(6)	0.006(7)	-.014(7)
C(10)	-.4659(4)	-.3734(8)	-.3750(7)	0.032(7)	0.073(9)	0.033(7)	-.013(7)	0.012(6)	-.011(7)
C(11)	-.4597(5)	-.6129(8)	-.4057(9)	0.067(9)	0.039(8)	0.075(10)	-.023(7)	0.011(8)	-.001(7)
C(12)	-.5040(6)	-.6711(8)	-.4224(10)	0.086(10)	0.044(8)	0.090(11)	-.026(8)	0.008(9)	-.003(8)
C(13)	-.4871(6)	-.7600(8)	-.4295(10)	0.101(12)	0.057(9)	0.080(11)	-.030(9)	0.002(10)	0.000(9)
C(14)	-.4310(6)	-.7818(9)	-.4236(8)	0.127(13)	0.052(9)	0.046(9)	0.009(9)	-.005(9)	-.003(7)
C(15)	-.3939(5)	-.7193(7)	-.4099(8)	0.008(10)	0.016(6)	0.066(9)	0.000(7)	0.007(8)	-.012(7)
C(16)	-.2875(4)	-.2455(7)	-.4134(6)	0.045(7)	0.034(6)	0.028(7)	-.005(6)	0.000(6)	-.009(5)
C(17)	-.2635(4)	-.1653(6)	-.4098(6)	0.038(7)	0.030(6)	0.030(6)	-.007(6)	-.001(6)	-.010(5)
C(18)	-.2185(5)	-.1525(8)	-.4535(7)	0.048(8)	0.066(9)	0.036(7)	0.015(7)	-.004(6)	0.009(7)
C(19)	-.1990(4)	-.2160(7)	-.5116(8)	0.056(8)	0.035(7)	0.042(8)	-.008(6)	0.002(7)	0.024(7)
C(20)	-.2236(4)	-.2945(7)	-.5076(7)	0.048(7)	0.032(8)	0.020(6)	0.004(6)	-.014(7)	0.022(6)
C(21)	-.1714(4)	-.4526(6)	-.4297(6)	0.040(6)	0.013(5)	0.021(6)	0.002(5)	0.008(5)	-.009(5)
C(22)	-.0228(4)	-.4809(8)	-.4594(7)	0.032(7)	0.048(8)	0.060(9)	-.005(6)	-.004(6)	0.002(7)

ATOM	x	y	z	U_{11}	U_{22}	U_{33}	U_{12}	U_{13}	U_{23}
C(23)	-.0697(4)	-.4594(7)	-.4199(7)	0.023(6)	0.054(8)	0.046(7)	-.006(6)	-.019(6)	0.0146)
C(24)	-.1194(4)	-.4769(6)	-.4612(6)	0.035(6)	0.017(6)	0.030(7)	0.005(5)	0.012(5)	0.007(5)
C(25)	-.2156(4)	-.4086(6)	-.3012(6)	0.053(7)	0.016(6)	0.025(6)	-.008(5)	-.004(6)	-.004(5)
C(26)	-.1995(5)	-.3948(8)	-.2177(7)	0.078(9)	0.065(9)	0.018(7)	0.014(7)	0.004(7)	-.019(6)
C(27)	-.2400(6)	-.4143(9)	-.1577(7)	0.078(10)	0.085(10)	0.030(7)	0.017(8)	-.009(7)	-.016(7)
C(28)	-.2936(5)	-.4399(9)	-.1823(7)	0.051(8)	0.084(10)	0.035(7)	0.002(8)	0.006(6)	-.001(8)
C(29)	-.3056(5)	-.4507(8)	-.2640(6)	0.084(10)	0.064(9)	0.012(6)	0.023(7)	0.026(6)	-.002(6)
N(2)	-.3927(3)	-.4640(5)	-.4166(6)	0.018(5)	0.048(6)	0.052(6)	0.003(4)	0.020(4)	-.013(5)
N(3)	-.3581(4)	-.3992(5)	-.4137(5)	0.042(6)	0.036(6)	0.035(6)	-.018(4)	0.010(5)	0.004(4)
N(4)	-.4774(4)	-.5268(6)	-.3990(7)	0.056(7)	0.052(7)	0.082(8)	-.016(5)	0.017(6)	-.017(6)
N(5)	-.3372(3)	-.2584(6)	-.3726(5)	0.028(6)	0.044(6)	0.044(6)	-.004(5)	0.001(5)	-.003(5)
N(6)	-.4084(4)	-.6562(7)	-.4017(6)	0.052(7)	0.064(7)	0.063(7)	-.006(6)	0.019(6)	-.008(7)
N(7)	-.2668(3)	-.3117(5)	-.4568(5)	0.044(6)	0.042(5)	0.018(5)	-.002(5)	-.007(4)	0.010(4)
N(8)	-.2166(3)	-.4715(5)	-.4670(4)	0.032(5)	0.044(6)	0.017(5)	-.019(4)	0.005(4)	0.002(4)
N(9)	-.1729(4)	-.4029(6)	-.3604(5)	0.051(6)	0.043(6)	0.014(5)	-.007(5)	0.008(5)	-.007(4)
N(10)	-.2645(4)	-.4306(6)	-.3244(5)	0.043(6)	0.062(6)	0.014(5)	0.007(6)	-.017(4)	-.014(5)

Table A.7

ATOM	x	y	z	U_{11}	U_{22}	U_{33}	U_{12}	U_{13}	U_{23}
Ni(1)	0.83885(14)	0.28194(19)	0.15616(8)	0.0376(15)	0.0438(16)	0.0320(14)	-.0009(14)	-.0043(12)	0.0026(13)
Ni(2)	0.70328(14)	0.43105(20)	0.10688(8)	0.0382(15)	0.0494(17)	0.0362(15)	0.0012(14)	-.0069(12)	0.0005(14)
Br(1)	0.26204(15)	0.39439(26)	0.08452(8)	0.0602(15)	0.1819(31)	0.0550(16)	0.0156(18)	-.0062(13)	0.0290(18)
Br(2)	0.48394(19)	0.28433(33)	0.35062(11)	0.0909(22)	0.235(4)	0.1012(24)	0.0313(25)	0.0343(19)	-.0129(27)
Br(3)	0.07928(14)	0.13579(17)	0.34383(7)	0.06770(15)	0.0555(15)	0.0466(13)	0.0170(13)	0.0007(11)	0.0034(12)
Br(4)	0.7776(4)	0.3950(5)	0.49327(18)	0.105(5)	0.131(6)	0.060(4)	0.032(4)	0.004(3)	0.005(4)
Br(5)	0.09796(29)	0.0183(4)	0.02892(16)	0.078(3)	0.112(4)	0.070(3)	0.026(3)	-.0063(27)	0.010(3)
O(1)	0.7094(6)	0.2714(9)	0.1323(4)	0.032(7)	0.051(8)	0.039(8)	0.002(7)	-.020(6)	0.016(7)
O(2)	0.8007(6)	0.4441(9)	0.1606(3)	0.042(7)	0.052(8)	0.011(6)	0.014(7)	-.008(6)	-.006(6)
O(3)	0.6796(10)	0.1098(11)	0.0777(5)	0.116(13)	0.076(12)	0.078(11)	-.017(10)	-.002(10)	-.021(9)
O(4)	0.2680(16)	0.1308(21)	0.0678(7)	0.240(27)	0.251(30)	0.134(20)	-.083(23)	-.067(18)	0.079(20)
O(5)	0.2811(14)	0.2544(21)	0.2840(7)	0.179(23)	0.247(29)	0.148(20)	0.066(20)	0.006(17)	0.015(19)
O(6)	0.4497(11)	0.4670(17)	0.4330(7)	0.112(15)	0.167(20)	0.173(21)	0.015(15)	-.015(14)	0.010(17)
O(7)	0.3975(15)	0.0479(22)	0.0255(8)	0.1998(25)	0.279(3)	0.171(23)	0.093(24)	-.034(19)	-.035(22)

ATOM	x	y	z	U_{11}	U_{22}	U_{33}	U_{12}	U_{13}	U_{23}
C(1A)	0.6124(11)	0.4903(14)	0.2274(6)	0.055(15)	0.046(15)	0.054(15)	0.009(12)	0.010(12)	-.002(12)
C(4A)	0.5332(11)	0.4694(15)	0.1438(6)	0.054(14)	0.046(15)	0.055(14)	0.008(12)	0.006(12)	0.005(12)
C(5A)	0.3948(11)	0.4946(16)	0.1716(7)	0.047(15)	0.062(17)	0.084(18)	-.014(13)	0.026(13)	-.014(14)
C(6A)	0.6498(12)	-.0030(16)	0.0906(8)	0.055(16)	0.047(16)	0.107(20)	-.014(13)	0.013(14)	0.024(15)
C(7A)	0.3884(14)	0.4969(18)	0.2564(8)	0.084(19)	0.063(19)	0.122(23)	0.002(16)	0.021(17)	0.012(17)
C(8A)	0.4786(12)	0.4968(16)	0.2633(8)	0.064(17)	0.052(17)	0.107(21)	0.002(14)	0.019(15)	-.002(15)
C(9A)	0.4804(11)	0.4863(16)	0.1787(7)	0.043(14)	0.059(16)	0.070(16)	0.004(12)	0.021(12)	0.006(13)
C(10A)	0.5245(12)	0.4899(14)	0.2233(6)	0.066(15)	0.043(14)	0.044(14)	-.016(12)	0.021(12)	0.005(11)
C(11A)	0.2569(13)	0.0107(16)	0.2202(6)	0.097(18)	0.058(15)	0.032(13)	-.025(14)	-.017(12)	0.004(11)
C(12A)	0.2325(14)	0.0317(20)	0.1738(7)	0.089(18)	0.114(12)	0.062(16)	-.042(16)	0.008(14)	-.005(15)
C(13A)	0.1457(15)	0.0417(19)	0.1616(8)	0.106(20)	0.097(21)	0.071(17)	-.042(17)	0.005(15)	0.015(16)
C(14A)	0.0891(14)	0.0315(16)	0.1920(7)	0.103(19)	0.063(16)	0.065(16)	-.027(14)	0.019(14)	0.008(13)
C(15A)	0.1221(12)	0.0138(17)	0.2381(7)	0.067(15)	0.077(18)	0.057(14)	-.001(14)	-.016(12)	0.001(13)
C(16A)	0.5233(12)	0.4099(15)	0.0644(6)	0.056(15)	0.056(16)	0.055(15)	0.000(12)	-.004(12)	0.025(12)
C(17A)	0.4591(12)	0.3834(18)	0.0274(7)	0.063(17)	0.110(21)	0.050(16)	0.000(15)	0.001(13)	-.004(15)
C(18A)	0.4830(12)	0.3339(17)	-.0098(7)	0.052(16)	0.081(19)	0.078(18)	-.009(14)	-.012(13)	0.007(15)

ATOM	x	y	z	U_{11}	U_{22}	U_{33}	U_{12}	U_{13}	U_{23}
C(19A)	0.5723(14)	0.1900(19)	0.4850(7)	0.081(18)	0.111(22)	0.047(16)	0.019(16)	-.013(14)	0.007(15)
C(20A)	0.6296(12)	0.3442(16)	0.0199(6)	0.052(14)	0.072(17)	0.043(14)	-.006(13)	-.016(11)	-.009(13)
N(2A)	0.6560(9)	0.4839(12)	0.1930(5)	0.052(11)	0.048(12)	0.049(12)	-.007(10)	0.004(9)	0.004(9)
N(3A)	0.6164(8)	0.4658(11)	0.1492(4)	0.038(10)	0.047(11)	0.039(10)	-.005(9)	-.009(8)	0.005(9)
N(4A)	0.3446(9)	0.0031(12)	0.2304(5)	0.062(12)	0.065(13)	0.039(11)	-.001(10)	0.009(9)	-.008(10)
N(5A)	0.4940(8)	0.4552(12)	0.1011(4)	0.045(11)	0.072(13)	0.031(10)	0.008(10)	0.004(9)	-.016(10)
N(6A)	0.2039(9)	0.0034(12)	0.2500(5)	0.057(11)	0.051(11)	0.043(10)	0.006(9)	0.011(8)	0.005(9)
N(7A)	0.6059(9)	0.3909(12)	0.0590(5)	0.041(11)	0.068(13)	0.042(11)	0.001(10)	-.013(8)	0.003(10)
C(1B)	0.8234(11)	0.4377(14)	0.0336(6)	0.045(13)	0.042(14)	0.047(14)	-.010(12)	-.014(11)	0.009(12)
C(4B)	0.9067(10)	0.2658(13)	0.0651(5)	0.027(11)	0.032(12)	0.031(12)	0.004(10)	0.005(9)	0.010(10)
C(5B)	0.9954(12)	0.2631(15)	-.0002(6)	0.062(15)	0.053(16)	0.049(14)	0.008(13)	0.008(12)	-.005(12)
C(6B)	1.0150(12)	0.3215(16)	-.0394(6)	0.058(15)	0.078(17)	0.042(14)	-.037(13)	0.004(12)	-.011(13)
C(7B)	0.9727(11)	0.4091(14)	-.0549(6)	0.045(14)	0.041(14)	0.056(14)	0.010(11)	0.004(11)	0.003(12)
C(8B)	0.9088(11)	0.4551(15)	-.0322(6)	0.048(14)	0.061(16)	0.037(14)	-.012(12)	0.004(11)	0.002(12)
C(9B)	0.9292(10)	0.3081(14)	0.0237(6)	0.030(12)	0.062(16)	0.040(13)	-.005(11)	0.005(10)	-.010(12)
C(10B)	0.8882(10)	0.3987(13)	0.0070(6)	0.042(13)	0.044(14)	0.027(12)	0.002(10)	0.008(10)	-.008(10)

ATOM	x	y	z	U_{11}	U_{22}	U_{33}	U_{12}	U_{13}	U_{23}
C(11B)	0.2490(11)	0.1066(15)	0.4534(6)	0.036(13)	0.057(16)	0.046(14)	0.005(11)	-.008(10)	-.013(12)
C(12B)	0.2393(12)	0.2123(15)	0.4690(6)	0.047(14)	0.050(16)	0.073(16)	0.002(12)	-.019(12)	-.024(13)
C(13B)	0.2672(12)	0.2960(17)	0.4425(7)	0.052(15)	0.079(18)	0.058(16)	-.004(14)	-.001(12)	0.000(14)
C(14B)	0.2982(12)	0.2696(15)	0.4025(7)	0.051(14)	0.049(15)	0.075(17)	-.005(13)	-.004(13)	0.006(13)
C(15B)	0.3051(11)	0.1663(15)	0.3896(6)	0.055(14)	0.044(15)	0.058(15)	0.009(12)	-.002(12)	0.002(12)
C(16B)	0.9092(10)	0.0974(14)	0.1091(6)	0.035(13)	0.058(16)	0.048(14)	-.006(11)	-.024(11)	0.006(12)
C(17B)	0.9268(11)	-.0117(15)	0.1006(6)	0.052(14)	0.050(16)	0.053(15)	0.005(12)	-.001(12)	-.016(12)
C(18B)	0.8956(13)	-.0864(15)	0.1269(6)	0.083(17)	0.045(15)	0.057(16)	0.004(13)	0.001(13)	0.010(12)
C(19B)	0.8460(12)	-.0547(15)	0.1613(6)	0.062(15)	0.046(16)	0.064(16)	-.002(13)	-.006(12)	0.008(13)
C(20B)	0.8289(12)	0.0519(15)	0.1672(6)	0.059(15)	0.051(16)	0.057(16)	-.023(13)	-.003(12)	0.008(12)
N(2B)	0.8051(9)	0.3944(11)	0.0711(4)	0.052(10)	0.043(10)	0.023(9)	0.000(8)	-.004(7)	-.002(7)
N(3B)	0.8524(8)	0.3084(11)	0.0886(4)	0.041(9)	0.042(10)	0.026(9)	0.006(8)	0.003(7)	0.004(8)
N(4B)	0.2183(9)	0.0270(12)	0.4817(5)	0.058(11)	0.050(11)	0.059(11)	-.018(9)	-.001(9)	-.001(9)
N(5B)	0.9449(9)	0.1729(12)	0.0799(5)	0.060(11)	0.058(12)	0.044(10)	-.004(10)	-.014(9)	0.012(9)
N(6B)	0.2826(8)	0.0845(11)	0.4150(5)	0.033(9)	0.045(10)	0.044(10)	-.002(8)	-.003(7)	-.003(8)
N(7B)	0.8621(9)	0.1266(12)	0.1416(5)	0.052(10)	0.062(12)	0.030(9)	0.004(9)	-.014(8)	-.004(8)

ATOM	x	y	z	U_{11}	U_{22}	U_{33}	U_{12}	U_{13}	U_{23}
C(1C)	0.8591(10)	0.2529(14)	0.2588(5)	0.028(11)	0.048(14)	0.025(11)	0.008(10)	-.004(9)	0.011(10)
C(4C)	0.6889(10)	0.2532(14)	0.2587(6)	0.034(12)	0.047(15)	0.042(13)	0.001(11)	0.000(10)	-.008(11)
C(5C)	0.7007(13)	0.2430(19)	0.3444(7)	0.072(18)	0.112(23)	0.061(18)	0.014(16)	0.027(15)	-.014(16)
C(6C)	0.7511(13)	0.2508(19)	0.3842(7)	0.061(16)	0.110(22)	0.070(18)	-.002(16)	0.007(14)	-.008(16)
C(7C)	0.8400(14)	0.2626(20)	0.3820(7)	0.091(20)	0.116(23)	0.048(16)	0.034(18)	0.007(14)	-.002(16)
C(8C)	0.8779(11)	0.2598(17)	0.3416(6)	0.040(13)	0.092(18)	0.046(14)	0.006(13)	0.014(11)	0.019(13)
C(9C)	0.7388(11)	0.2486(15)	0.3016(6)	0.050(14)	0.064(16)	0.023(12)	0.004(12)	-.001(10)	-.005(11)
C(10C)	0.8261(11)	0.2516(15)	0.3007(5)	0.046(13)	0.069(16)	0.022(12)	0.014(12)	0.009(10)	0.002(11)
C(11C)	0.9941(10)	0.2802(14)	0.2244(6)	0.037(12)	0.045(14)	0.038(13)	0.006(11)	0.004(10)	-.004(11)
C(12C)	1.0972(13)	0.3674(17)	0.1665(6)	0.069(16)	0.081(18)	0.052(15)	-.017(15)	0.017(13)	0.000(14)
C(13C)	1.0129(10)	0.3566(14)	0.1544(6)	0.034(12)	0.039(14)	0.055(14)	-.005(11)	0.012(10)	0.001(11)
C(14C)	1.1355(13)	0.3302(17)	0.2082(7)	0.072(17)	0.082(18)	0.055(16)	-.009(15)	0.003(13)	0.016(14)
C(15C)	1.0813(10)	0.2862(15)	0.2364(6)	0.035(13)	0.053(15)	0.046(13)	0.002(11)	0.009(10)	-.018(12)
C(16C)	0.5446(11)	0.2358(15)	0.2212(7)	0.039(13)	0.040(14)	0.108(19)	0.014(11)	0.001(12)	-.003(13)
C(17C)	0.4595(11)	0.2424(16)	0.2292(8)	0.021(11)	0.058(16)	0.121(20)	0.010(11)	0.000(12)	0.000(14)
C(18C)	0.4022(12)	0.2306(16)	0.1908(7)	0.043(13)	0.058(15)	0.092(18)	-.014(12)	0.001(12)	0.007(13)

ATOM	x	y	z	U_{11}	U_{22}	U_{33}	U_{12}	U_{13}	U_{23}
C(19C)	0.4271(13)	0.2098(19)	0.1512(7)	0.058(15)	0.108(20)	0.079(17)	-.015(15)	-.016(13)	0.019(16)
C(20C)	0.5103(12)	0.2029(16)	0.1448(7)	0.063(15)	0.074(18)	0.069(16)	-.017(13)	-.023(13)	0.007(14)
N(2C)	0.8096(8)	0.2565(12)	0.2210(5)	0.028(10)	0.069(13)	0.041(11)	-.009(9)	-.002(8)	0.001(9)
N(3C)	0.7263(8)	0.2609(11)	0.2212(4)	0.035(10)	0.050(12)	0.038(10)	-.002(9)	0.008(8)	0.001(9)
N(4C)	0.9436(9)	0.2439(12)	0.2560(5)	0.050(11)	0.072(13)	0.034(10)	0.009(10)	0.007(9)	0.014(9)
N(5C)	0.6035(8)	0.2506(11)	0.2586(5)	0.031(10)	0.042(11)	0.047(11)	0.000(9)	-.002(8)	-.003(9)
N(6C)	0.9624(8)	0.3168(11)	0.1831(4)	0.028(10)	0.044(11)	0.038(10)	-.001(8)	-.004(8)	0.005(8)
N(7C)	0.5725(10)	0.2214(14)	0.1792(5)	0.053(11)	0.091(14)	0.056(12)	0.002(11)	-.022(9)	0.012(11)